POLITECNICO
MILANO 1863

Simulation of gas flows through connected microchannels for attosecond soft X radiation sources with ANSYS Fluent

Emma Serrano San Cristóbal

Tutor: Aldo Frezzotti

Final Thesis

School of Industrial Engineering
Academic Year 2017 -2018

Abstract

The objective of this project is to make an approach to the behaviour of a flow being ejected through a set of nozzles into a volume, in which another set of outlet orifices is found, with a discharge pressure as low as possible in order to simulate vacuum conditions. The study of the case is started by testing simple and schematic models with the software ANSYS Fluent, through which results are obtained and validated by comparing them to the expected solutions given by the theory.

For the initial approach a *2D* case with one inlet discharging into an open volume has been defined, and solved by applying the inviscid theory through ANSYS Fluent. Further evolutions of this base model, such as the addition of a second inlet or the enclosing of the system into a closed volume with an outlet, have matched the predicted results regarding the theory application as well.

The final geometry, consisting on a channel with two main outlets on its extremes and a set of inlet and outlet flow orifices along its length, has been tested through the software in order to study the dependence of the flow behaviour on the variation of different parameters regarding the channel geometry or the boundary conditions of the case. The profile of the variables of interest along the channel, such as the density, the static temperature and pressure, and the velocity magnitude, has been extracted, and final suggestions, regarding geometry and flow concerns, have been provided in order to get the desired evolution of the flow along the channel axis.

Nomenclature

e	Internal energy
g	Gravity acceleration
h	Enthalpy
$\dot{m}$	Mass flow rate
$\dot{m}_{in}$	Inlet mass flow rate
$\dot{m}_{out}$	Outlet mass flow rate
$\boldsymbol{u}$	Flow velocity vector
u_m	Magnitude of the velocity
u	Component of the velocity vector in the x direction
v	Component of the velocity vector in the y direction
w	Component of the velocity vector in the z direction
C	Courant number
D_c	Characteristic dimension
Kn	Knudsen number
L	Length
L_{REF}	Reference length
L_{ic}	Length of the inlet channel
L_{mc}	Half of the length of the main channel
P	Pressure
P	Pressure
P_{in}	Inlet pressure
P_{int}	Internal pressure
P_{out}	Outlet pressure
P_0	External pressure
P_1	Pressure at inlets
$P(x_i)$	Pressure at the feeding channel located at position x_i
R	Radius
R_{ic}	Radius of the inlet channel
R_{mc}	Radius of the main channel
R_{oc}	Radius of the outlet channel

R'	Ideal gas constant
T	Temperature
U_c	Characteristic velocity
V	Velocity magnitude
V_0	Initial velocity magnitude
V_F	Final velocity magnitude
γ	Heat capacity ratio
ϕ	Magnitude of interest in the conservation equation
ρ	Density
μ	Dynamic viscosity
∇	Nabla operator (gradient)
Δt	Time step
Δx	Length interval

Content

List of figures

List of tables

Chapter 1 Introduction

1.1 Motivation

The study of supersonic flow aerodynamic windows focused on the application for high-power lasers is an issue of interest, since the absence of solid windows would imply that there would not be additional surfaces absorbing energy from the laser through excessive heating. This benefit is especially remarkable in the field of extreme ultraviolet radiation, considered as the most highly absorbed component of the electromagnetic spectrum, requiring high vacuum for transmission.

The extreme ultraviolet radiation (XUV) is electromagnetic radiation in the part of the electromagnetic spectrum spanning wavelengths from *124 nm* to *10 nm*, and its main uses are photoelectron spectroscopy, solar imaging and lithography. The XUV can be generated by a high-power pulsed laser system and a setup consisting of a combination of vacuum chambers and expanding jets of a gas such as krypton, argon, neon or helium, and by means of variating the full spectrum laser intensity and the expanded gas density it is possible to obtain fluctuations in the XUV-light intensity.

Focusing on the generation of extreme ultraviolet radiation from a full spectrum laser, the details of the setup in order to obtain the desired output signal need to be known, and taking into account the fact that this signal generation will be implemented through a set of expanding gas jets in an environment close to vacuum, it is essential to perform an initial analysis of the fluid behaviour in the design so that the validity of it is verified. This way it will also be possible to be aware of the relevant parameters of the setup in a way that further suggestions and modifications can be made in order to generate the most accurate environment for the XUV generation.

The study of the gas behaviour will be performed through computational fluid dynamics, a branch of fluid mechanics that uses numerical analysis and data structures to solve and analyse problems that involve fluid flows. Therefore the main tool needed for this approach will be a computer, and the chosen software is ANSYS Fluent.

1.2 Objectives

The main objectives of this project, which will be used as the guide to approach the final case display, are the following:

- Perform an initial research of the existing experiments and papers related to the case of interest in order to establish a baseline from where to start the preliminary designs to test.
- Create base geometry with the most essential features of the case setup and obtain the fluid behaviour through ANSYS Fluent. Modify sequentially this initial approach, by adding geometrical features and additional considerations regarding the boundary conditions of the calculation, so that the final case matches and represents the real experiment as much as possible.
- Verify the results obtained by validating them through relevant theory and external experiments already validated.
- Build up the testing setups in order to direct them to a concluding case that best represents the real setup.
- Obtain the evolution of the fluid variables of interest, such as pressure, velocity, and specially density, along the main channel direction and establish the relationship or dependence of this evolution with the features of the setup.
- Once all the results are obtained and validated, suggest further modifications in the computational approach and in the final setup of the real case in order to obtain a fluid profile that fits the required characteristics of the model in a more suitable way that the ones reached with the actual focusing.

1.3 Scope

The analysis of the case will be started by a brief research and study of the flow conditions expected to take place in the initial design. Documentation will be obtained from papers of previous studies related to the topic and theory books and websites that cover such conditions. Once the relevant features of the flow behaviour are set and known, the computational fluid dynamics analysis will take place, starting off with the most basic solution approach consisting on an orifice from which argon flows at the defined conditions of the case, discharging mass into a *2D* open control volume.

The next setup will be completely analogue to the first one, but studying the interaction between two orifices with the exact same conditions. After this, the third

approach will account for the *3D* effects giving this way a more realistic representation of the case.

Finally, a *3D* setup consisting on a closed control volume with one inlet orifice, and another one for the outlet, will be tested and sequentially modified by adding more details, until the final configuration of *30* inlets and *30* outlets along an open channel discharging into conditions close to vacuum is reached. Once this design is verified some variations will be tested on it, such as the distribution of the outlets with respect to the position of the inlets, or the size of the diameter of these, among other possibilities. In this phase of the project the main target will be to obtain the dependence of the density profile along the main channel on the geometric and flow conditions, so that further suggestions regarding the final design of the laser system can be stated for achieving de desired profile evolution.

Chapter 2 Problem to solve

2.1 Problem description

In order to understand the analysis to perform and the scope of it, it is essential to consider the already mentioned extreme ultraviolet radiation, XUV. For XUV to take place it is first necessary to have free electrons and ions. Therefore, ionization must take place. The reason of this is that neutral atoms or condensed matter are not capable of emitting XUV radiation, since XUV light can only be emitted by electrons which are bound to multi-charged positive ions. This situation is naturally recreated by the solar corona (an aura of plasma that surrounds the Sun and other stars), but it can also be artificially achieved by means of the existence of a hot dense plasma. In a parallel way, though, the free electrons and ions can be temporarily generated by a laser beam suitably composing a setup with freely expanding jets of a proper gas into a vacuum-condition reservoir.

Different applications are derived from the extreme ultraviolet radiation, such as photoelectron spectroscopy (energy measurement of electrons emitted from solids or liquids in order to determine the binding energies of electrons in a substance), solar imaging (through the Extreme ultraviolet Imaging Telescope, EIT, high resolution images of the solar corona in the ultraviolet range can be captured) and lithography (being the Extreme ultraviolet lithography, EUVL, considered as a next generation lithography technology).

With the aim of recreating the last of the stated methods regarding artificial generation of extreme ultraviolet radiation, a preliminary design has been provided in which a set of *30* channels discharges the gas into a main channel, along which the laser signal will travel. The gas leaves the volume through the main channel extremes and through another set of *30* outlets, initially placed aligned with the inlets. A rough scheme (not to scale) is representing the setup in the following figure.

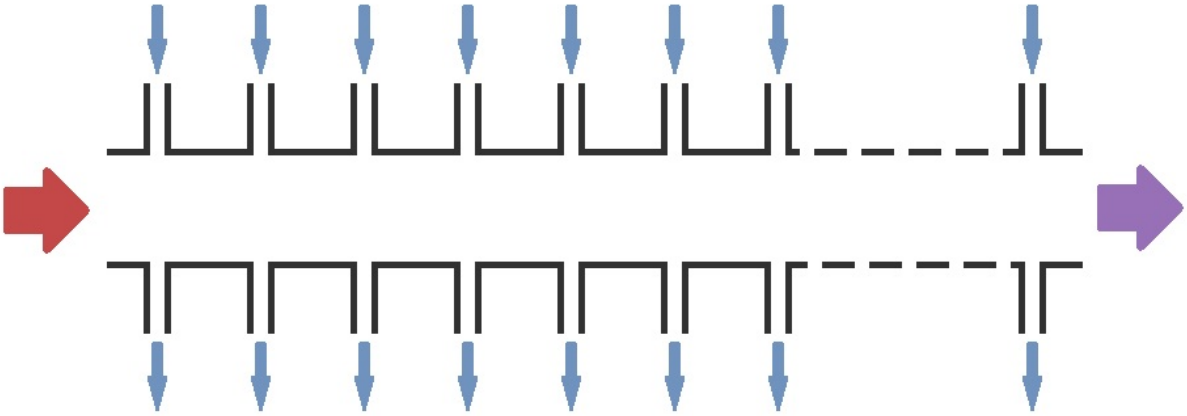

Figure 1: Schematic representation of the channel along which the laser beam travels.

The image above represents the main channel travelled by the laser. The red arrow stands for the full spectrum laser signal, while the purple one represents the XUV output signal. The blue arrows are depicting the main gas flow, although, as already said, it also flows out from the volume through the extremes of the principal channel, but for the aim of the simplicity of the representation no schematic remark has been added to this zone.

Regarding the fluid-dynamic contribution to the development of the experiment and to the resulting XUV signal, it is known that variations in the gas density have an influence in the pulse-to-pulse fluctuations that the XUV-light intensity may experience. This turns the flow density into one of the most relevant parameters when analysing the solutions to implement. Particularly, the evolution of the density along the main channel axis will be the most meaningful information in terms of the laser signal outcome.

In order to perform decent approximations to the target design it is necessary to take some initial assumptions regarding the nature of the flow. Bearing in mind the low pressures and the relatively high values for the velocity of the gas, and considering the fact that low gas-wall interaction will take place in the domain of interest, a valid starting point would be considering the flow as inviscid, which would imply the absence of a boundary layer development and existence. For a fluid to be considered as inviscid its Reynolds number ($Re = \frac{\rho \cdot U_c \cdot D_c}{\mu}$, non-dimensional parameter that represents the relationship between the inertial forces and the viscous forces) needs to be very high. Thanks to this assumption it is possible to reduce the Navier-Stokes equations, which describe the motion of viscous fluid substances, to the Euler equations:

$$\frac{D\rho}{Dt} = -\rho\nabla \cdot \boldsymbol{u}$$
$$\frac{D\boldsymbol{u}}{Dt} = -\frac{\nabla p}{\rho} + g \qquad (1)$$
$$\frac{De}{Dt} = -\frac{p}{\rho}\nabla \cdot \boldsymbol{u}$$

This last set of equations allows to simplify the solution of the fluid-dynamic behaviour of the gas flowing through the volume previously defined. Nevertheless, it is essential to bear in mind the fact that the solution provided by the Euler equations is no longer valid in the region of fluid near a solid boundary.

Therefore the initial approximations implemented by means of the already mentioned software ANSYS Fluent will be based on an inviscid model.

2.2 Operating conditions

The provided data from which the simulations will be pictured is the one gathered in the following table:

Parameter	Value
Pressure in the vacuum chamber *[mbar]*	*10^{-4}*
Backing pressure *[mbar]*	*20-300*
Jet Mach number *[-]*	*1*
Diameter of the jet nozzle *[mm]*	*3*
Gas to be used: krypton, argon, neon, helium	

Table 1: Operating conditions.

Considering the previous operating conditions, the outlet pressure for the flow exit orifices will be set to *10^{-4} mbar*, while the flow inlet orifices will be defined to have a backing pressure of *120 mbar* and a velocity equal to Mach *1*. As for the fluid composition, the gas chosen will be argon under the consideration of ideal gas.

The temperature will be set to *300 K*, and in the initial simulations no heat flux will be considered between the fluid and the volume walls, being the last ones set as adiabatic.

Even though the geometric details will be specified for every simulation ahead, for the initial ones no channels will be accounted for the inlet and outlet orifices through which the gas is injected in and extracted from the volume. Therefore the conditions

given in these inlets and outlets will be the ones that are supposed to take place in the surface of these that intersects with the main channel walls, which would be, respectively, the end of the inlets channels and the beginning of the outlets channels.

Regarding the geometric specifications, those will be deeply defined in the corresponding sections of each of the simulations.

Chapter 3 Methodology

3.1 Sequence of performance

As it has already been commented, the target of the studies to develop is the definition of the evolution of the density profile along the main channel, which will have direct influence on the resulting laser signal. In order to do that, the basic steps to follow will be the ones briefly stated below:

- Analyse the conditions of the case to study in order to obtain a generic scheme of the expected behaviour of the fluid. This step is essential for setting the correct configuration options when starting the computational simulations, and it also provides the theoretical approach to the solution in a way that it can eventually become a validation reference for the results given by the analysis.
- Translate the assumptions taken in the first step into parameters and models that can be provided to the computational fluid dynamics tool used, in this case ANSYS Fluent.
- By means of a proper software, define the geometry of the model in the most accurate way possible, representing each of the main parts of the volume of interest. It is also useful to tag the main parts of the geometry with representative labels, like “inlet”, “outlet” or “walls”. This additional step will ease future settings.
- Once the geometry has been obtained it needs to be meshed in a proper way so that the software can analyse the applicable models.
- Prepare the setup of the solution calculation taking into account the assumptions, simplifications and considerations minded in the first step.
- Evaluate the obtained solution. Validate it by comparing it with the proper theory that represents the fluid dynamic behaviour under the conditions of the case of interest determined in the first step. In case the solution is satisfactory, extract the parameters of interest from it.
- If the solution obtained is not matching the expected results and does not fit in the validation prediction, move backwards and check the software settings and assumptions taken in order to find the error or misconception that leads to such result, and repeat the calculation until the solution can be accepted.

Further details of the procedure applied on each one of the previous steps will be specified in the coming contents.

3.2 Operating tool: ANSYS Fluent

When it comes to finding the solution of the problem, which in this case is the definition of the fluid dynamic behaviour of the gas that enters into the defined volume, since the purpose of it is designing the density profile of the gas along the channel, which is the ultimate interest, it is necessary to enter in the field of computational fluid dynamics.

During the engineering process of designing and creating a new product such the one treated in this case, aerodynamics represent an essential role. Unfortunately, these are not easily pictured out during the concept phase of the design. Therefore it is crucial to create and test prototypes that can offer an estimation of the final situation to expect. But since the creation and testing of physical prototypes would mean a considerable investment of time and economical resources (designing the prototype, constructing it, testing it, studying the results, redesigning it and constructing it again in order to repeat the tests until the desired configuration is achieved), and bearing in mind the fact that computers development and capacity are continuously rising, the use of computational fluid dynamics, CFD, as a helpful tool has become a common issue when it comes to generating solutions for fluid flows.

A CFD calculation provides the behaviour of a fluid flow by considering and calculating the values of its physical properties in a simultaneous way, so that the target of a representative solution can be reached. CFD solvers are based on a mathematical model that represents the physical case in accordance with the content of the problem, and a numerical method to generate a path through the solution of it.

There are several CFD softwares available nowadays, but particularly in this case the chosen one is Fluent, the one provided by the brand ANSYS.

In order to create a suitable background of the project, along this section a description of each of the ANSYS platforms, used to obtain the ultimate solutions, will be given.

ANSYS is a general purpose software, not only used for treating fluid dynamic concerns but also applicable to other fields that imply interactions of all disciplines of physics, structural, vibration, fluid dynamics, heat transfer and electromagnetic.

ANSYS is, therefore, a tool that can simulate tests in order to provide a virtual environment before manufacturing physical prototypes of products, saving time and economical resources from all the design, development and production process. The program offers different platforms, in order to cover each of the available solvers (Samcef, Polyflow, CFX, Fluent, Forte,...) gathered in a principal menu displayed in the so-called Workbench. This graphic interface allows to create a project from the design geometry to the post-processing of the obtained results.

In the following subsections deeper descriptions of each of the platforms offered by ANSYS Workbench used in the process will be given.

3.2.1. Creating the geometry: DesignModeler

DesignModeler offers a graphical user interface through which designing the geometry of the physical case to test. By means of this platform the user can create *2D* or *3D* models starting from a sketch based on geometrical figures such as lines, rectangles, polygons, circles and many others. From this sketches surfaces can be constructed and extruded or revolved, among other possibilities. The program also allows to merge different bodies in order to create a more detailed final one, or to import directly an already generated computer-aided design (CAD) geometry created by means of other software platforms of design.

Even though it needs some practice in order to master the tool, DesignModeler, thanks to its interface, is quite an intuitive tool that eases the process of the geometry design.

Focusing the attention on the designs performed along this project, the creation of those through the DesignModeler platform will not suppose further difficulties since the main geometrical shapes used to generate them are easy to replicate with the given options.

3.2.2. Meshing the volume

Once the volume that will be occupied by the fluid has been generated it needs to be divided into discrete cells, it needs to be meshed. The reason of this step is the fact that the partial differential equations that govern fluid dynamic behaviour are not usually related to an easily feasible analytical solution, unless the approached case is really simple. Therefore these equations are discretized and solved inside each of these subdomains. The collection of all of these subdomains is named mesh.

The main classifications for the type of mesh are structured or non-structured meshes.

Structured meshes are organized and have a regular and trivial connectivity. This type of meshes are really efficient, being the element position and, hence, the connectivity, defined by the place they occupy in the vector where the information of the mesh is collected. For *2D* the cells are quadrilaterals, and for *3D* they are hexahedrons. The most remarkable advantage of this kind of meshes is the fact that, for the same number of cells and same mesh quality, structured meshes provide better convergence and better precision that those given by non-structured meshes. The drawback of this type of mesh, though, lays on the difficulty of generation for complex geometries, requiring a lot of interaction from the designer.

On the other hand, non-structured meshes are irregular and the storage of the elements is not trivial in this case. The computational cost associated is much bigger than the one given for structured meshes. Normally triangles are the shape used for the *2D* cells, while tetrahedrons are selected for the *3D* meshes, even though other elements can be used. The main advantage of this type of mesh is that they are easily generated in an automatic way.

It is also possible to generate hybrid meshes that contain differentiated parts on them that can be identified with both classifications.

The importance of keeping a good quality mesh is remarkable: in general it is desirable to preserve a smooth transition between cells. The order of magnitude among adjacent cells should not vary, and the cells should not be considerably larger in one of the dimensions, unless flow characteristics allow it. Lastly, cells may not be too deformed, and the mesh should be refined in the suitable zones where phenomena such boundary layers, shock waves or high gradients of the parameters take place.

Considering the characteristics of the geometry of interest for this particular project, and as it will be later shown, a structured mesh composition has been chosen, since the shape of the volume of interest to be tested is suitable for such meshing option, and also considering the already mention fact that this type of mesh is preferable.

3.2.3. Setup of the calculation and solution visualization: Fluent

As it has previously been introduced, Fluent is the computational fluid dynamics tool provided by ANSYS. This software bases its solution on the finite volumes method (FVM), where the volume is discretized in a set of finite control volumes in which the equations of conservation of mass, momentum, energy or species, among others, are solved. The differential equations are discretized into an algebraic equation system, and all these algebraic equations are numerically computed in order to find the solution. The control volumes in Fluent are cell-centred, corresponding to the actual volumes defined by the mesh, and the variables are located at the centre of such volumes.

The conservation equations solved by Fluent are described by the following expression:

$$\frac{\partial}{\partial t}\int_V \rho\phi \, dV + \oint_A \rho\phi V \, dA = \oint_A \Gamma_\phi \nabla\phi \, dA + \int_V S_\phi \, dV \qquad (2)$$

Where each of the terms are identified as cumulative, convection, diffusion and source term respectively. As for ϕ, its corresponding value is specified in the following table:

Equation	$\boldsymbol{\phi}$
Continuity	*1*
Momentum in X	u
Momentum in Y	v
Momentum in Z	w
Energy	h

Table 2: Magnitudes to consider for each of the conservation equations.

These expressions, as it has already been commented, are suitable to be simplified in case the problem faced allows it. In any case, they need to be expressed in their differential form, by performing some steps applying the Reynolds transport theorem and the divergence theorem, so that they can be treated through numerical methods and given this way to the solver. Nevertheless, this is a step performed directly by the program, but it is interesting to know the expressions since they may be useful for future validation of the solution obtained.

Through Fluent the remaining details of the case can be set, considering that the geometry and the mesh have already been configured through the previous tools offered by ANSYS.

Fluent shows three main separated sections, displayed in the suitable order matching the chronological priority of setting: setup, solution and results. A more detailed description can be seen below.

- Setup. In this section the general settings are chosen. There are several submenus corresponding to the following topics.
  - General. In this paragraph it is stated whether the solution will be calculated as transient (time dependent) or steady. Also the velocity formulation and the type of solver (pressure-based or density-based, being the last one the most appropriate for compressible fluids) are defined.
  - Models. The equations to be solved are ticked in this section. The minimum required one is the energy model, but there are many others to choose as the viscosity one, in which the expected flow can be considered as inviscid, laminar or turbulent, having a variety of models for representing phenomena of turbulence for the last case.
  - Materials. In this section the materials for both fluid and solid parts is selected. Fluent also offers a database in which several options are displayed. These options can also be modified in order to match some considerations or simplifications, as, for example, the ideal gas law.
  - Cell Zone Conditions. The operating conditions of the simulation and the materials composing each of the entities defined by the geometry can be set in this part.
  - Boundary Conditions. This is one of the most important settings of the whole CFD simulation process. If boundary conditions are not wisely chosen the time to find the solution can increase considerably and lead to inaccurate and clumsy calculations. Through the boundary conditions the solver obtains a set of known values for some parameters at specific zones of the domain. The main zones are usually the inlet and outlet through which the fluid flows across the volume, and the walls and interior zones. There are different types of boundary conditions, but they all mainly refer to the values of pressure, temperature and velocity or mass flow.

- Dynamic Mesh. This paragraph gives the possibility to modify the mesh as the calculation runs once the program detects the zones where there are high gradients and more precision for the solution is needed.
- Reference Values. Here the defined parameters are the reference quantities used for computing normalized flow-field variables.

- Solution. The aim of this part is to define the details of the solution implementation.
  - Methods. The main setting of this part is the solver formulation, being possible to choose between implicit and explicit. Explicit schemes have more tendency to instability than implicit ones, but are easy to program with simple calculations, while implicit schemes are more difficult and can involve many iterations, but are very stable. Depending on the scheme chosen the program will request further settings regarding spatial discretization.
  - Controls. Different parameters regarding the stability of the convergence behaviour are defined in this display. Such parameters will depend on the type of solver chosen.
  - Report Definitions, Monitors, Cell Registers, Calculation Activities. These sections allow to define the record of some output parameters of interest in order to monitor them along the simulation. It is also possible to store them in order to treat them later. In the Monitors section the residuals can be modified, redefining this way the convergence requirements.
  - Initialization. An initial estimation to the solution of the flow field needs to be provided to the program. Fluent offers a standard initialization, in which the user needs to provide the values of the parameters on the volume, and a hybrid initialization, where the program estimates the initial approach to the solution by interpolating the data provided in the boundary conditions.
  - Run Calculation. The number of iterations needs to be set, and if a transient calculation has been chosen, it is also necessary to choose the time step and the maximum number of time steps to perform.
- Results. In here different tools are given for visualizing the results obtained, like XY plots and contour plots. It is also possible to visualize the results in an animation in the case of the transient calculations.

Since the settings listed above may vary among different simulations to perform, they will be specified for the corresponding case in the pertinent section.

3.2.4. Validation of the solution and convergence

Once the program has provided an apparently satisfactory solution, it is necessary to verify the validity of it, as it has already been commented. In order to do that the assumptions and simplifications accepted for the case have to be retaken and applied to the fluid dynamics theory, in order to find an expression, correlation or an already validated experiment previously performed that can be compared to the CFD solution. If the solution is coherent, then the results can be extracted and treated in the suitable way. On the contrary, if the comparison brings out the conclusion that the analysis is not reliable, then the user needs to move backwards in order to verify the quality of the mesh and the imposed settings all along the Fluent sections, paying special attention to the boundary conditions assumed.

3.2.5. Properties of the numerical methods solutions

Will the aim of providing some criteria to judge the validity of the solutions obtained with Fluent, the properties of the numerical methods solutions are given below:

- Accuracy. Numerical solutions are only approximate solutions, so it is desirable to obtain the closest result to the physical case.
- Agreement with the boundary conditions. Numerical solutions are expected to be within the bounds provided to the corresponding physical quantities.
- Conservation. The conservation laws imposed to the procedure need to be accomplished.
- Convergence. The solutions obtained have to show a tendency to the same result, regardless the mesh used.
- Consistency. Those points that are close in the domain with respect to the other should show a consistent solution: the value of an observed parameter should be similar among them, showing a smooth transition of it along the domain.
- Realizability. In case the model that represents the phenomena of study is too complex to be treated directly, it has to be processed in order to guarantee physically realistic solutions.

- Stability. A satisfactory CFD analysis provides a stable solution even under perturbations.

Chapter 4 Cases

In this chapter the models tested and the results obtained are exposed. For every setup a brief description is given regarding the configuration chosen, and also the results of interest of each of the problems are shown and commented.

The procedure followed starts from the very basic simplification of the case of study. From this basis the final case will be sequentially approached by adding more features and considerations.

4.1 Initial approach

4.1.1. Geometry definition

Considering the basic case definition and the operating conditions already provided, the initial approach to the case will be composed by a *2D* geometry representing the control volume of interest as a fluid surface. This initial geometry is formed by a rectangle, the sides of which measure *10* nozzle diameters and *20* nozzle diameters (*30* and *60 mm* respectively), and it is defined by means of the software DesignModeler. The nozzle is placed in the middle of the smallest side, as can be seen at the left part of the following image.

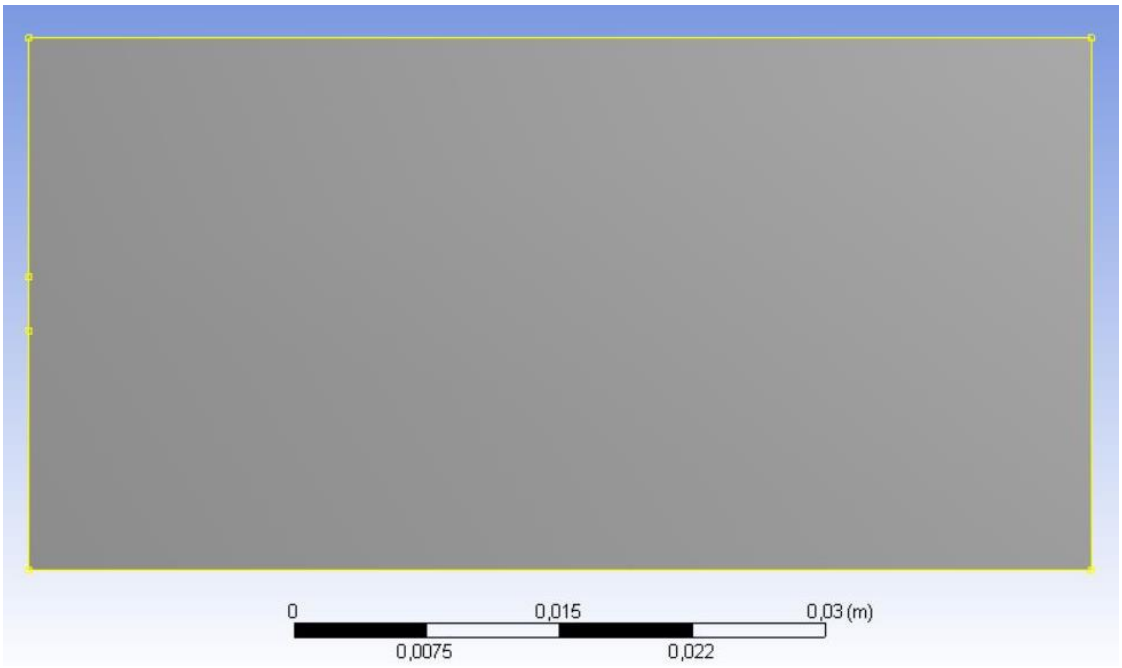

Figure 2: Geometry of the initial approach.

In order to define the boundary conditions of the control volume, the different surfaces have been identified and tagged so that they can be easily recognised:

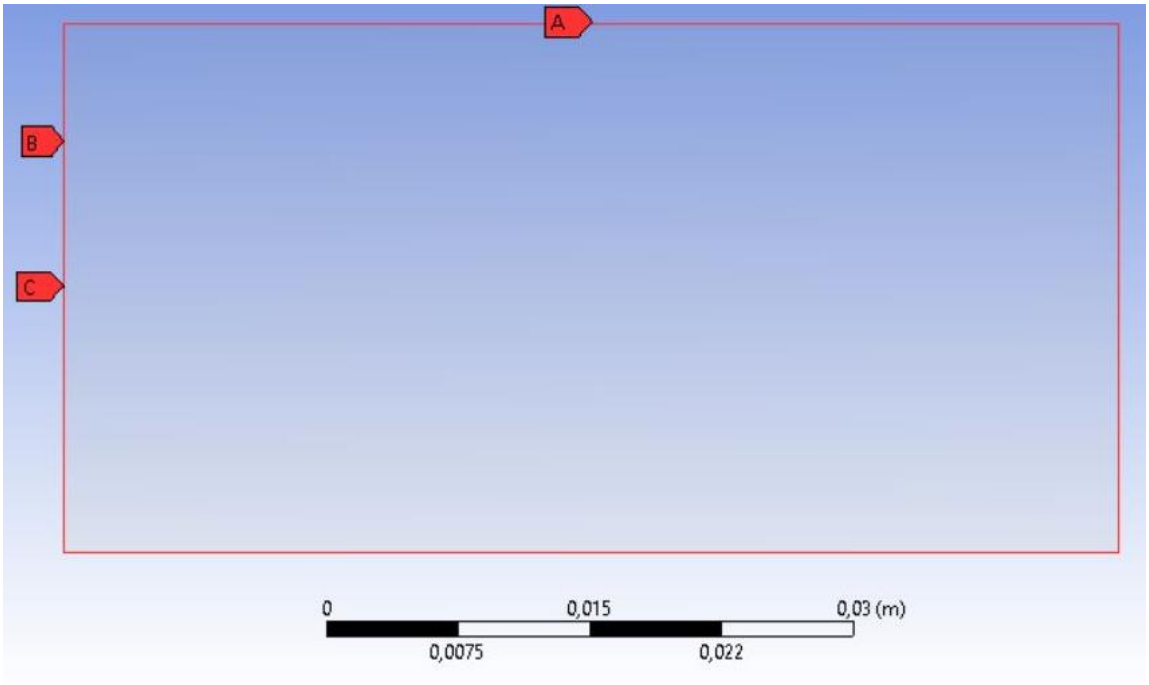

Figure 3: Surfaces of the volume. *A* represents the outlet boundary condition, while *B* stands for the wall condition, and *C* for the inlet.

4.1.2. Meshing

In order to analyse the problem through ANSYS Fluent, it is necessary to define the geometry and mesh it properly, finding an equilibrium between the convergence of the solution and the quality of it, and the time it takes for the calculation to be completed. Both the quality of the solution and the time to achieve it will increase with the quality of the mesh, so it is necessary to arrange an acceptable compromise between them. The mesh configuration chosen is the one suggested by default by the program, but modifying the following fields:

Parameter	**Value**
Size Function	Curvature
Max Face Size *[m]*	$1.2 \cdot 10^{-4}$
Min Size *[m]*	$1.2 \cdot 10^{-6}$
Smoothing	High

Table 3: Meshing settings.

The outcome of the mesh settings can be seen in the figure:

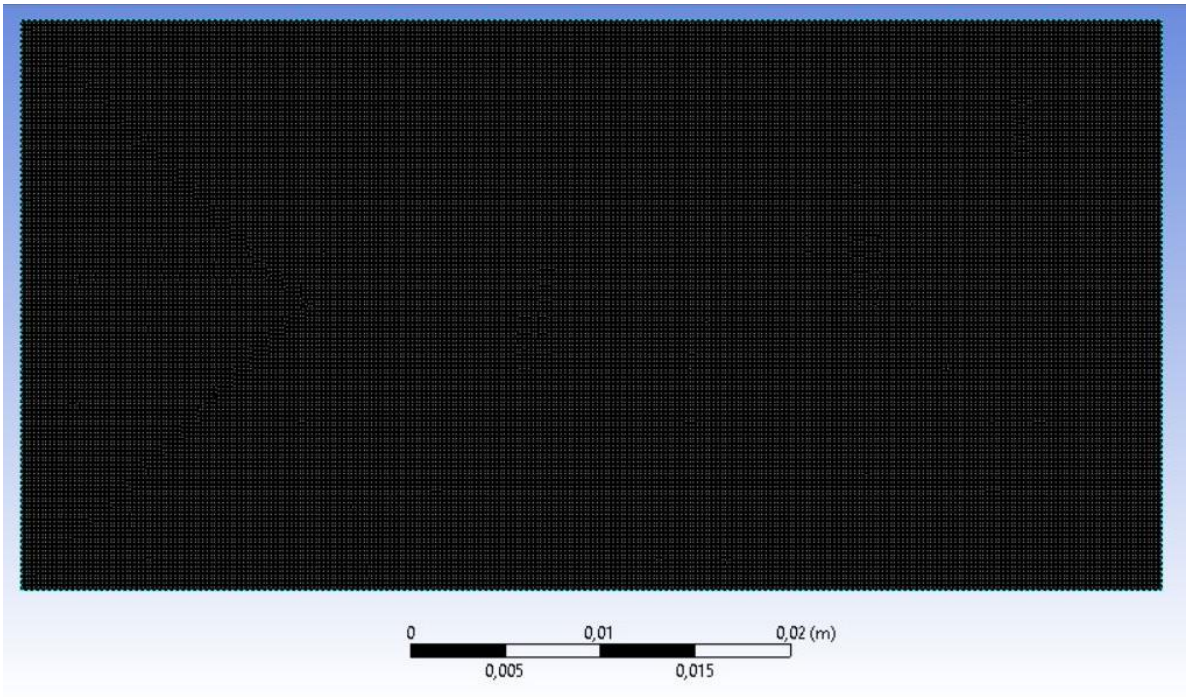

Table 4: Meshed geometry.

As it can be seen, the mesh has a large number of elements, but as it will be tested during the calculation, and considering the fact that, so far, it is a *2D* domain, the computational cost is not very large since the solution is found considerably fast. Besides the computational cost for the meshing process is low as well, due to the regularity and simplicity of the geometry.

4.1.3. Case setup

The configuration chosen in ANSYS Fluent in order to analyse the problem is the one stated below. Those sections belonging to the Fluent setup that are not mentioned remain as given by default by the program.

4.1.3.1. General

In this section the type of solver has been set as density-based (ideal for supersonic cases) and absolute as for the velocity formulation. The approach timewise chosen has been steady.

4.1.3.2. Models

Only energy and viscous models are enabled, choosing the inviscid option for the second one.

4.1.3.3. Materials

Though the ANSYS Fluent database, argon has been added to the materials library, and set as an ideal gas, in the "fluid" subsection.

4.1.3.4. Cell zone conditions

Argon has been set as the element composing the fluid control volume.

4.1.3.5. Boundary conditions

Bearing in mind the volume surfaces scheme previously shown and the operating conditions, the following settings have been applied.

a. **Inlet**. It has been defined as a "pressure-far-field" inlet with a Gauge pressure of *11999.99 Pa* and a Mach number equal to *1*.
b. **Outlet**. Set as a "pressure-outlet" with a Gauge pressure equal to 10^{-12} *Pa* (this value has been chosen in order to avoid entering *0*, and solving this way a Fluent warning when calculating the solution).
c. **Wall**. The boundary condition type in this case is "wall", with no further modifications.
d. **Interior**. Set as "interior".

In the option "Operating Conditions..." the operating pressure is set to 0.01 Pa in order to match the original requirements of the case.

4.1.3.6. Solution: Monitors

In this section, the convergence limit has been set for all the residuals to drop under the value on 10^{-6}, assuming this way a conservative approach to the solution. Even though the optimal case would be that all the residuals dropped to a final value lower than 10^{-6} (which would imply that the calculated solution can be considered as constant along the iterations performed from that point, so it is have converged) it is also necessary to monitor the convergence of a determined parameter in order to guarantee the convergence of the solution. The chosen parameter for this project is the mass flow rate, stating that when the registered mass flow rate through the outlet equals the one in the inlet, the solution can be considered as converged.

Therefore in the subsection “Report Files” these two parameters need to be set so that the program registers them.

4.1.3.7. Calculate

The number of iterations is set to *10000*. In case the convergence criteria is achieved before performing such number of repetitions, the calculation will automatically stop.

4.1.4. Solution

The solution found by means of the settings previously stated will be illustrated through the contour plots of static temperature, velocity magnitude, density and static pressure.

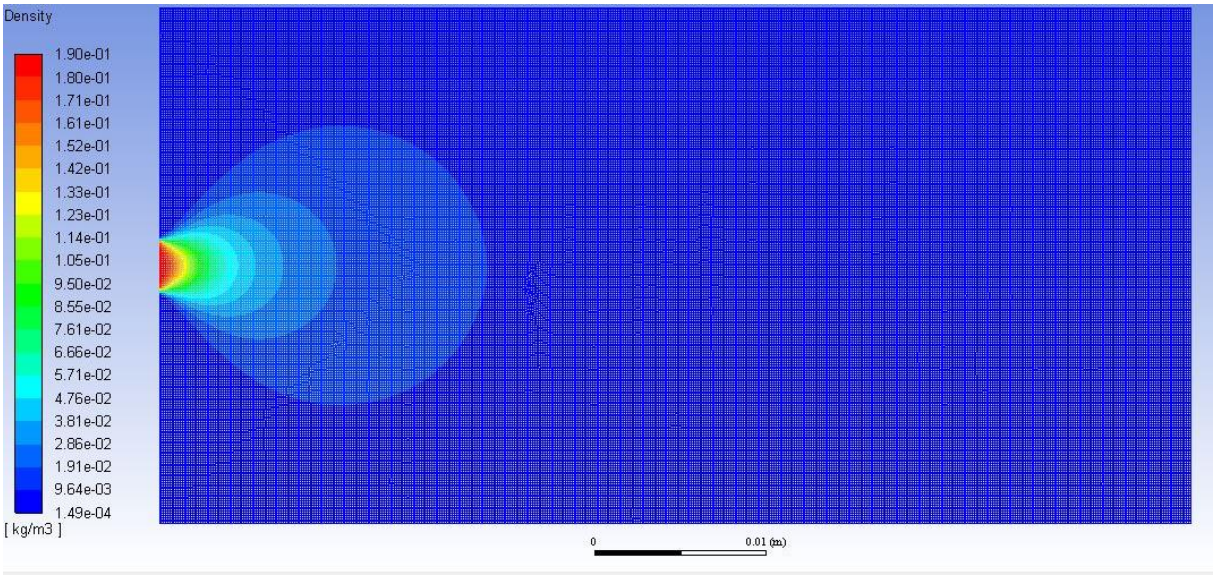

Figure 4: Density evolution along the domain.

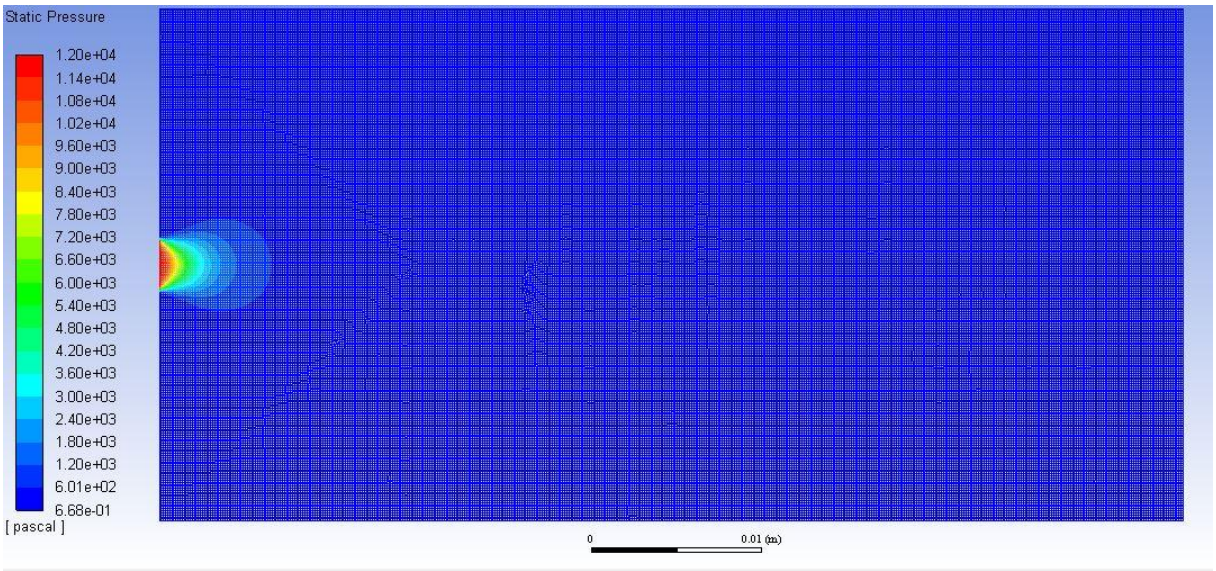

Figure 5: Static pressure evolution along the domain.

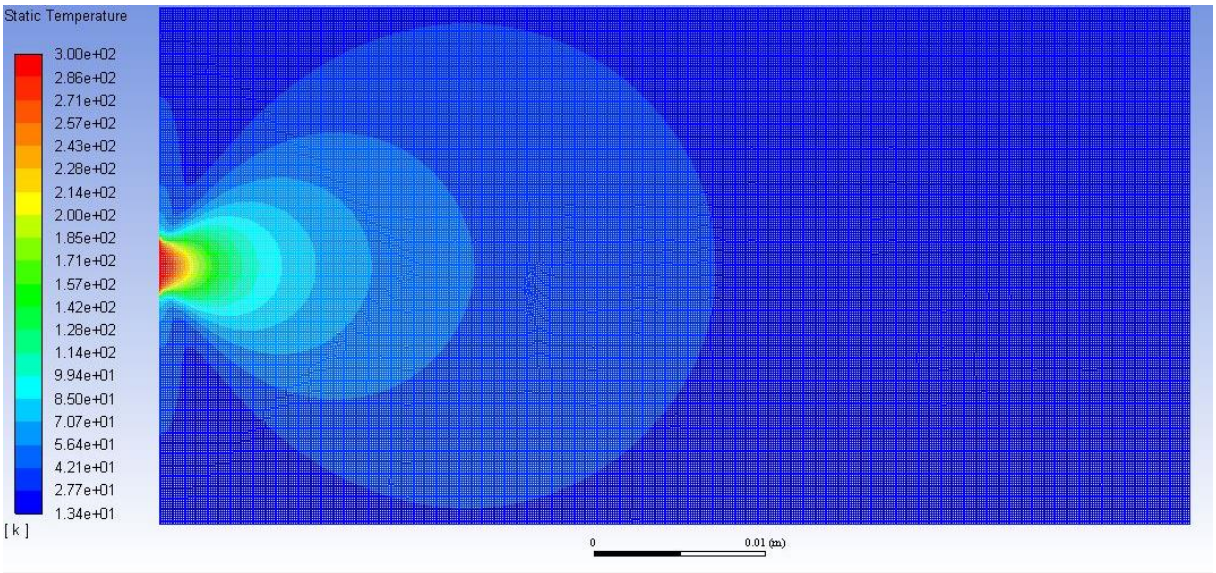

Figure 6: Static temperature along the domain.

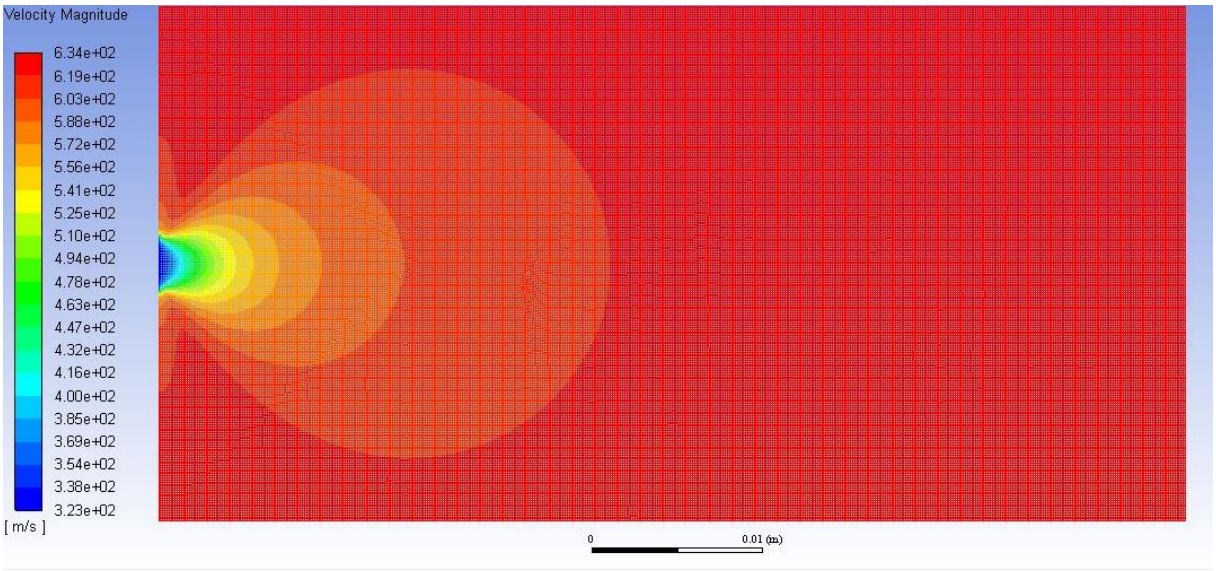

Figure 7: Velocity magnitude evolution along the domain.

These results have been achieved once the mass flow rate comparison between inlet and outlet resulted equal. Besides, the residuals evolution is also satisfactory.

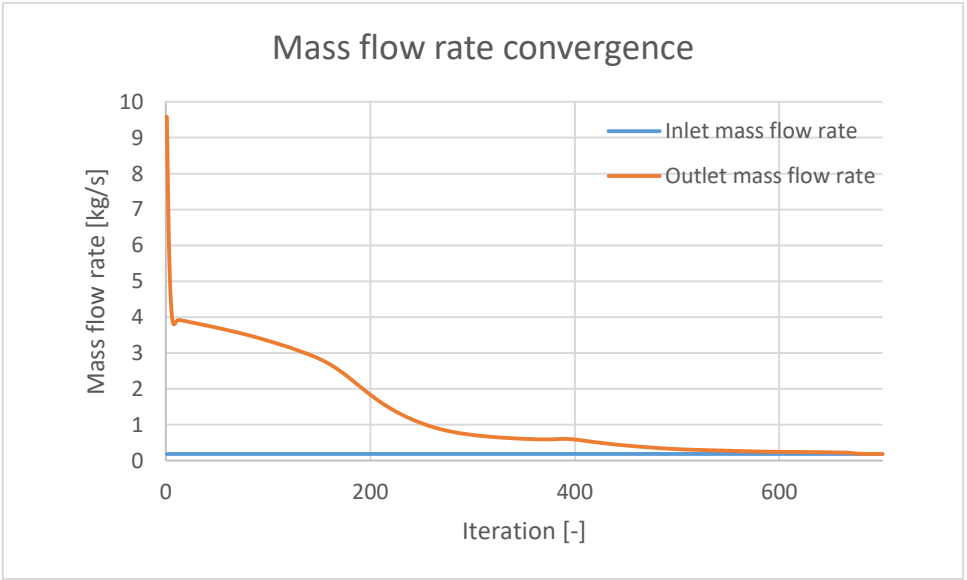

Figure 8: Mass flow rate convergence.

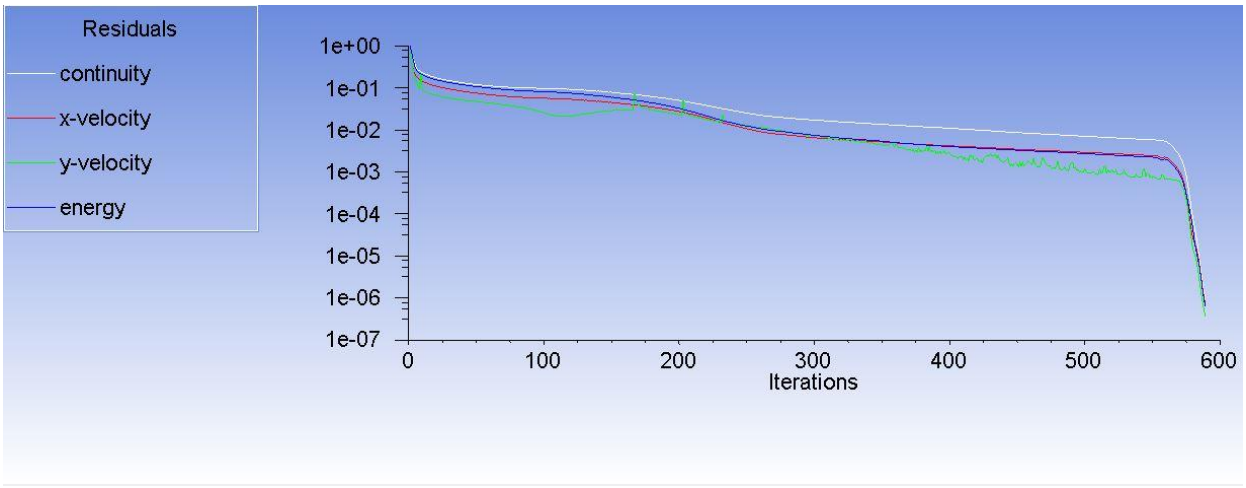

Figure 9: Evolution of the residuals.

As expected, the flow expands along the direction of the jet axis (horizontal direction from the nozzle exit), increasing the velocity and decreasing the density.

In order to verify the results obtained, and bearing in mind the fact that the process studied is an isentropic expansion in a supersonic regime, the following relationships can be established regarding the value of some magnitudes along the jet axis, being $\gamma = 1.67$ the heat capacity ratio for argon at atmospheric temperature, T/T_0 and ρ/ρ_0 the temperature and density ratio respect to a reference point, and V_F, V_0 the final and initial velocity magnitude for the flow along the jet axis:

$$ln\left(\frac{T}{T_0}\right) = (\gamma - 1) ln\left(\frac{\rho}{\rho_0}\right) \tag{3}$$

$$V_F = \sqrt{\frac{\gamma + 1}{\gamma - 1}} V_0 \tag{4}$$

These expressions have been verified graphically, as shown in the following figures:

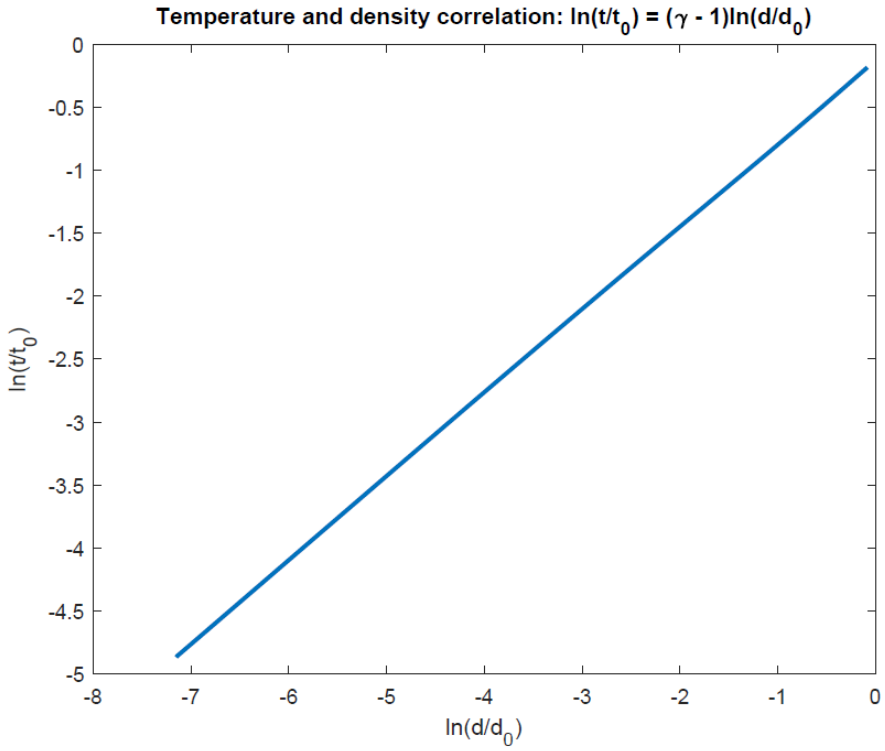

Figure 10: Verification of the velocity magnitude tendency along the jet axis.

It is verified that the relationship between the logarithms of the ratios of density and temperature with respect to a reference point describe a straight line with slope equal to $\gamma - 1$. Furthermore, and as it can be seen in the following image, the final value of the velocity magnitude along the axis also converges to the final value estimated through the theory:

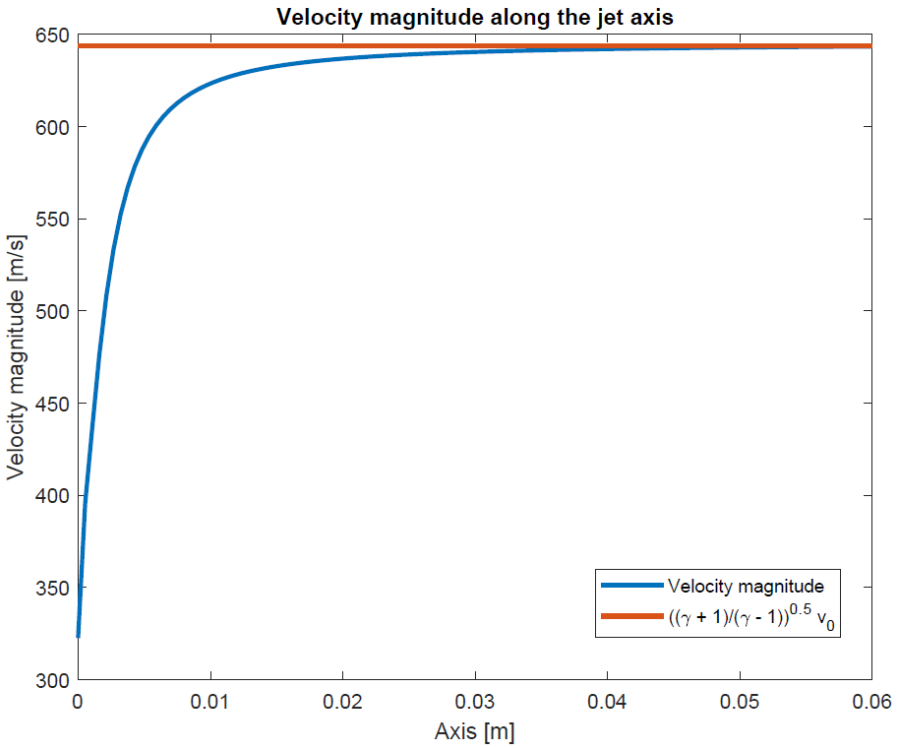

Figure 11: Verification of the velocity magnitude tendency along the jet axis.

The errors obtained when comparing the values of γ and V_F provided by the calculations and the ones given by the theory are the following ones:

Solution error	
ε_{VF}	$0.0658\ \%$
ε_{γ}	$0.8338\ \%$

Table 5: Error of the solution.

Therefore, the first solution approximation obtained can be assumed as valid. This will be the base point from where future calculations will be developed.

4.2 Basic *3D* approach

4.2.1. Geometry definition

In this case the geometry will be analogue to the one adopted in the *2D* case: the control volume will be formed by a prism created from an $30 \cdot 30\ mm^2$ square extruded $60\ mm$ in the same direction of the axis of the jet, the inlet of which will be a circle of $3\ mm$ of diameter:

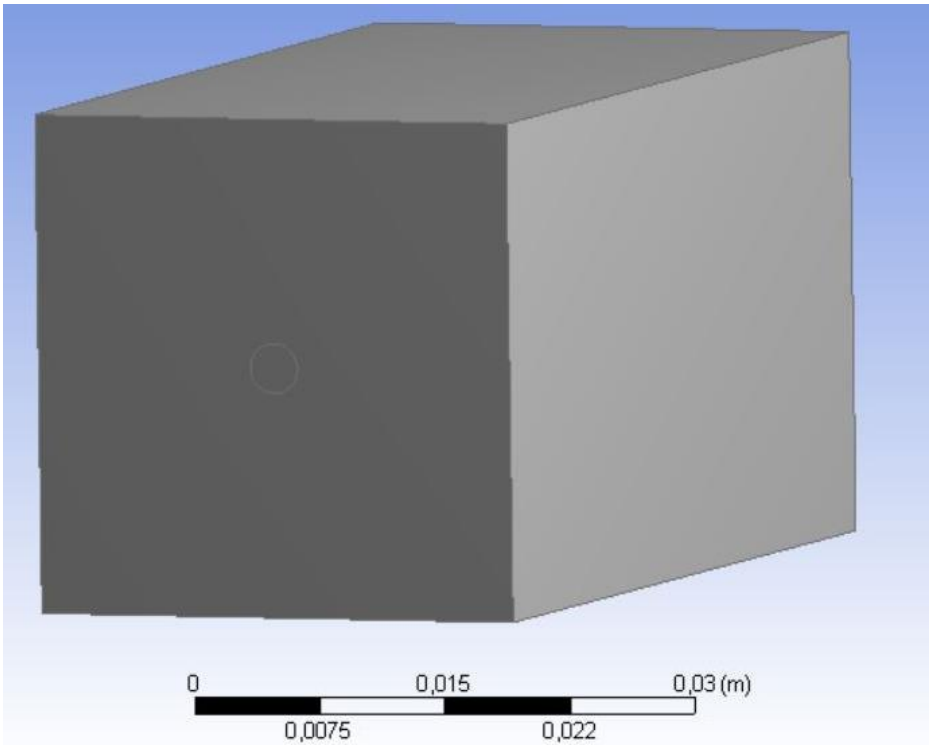

Figure 12: *3D* geometry.

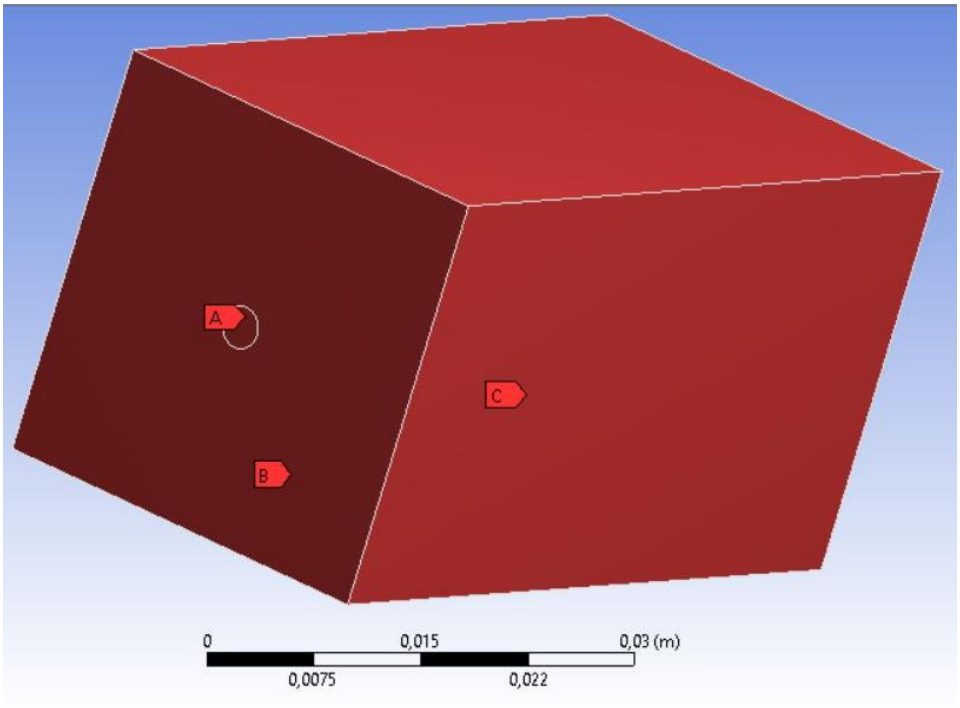

Figure 13: Surfaces of the volume. A represents the inlet boundary condition, while B stands for the wall condition, and C for the outlet.

4.2.2. Meshing

Regarding the mesh configuration, in this case the following setting has been chosen:

Parameter	Value
Size Function	Proximity and curvature
Max Face Size *[m]*	$5.36 \cdot 10^{-4}$
Min Size *[m]*	$1.68 \cdot 10^{-6}$
Smoothing	High
Assembly Method	Cutcell

Table 6: Meshing settings.

The mesh obtained under these requirements is:

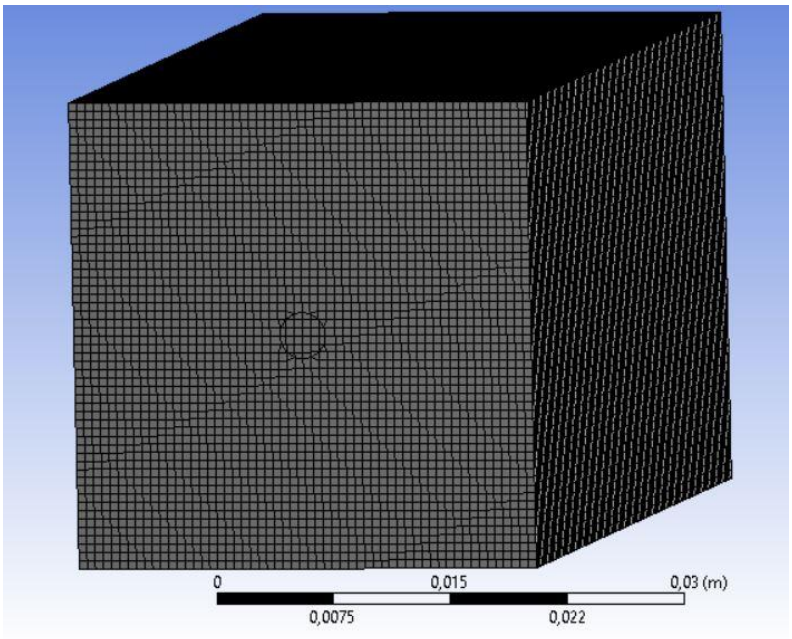

Figure 14: Meshed 3D volume.

4.2.3. Case setup

The configuration regarding to the solution setup is completely analogue to the one previously chosen for the *2D* approach.

4.2.4. Solution

In order to visualize the results, a view similar to the *2D* case has been selected, in which the intersection of the volume with the horizontal plane along the axis is

obtained. It has also been verified that both vertical and horizontal intersections give the same contour plots, being the flow field axisymmetric.

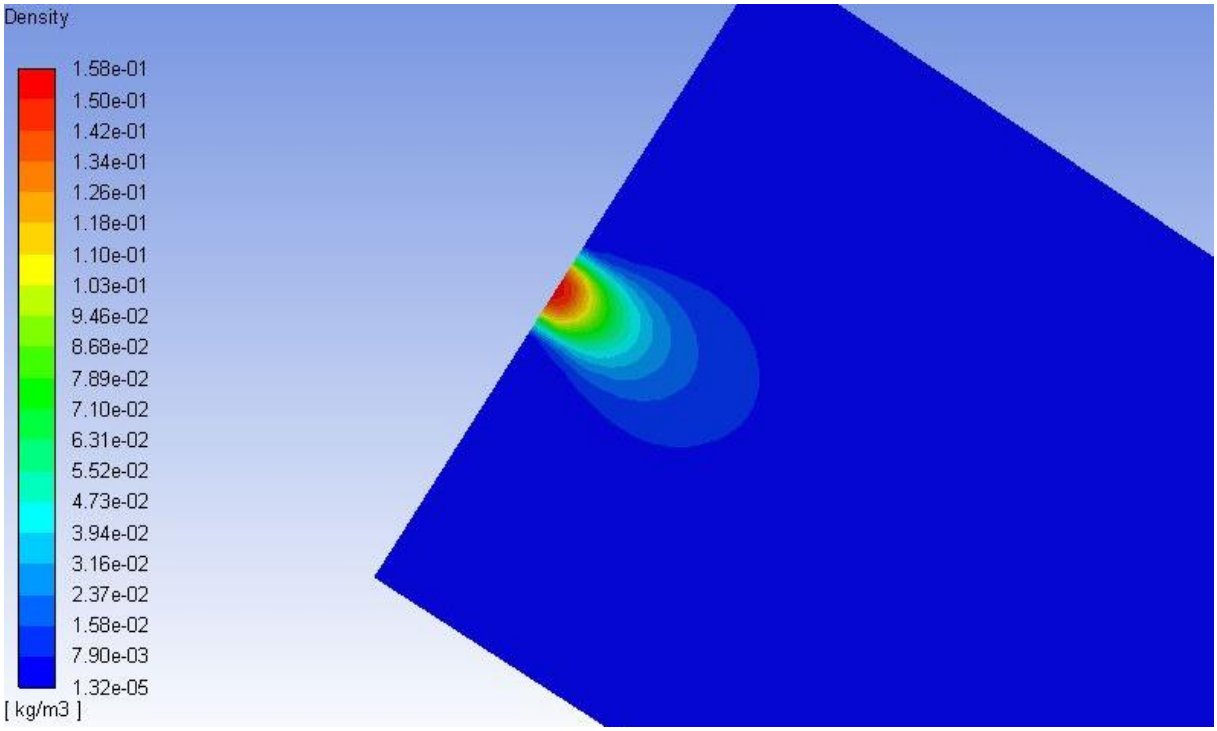

Figure 15: Density evolution along the horizontal plane in the centre of the domain.

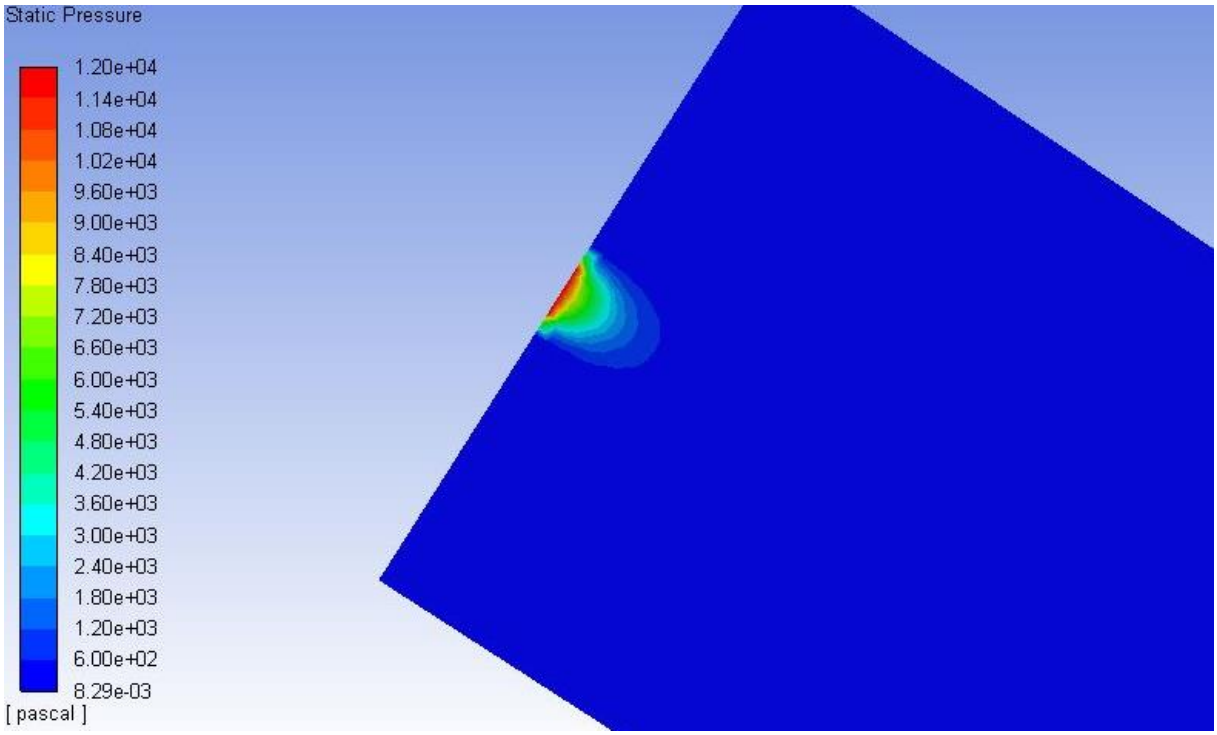

Figure 16: Static pressure evolution along the horizontal plane in the centre of the domain.

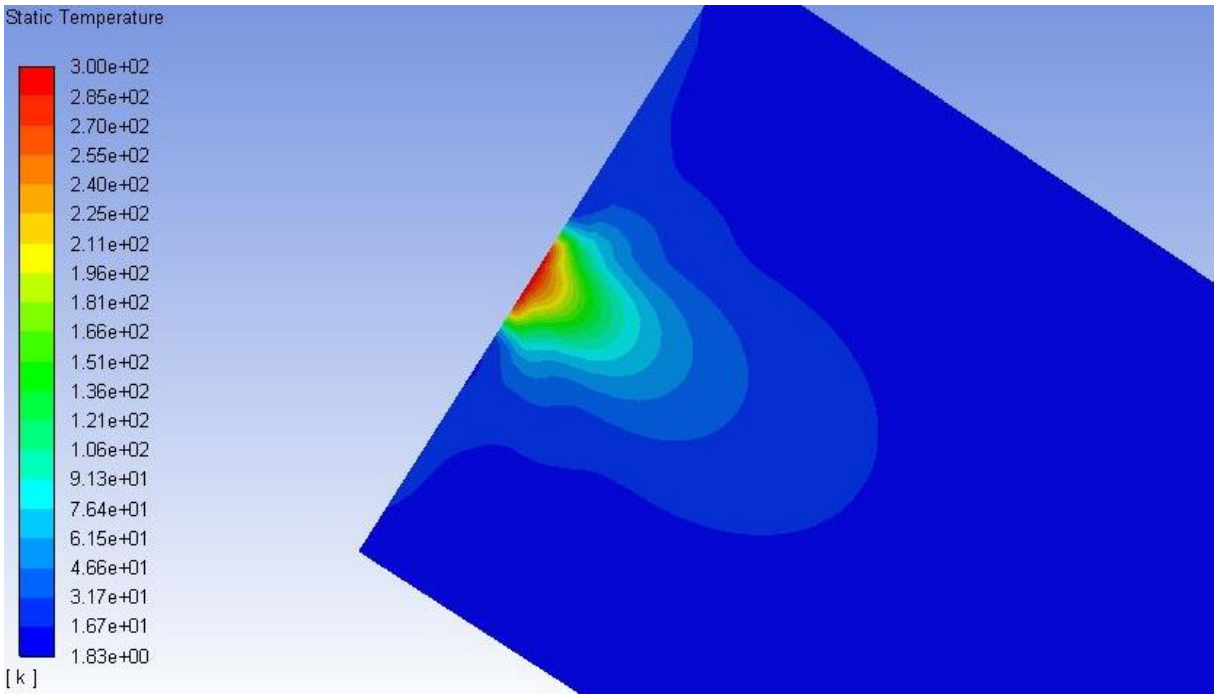

Figure 17: Static temperature evolution along the horizontal plane in the centre of the domain.

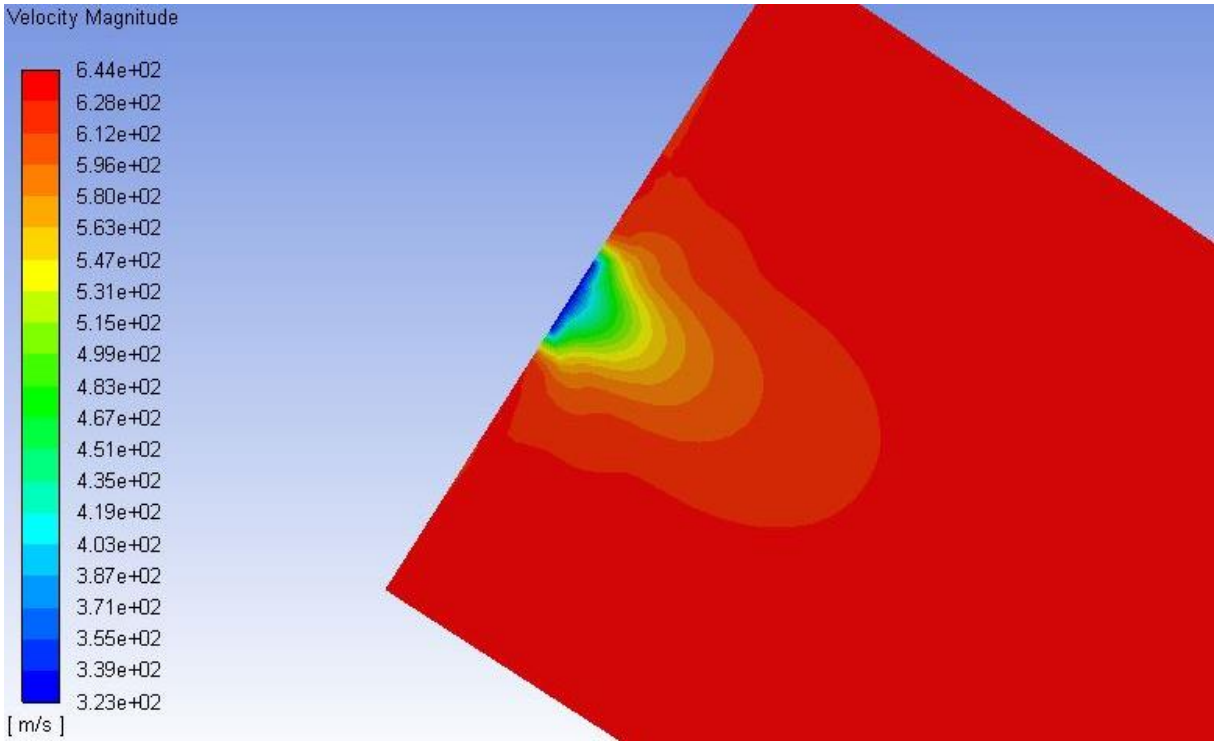

Figure 18: Velocity magnitude evolution along the horizontal plane in the centre of the domain.

As for the convergence criteria:

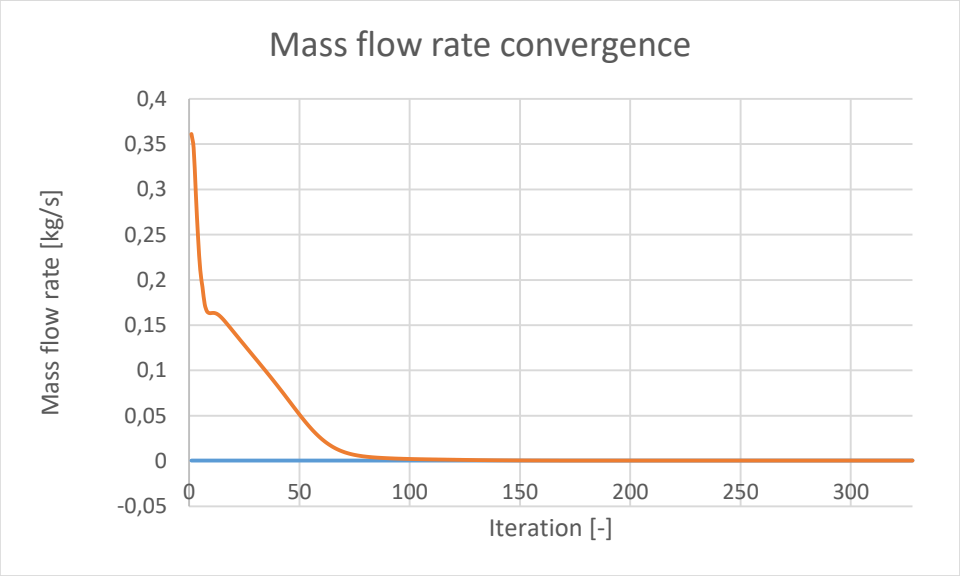

Figure 19: Mass flow rate convergence.

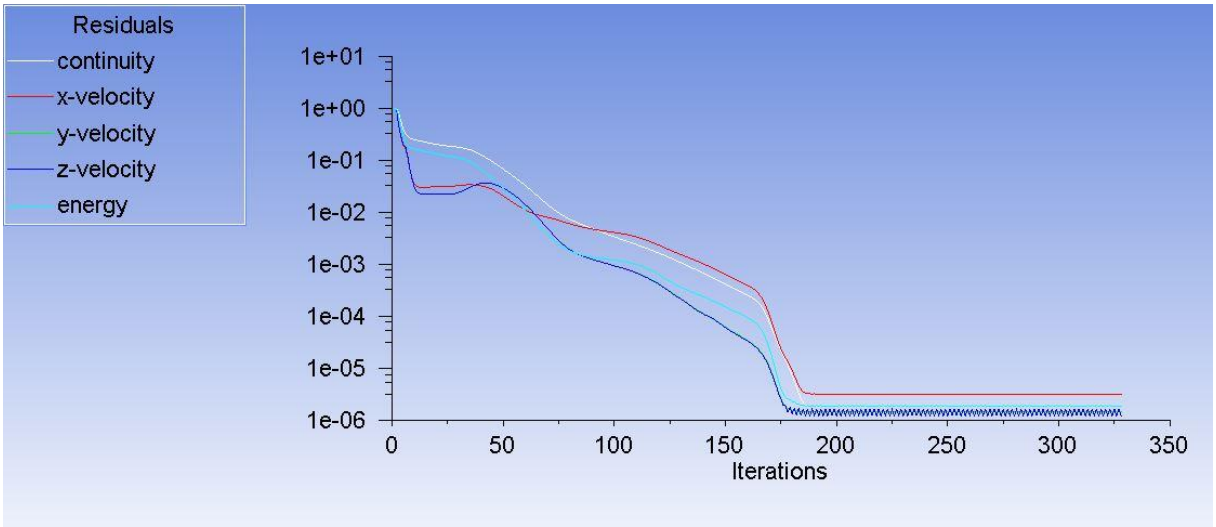

Figure 20: Evolution of the residuals.

By applying the same verification method for the obtained results as in the *2D* approach, the graphical correlations are the ones shown below:

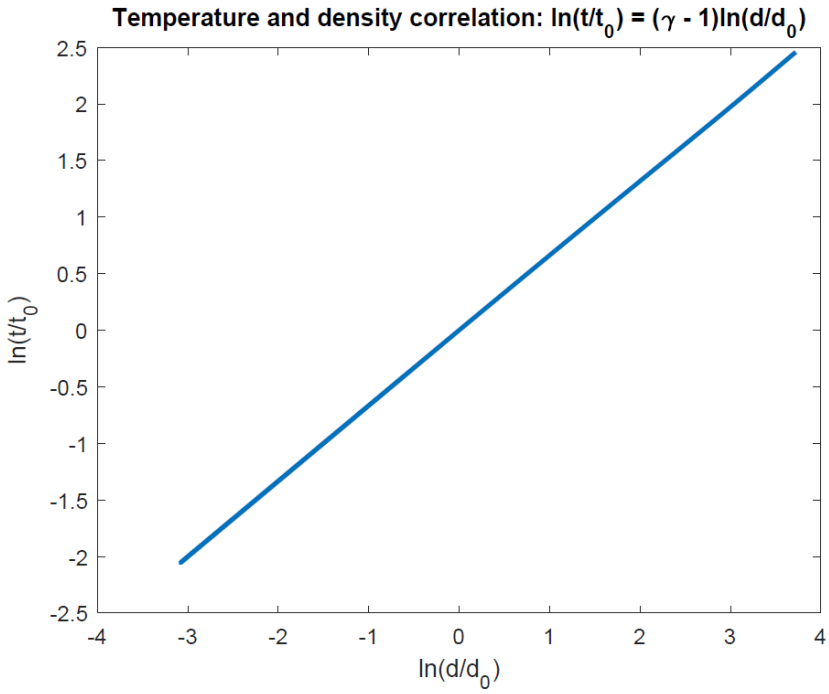

Figure 21: Verification of the temperature and density correlation for the *3D* case.

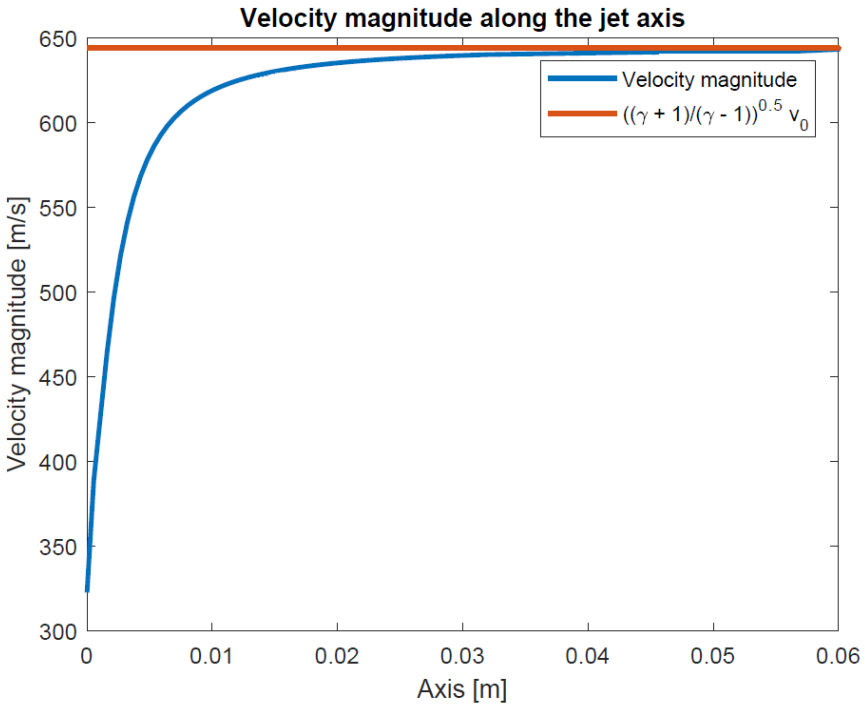

Figure 22: Verification of the velocity magnitude tendency along the jet axis for the *3D* case.

The magnitude errors in this case would be:

Solution error	
ε_{VF}	*0.1262 %*
ε_{γ}	*0.8441 %*

Table 7: Solution errors for the *3D* case.

The heat capacity ratio error has slightly increased, and the final velocity error is twice the one obtained comparing to the results of the *2D* case, but both of them can be still considered as small, therefore this approach to the case can be considered as valid.

4.3 Double inlet approach

4.3.1. Geometry definition

The final design would hold a set of circular inlet nozzles with the characteristics defined for the single nozzle of the previous approach. For this reason, the next step is redefining the control volume with two identical circular inlets, which will keep a diameter of *3 mm* each with a gap of one diameter among them. In this case the prism will be generated by a *60 mm* extrusion of a $36 \cdot 30\ mm^2$ rectangle. Through this configuration it is possible to obtain information about the interaction of the flow expelled by both inlets, as the distance among them is low enough for them to have an impact on each other. This approach is of interest considering the fact that, in the final setup, interaction among nozzles will take place.

As in the previous setup and in an analogue way, an overview of the geometry and the parts of the control volume is attached in the following figures:

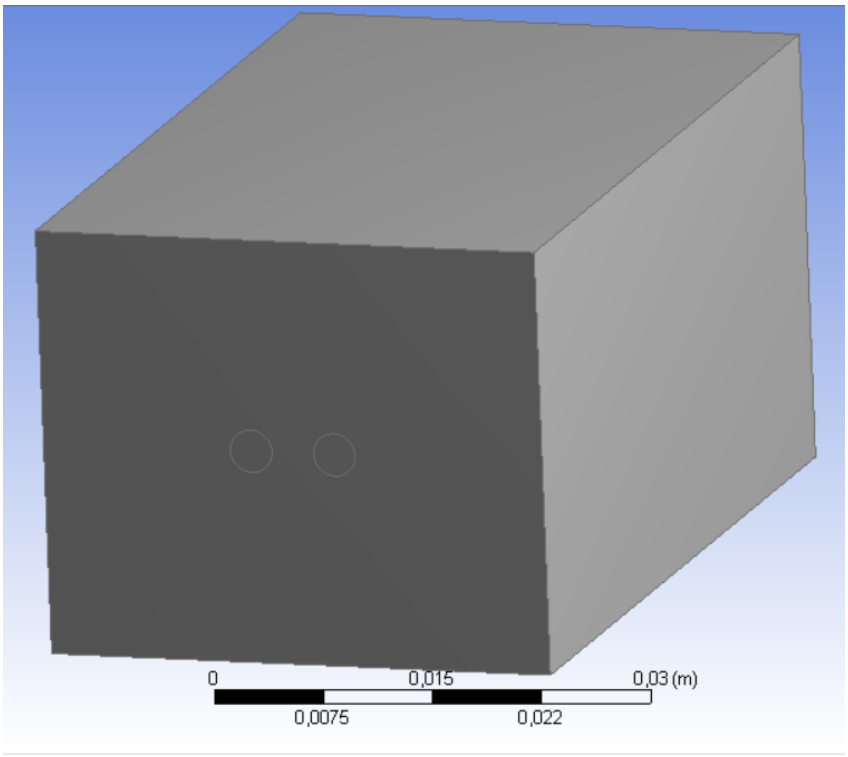

Figure 23: *3D* geometry with two inlets.

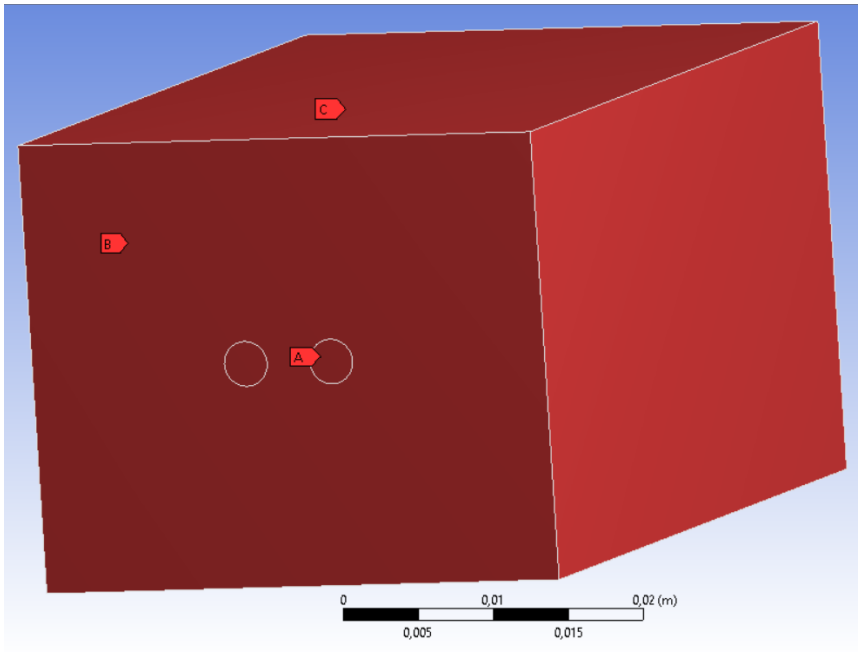

Figure 24: Surfaces of the volume. *A* represents the inlet boundary condition, while *B* stands for the wall condition, and *C* for the outlet.

4.3.2. Meshing

In this case the setup of the meshing is as follows, reducing the minimum and maximum size in order to provide a more refined mesh near the inlets:

Parameter	Value
Size Function	Proximity and curvature
Max Face Size *[m]*	$5.079 \cdot 10^{-4}$
Min Size *[m]*	$6.2 \cdot 10^{-8}$
Smoothing	High
Assembly Method	Cutcell

Table 8: Meshing settings.

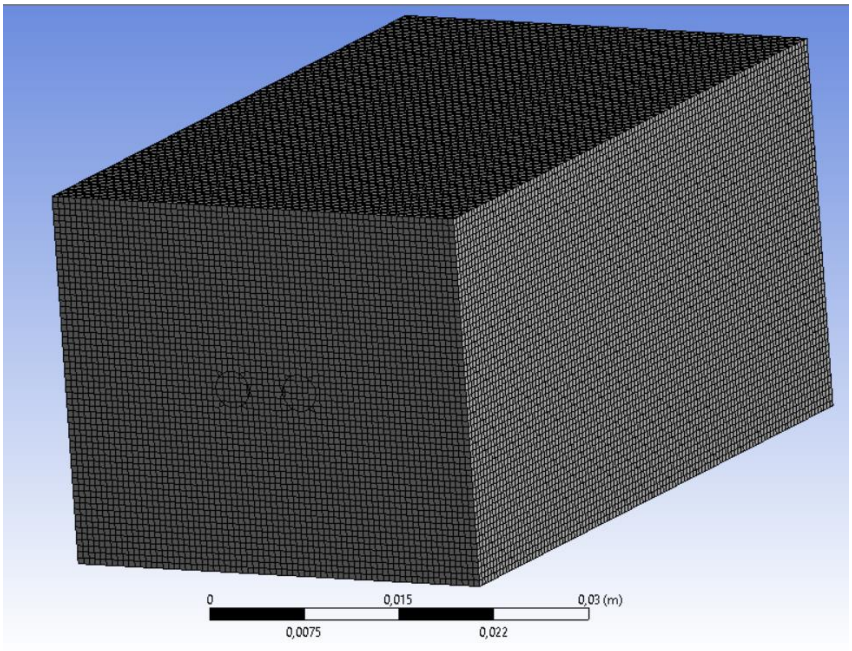

Figure 25: Meshed *3D* volume with *2* inlets.

4.3.3. Case setup

The case setup is exactly the same as the one chosen for the *3D* case with one single inlet.

4.3.4. Solution

As in this case there is an interaction between the two inlets flows that causes a discontinuity, the inviscid model is not valid for obtaining a converged solution through the ANSYS Fluent software as it can be observed in the solution residuals track, even though from the theoretical point of view this case fits in this category.

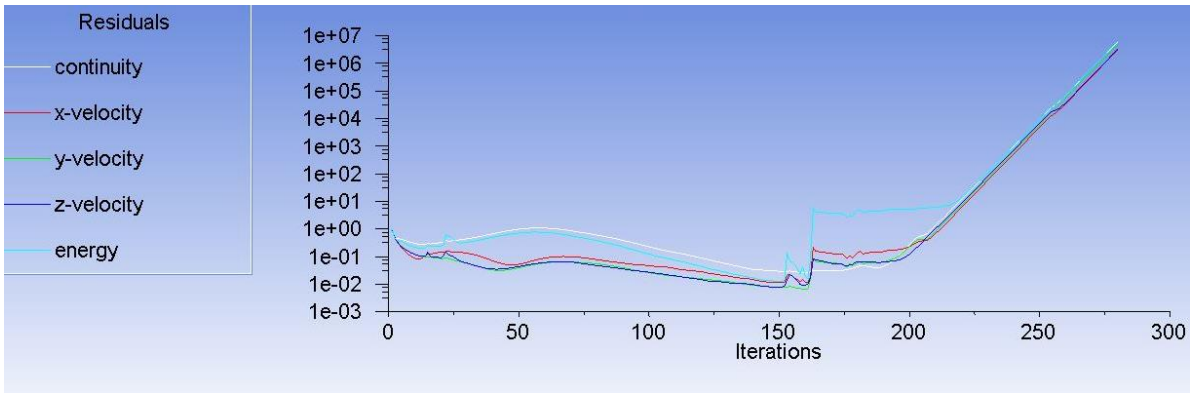

Figure 26: Residuals evolution: divergence for the inviscid model.

Therefore, it will be necessary to consider the viscosity in order to obtain a converged solution of the problem.

4.3.5. Solution considering viscosity: laminar fluid

The only change performed in the case setup will be the activation of the laminar model instead of choosing the inviscid option. The rest of the setup options remain as in the previous trial. With this new configuration, the obtained results are:

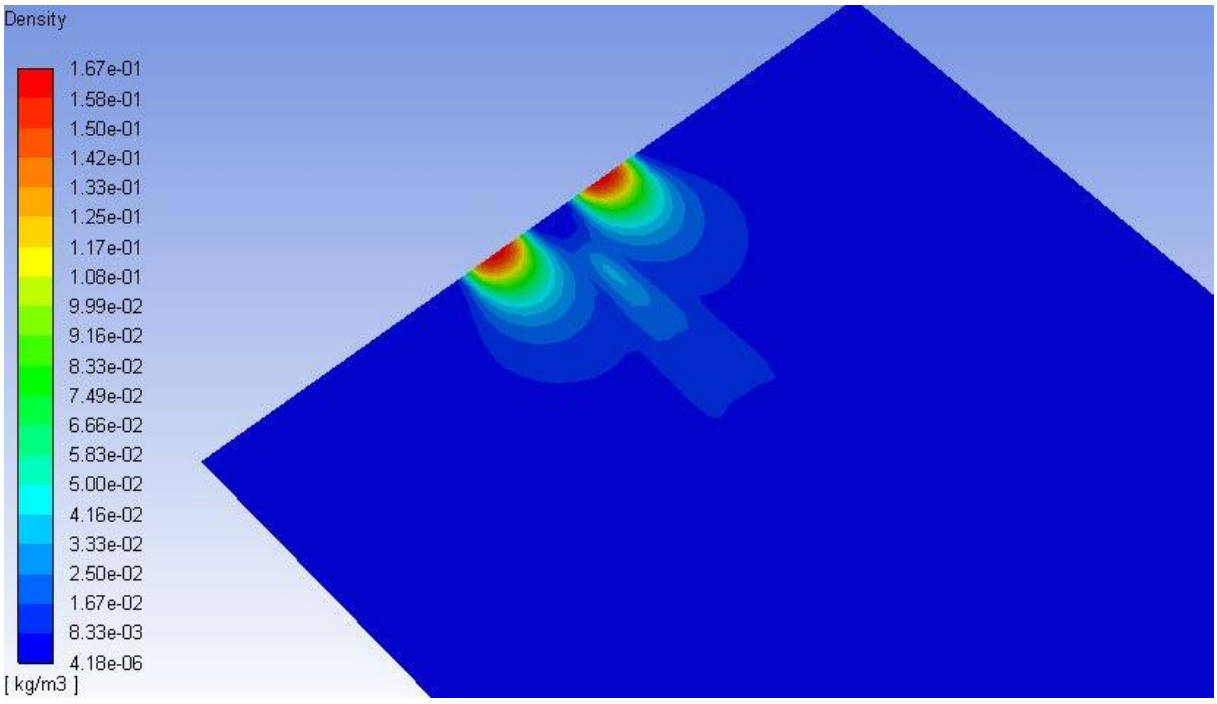

Figure 27: Density evolution along the horizontal plane in the centre of the domain.

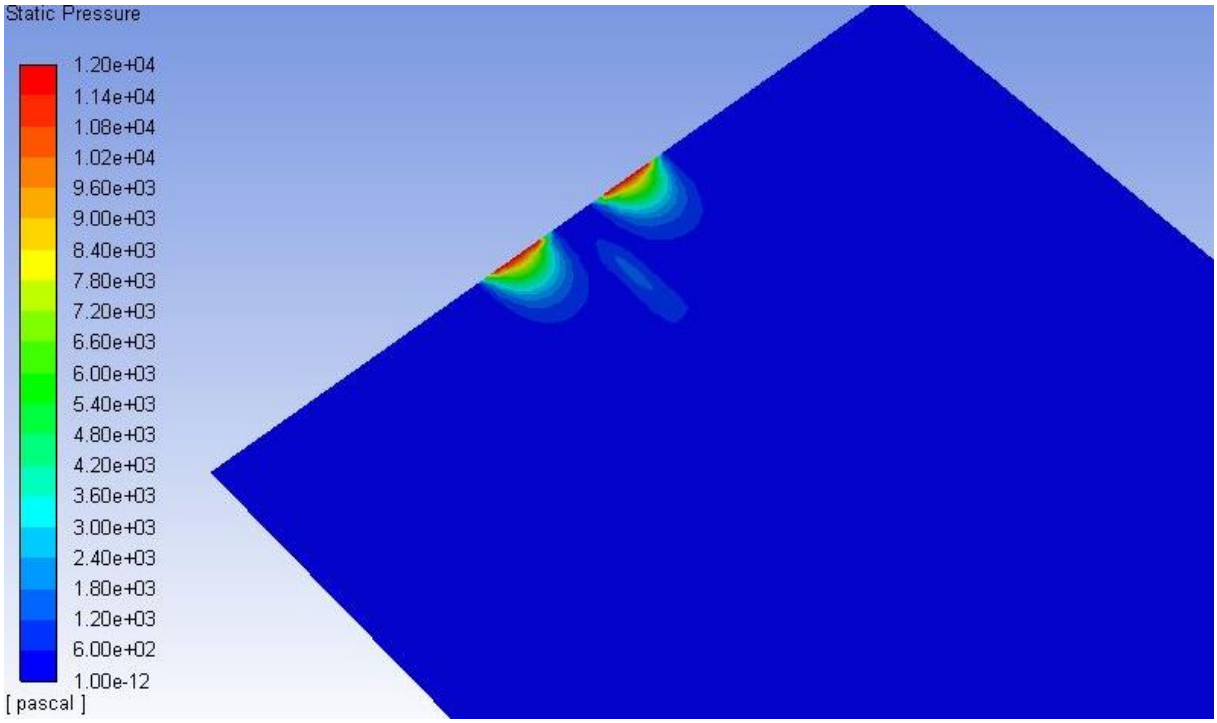

Figure 28: Static pressure evolution along the horizontal plane in the centre of the domain.

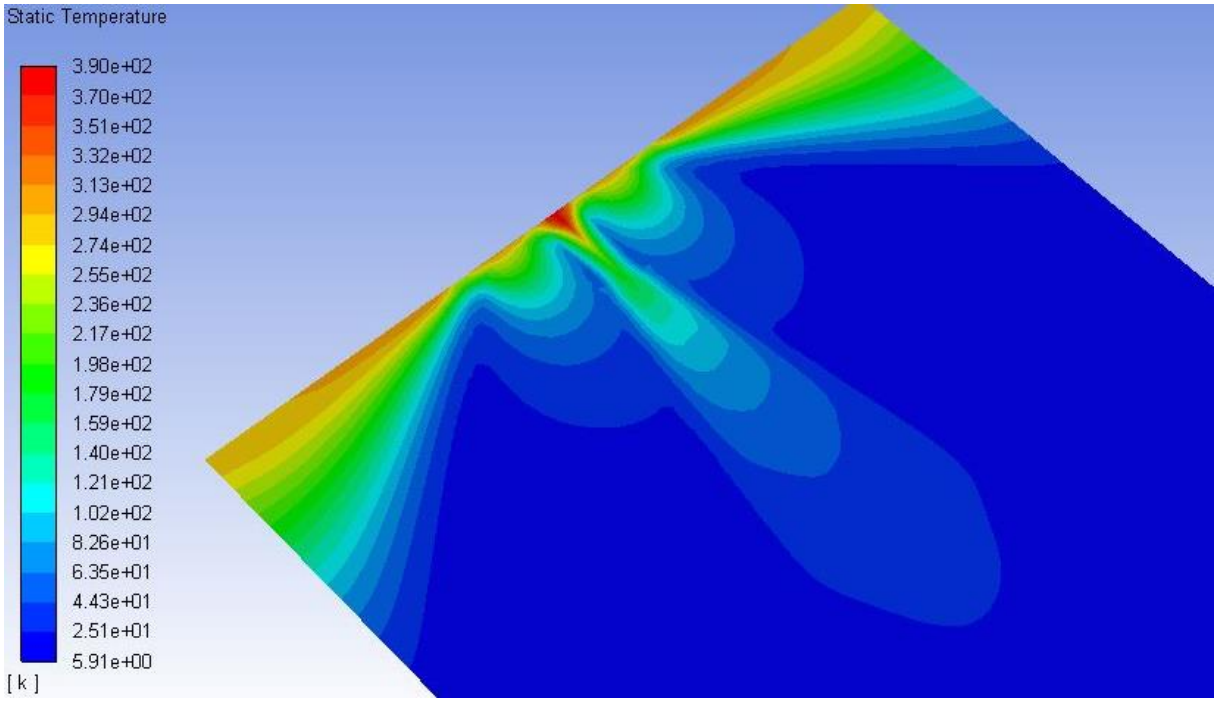

Figure 29: Static temperature evolution along the horizontal plane in the centre of the domain.

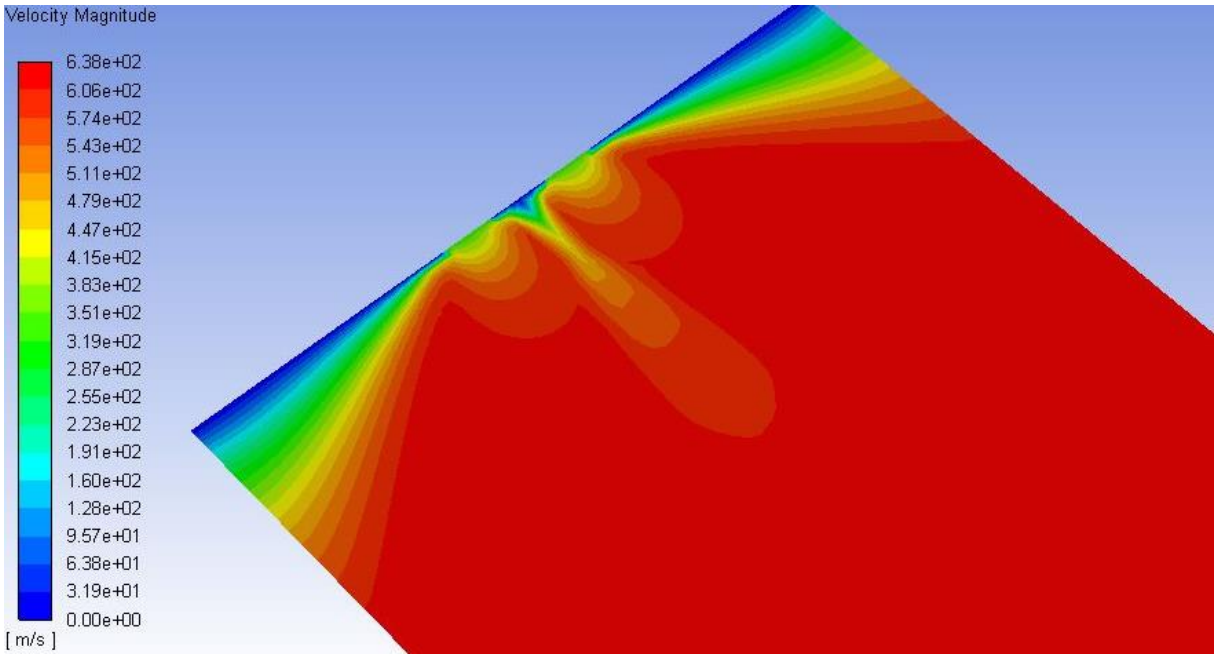

Figure 30: Velocity magnitude evolution along the horizontal plane in the centre of the domain.

It can be seen that, due to the interaction of the two nozzles, the flow properties are not constant between both inlets, proving that they are influencing each other. Nevertheless, by comparing the results of this configuration with the ones obtained for the setup with one single inlet, it is verified that even with the two inlets interaction, the flow behaviour keeps fitting the inviscid theory once it has advanced enough through the X axis from the origin. In order to visualize this property, the evolution of the density, the velocity magnitude and the static temperature along the X axis, from the centre of one of the inlets (valid for both of them as the solution is symmetrical with respect to the XY plane intersecting the origin) has been compared with the ones obtained for the single inlet case analysed by using the inviscid model in ANSYS Fluent:

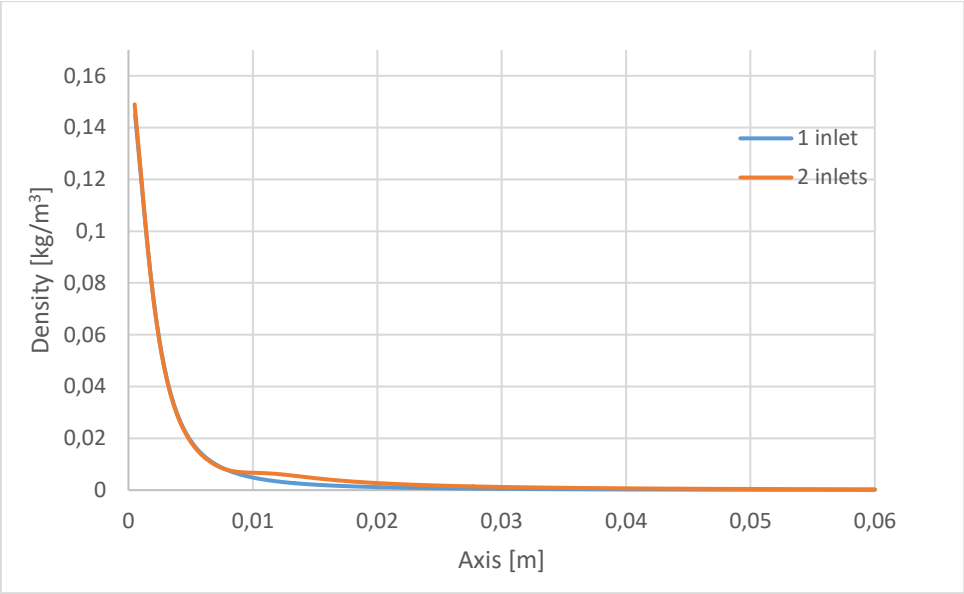

Figure 31: Comparison of the density evolution along the X axis between the one inlet model and the two inlets model.

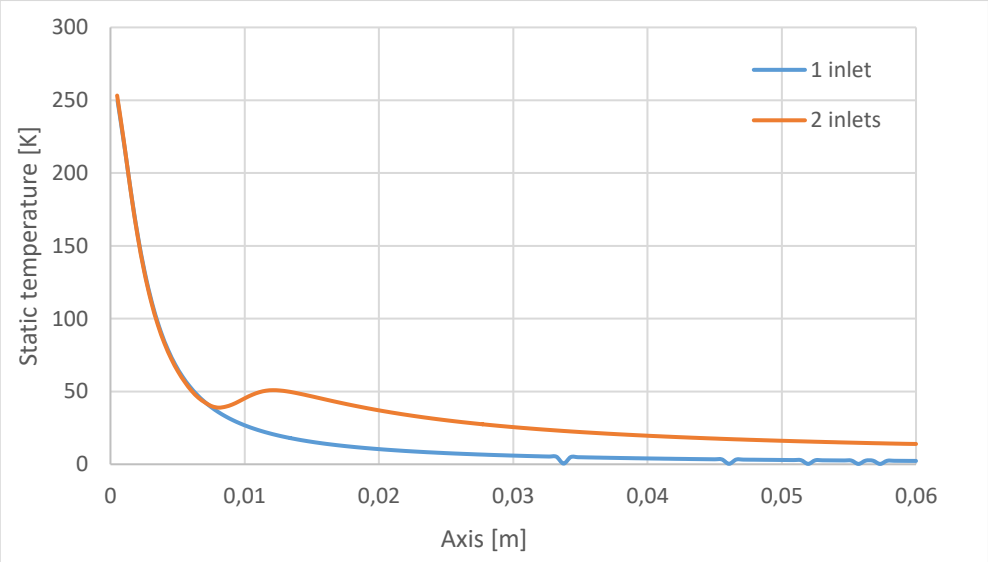

Figure 32: Comparison of the static temperature evolution along the X axis between the one inlet model and the two inlets model.

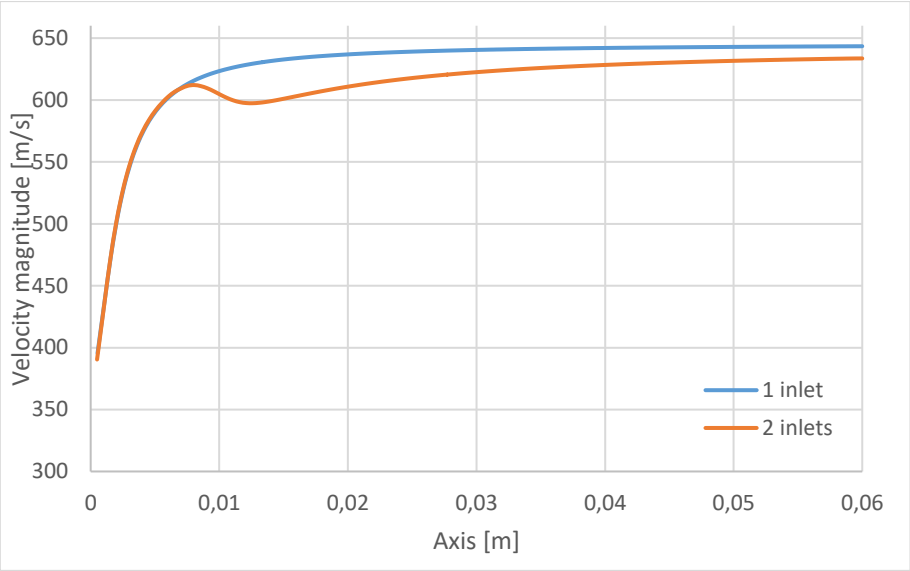

Figure 33: Comparison of the velocity magnitude evolution along the X axis between the one inlet model and the two inlets model.

It can be seen that the tendency of both solutions is the same. The main difference among them can be found at around *0.012* meters from the inlet along the X direction, where a bump appears for the two inlets case. This peak is related to the interaction between both nozzles, as it was seen in the *2D* contour plots before. Therefore it is demonstrated that, even though it has been necessary to activate a viscous model for solving the two inlet configuration, the output obtained matches the inviscid prediction, as it coincides with the inviscid solution of one inlet for the downstream flow considered to be far away from the origin (around *20* inlet diameters).

Considering the three last variables represented through the plots along the X axis, it is also seen that the final values for the parameters, especially the ones of the velocity magnitude and the static temperature, do not converge in the exact way. This is due to the interaction of the nozzles that takes place upstream.

As for the convergence of the solution:

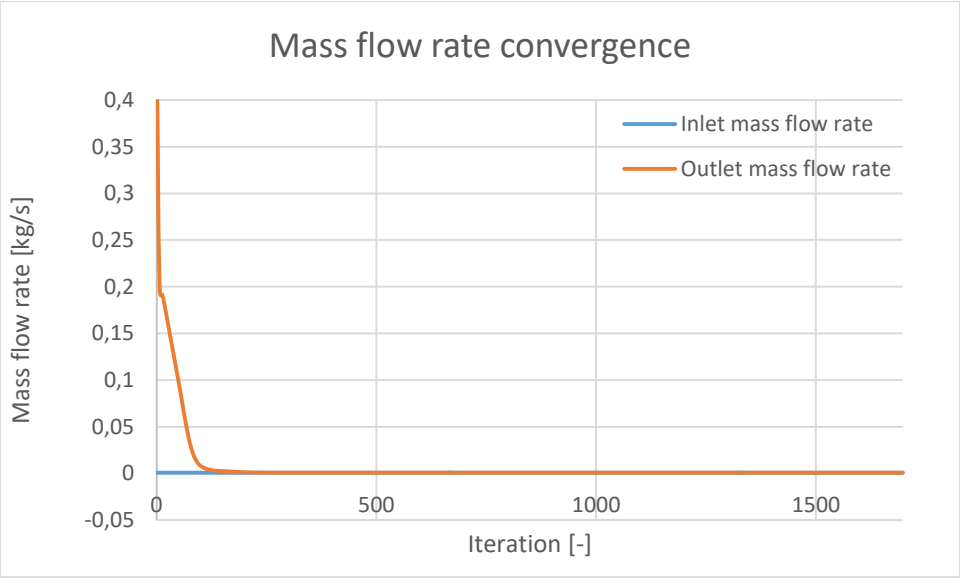

Figure 34: Mass flow rate convergence.

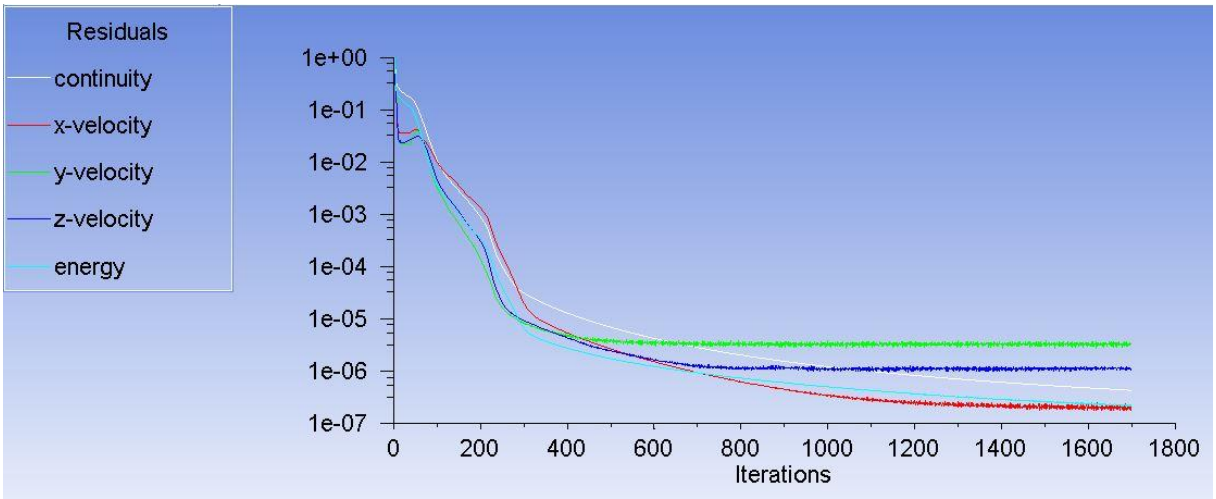

Figure 35: Evolution of the residuals.

4.3.6. Validation of the viscous model

In order to accept the viscous model solution for the two inlets configuration as valid, it is necessary to verify that this solution meets the results obtained through the inviscid consideration. As a way of verifying this statement, the initial *3D* configuration (one inlet control volume) has been recalculated through laminar viscous model. In this case the comparison among the evolution of the variables is the one defined by the following graphs:

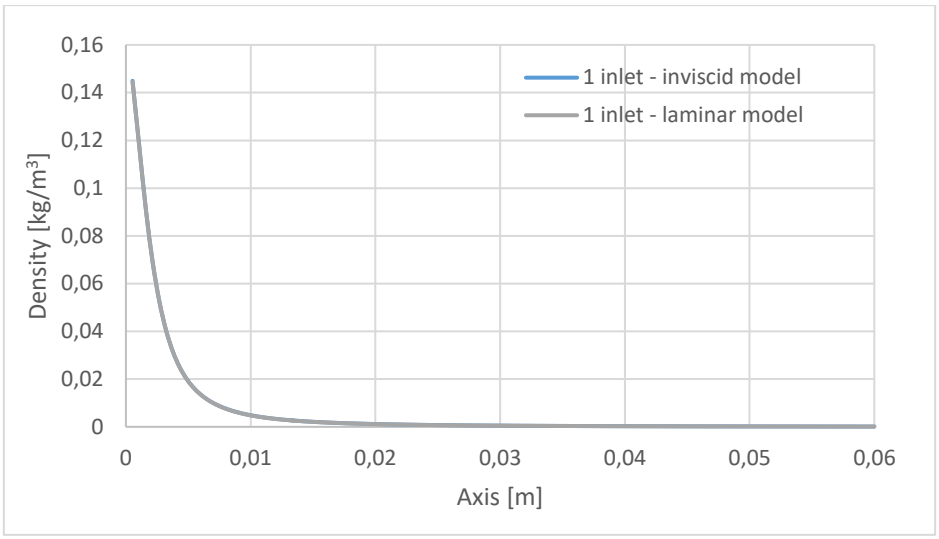

Figure 36: Comparison of the density evolution along the X axis for inviscid and laminar models.

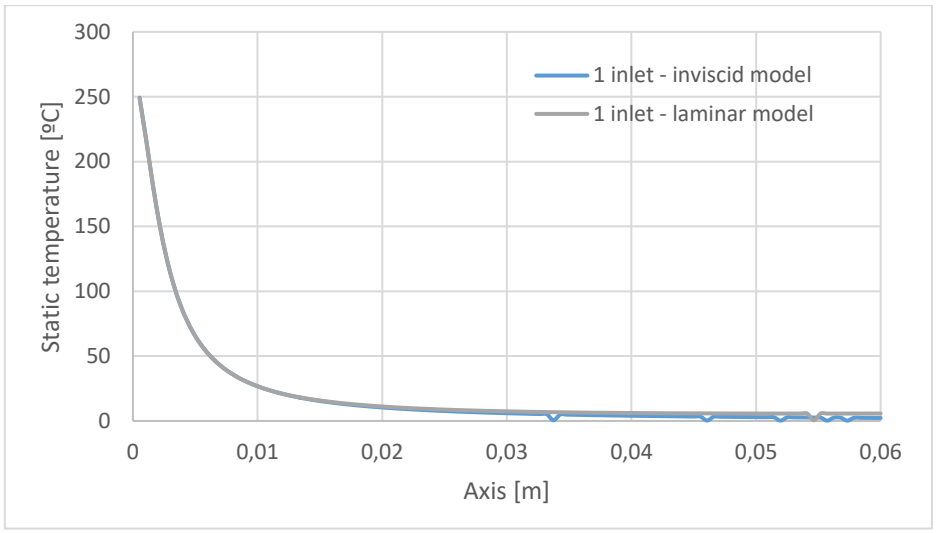

Figure 37: Comparison of the static temperature evolution along the X axis for inviscid and laminar models.

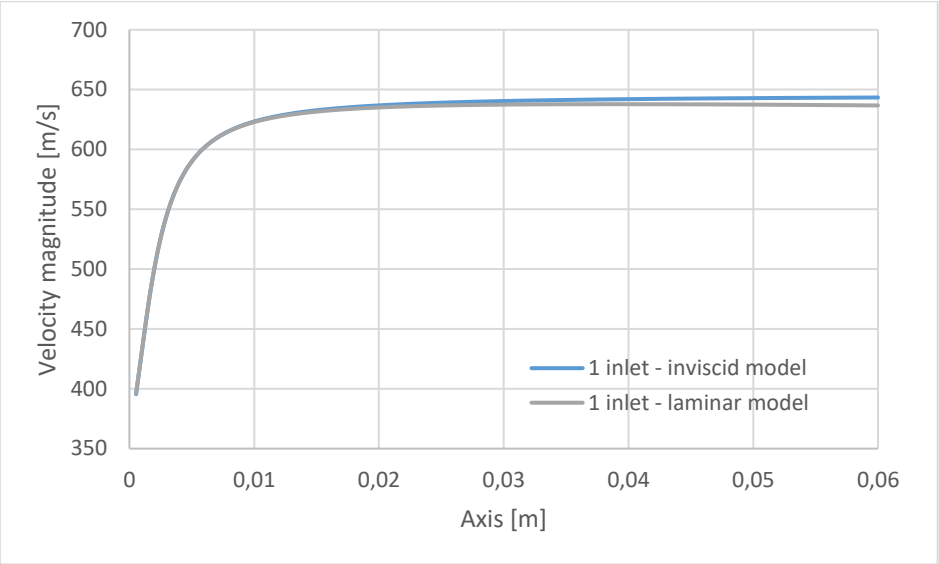

Figure 38: Comparison of the velocity magnitude evolution along the X axis for inviscid and laminar models.

The graphs above show that the results obtained through the inviscid and the viscous model converge to a quite close value, being possible to consider the viscous model solution as a valid approach to the theoretical inviscid result downstream. Therefore it is acceptable to use the laminar model for the two inlet configuration setup.

There is still a small difference between the results obtained. This difference is due to the fact that the results have not converged with the same accuracy in both calculations. Besides, the viscous model introduces some dissipation in order to reach the result, which leads to a smaller value for the final velocity magnitude than the one obtained through the inviscid consideration.

4.4 Closed volume with one inlet and one outlet

4.4.1. Geometry definition

Once all the previous verifications have been performed, the laminar model has been accepted as the one chosen for the next calculations. Regarding the geometry, it is known that the target design will be a channel of approximately *6* mm long and *100* μm wide with *30* inlets of *20* μm of diameter and *30* outlets with *30* μm of diameter. Therefore an initial evaluation is set in which the geometry is composed by a volume formed by a square of *220* μm side extruded *100* μm. In the centre of each of the extruded faces the *20* μm diameter inlet and the *30* μm diameter outlet will be placed, respectively.

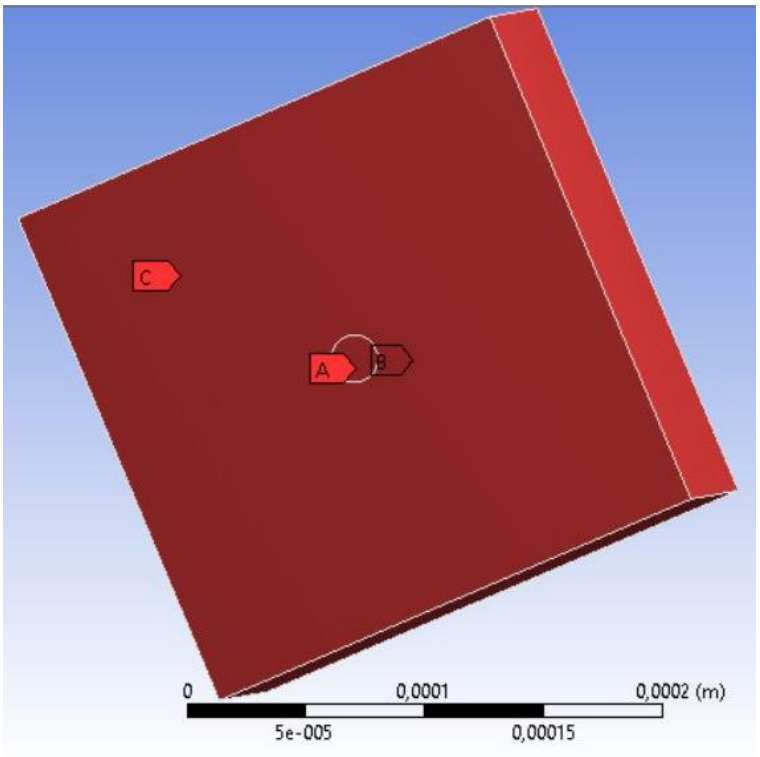

Figure 39: Surfaces of the volume. A represents the inlet boundary condition, while C stands for the wall condition, and B for the outlet.

4.4.2. Meshing

In this case the chosen setup is:

Parameter	Value
Size Function	Proximity and curvature
Max Face Size *[m]*	$2.022 \cdot 10^{-6}$
Min Size *[m]*	$7.9 \cdot 10^{-9}$
Smoothing	High

Table 9: Meshing settings.

Since the outcome of the mesh shows the same distribution as the previous ones, and considering that this structure will be kept along the following simulations, the capture of the aspect of the mesh will be omitted.

4.4.3. Case setup

The case setup is exactly the same as the one considered so far, but bearing in mind that in the new geometry the interaction of the flow with the walls increases, since there is more surface of the volume belonging to this boundary condition. Therefore it

is stated that there will be heat exchange between the fluid and the walls. In order to do that, in the thermal display of the boundary condition of wall it is set that the walls are at a standard temperature of *300 K*, with no further information is given regarding the material or the thickness.

4.4.4. Solution

In this case the parameters evolution obtained is the following one, being the upper zone the one corresponding to the inlet and the lower one the one of the outlet:

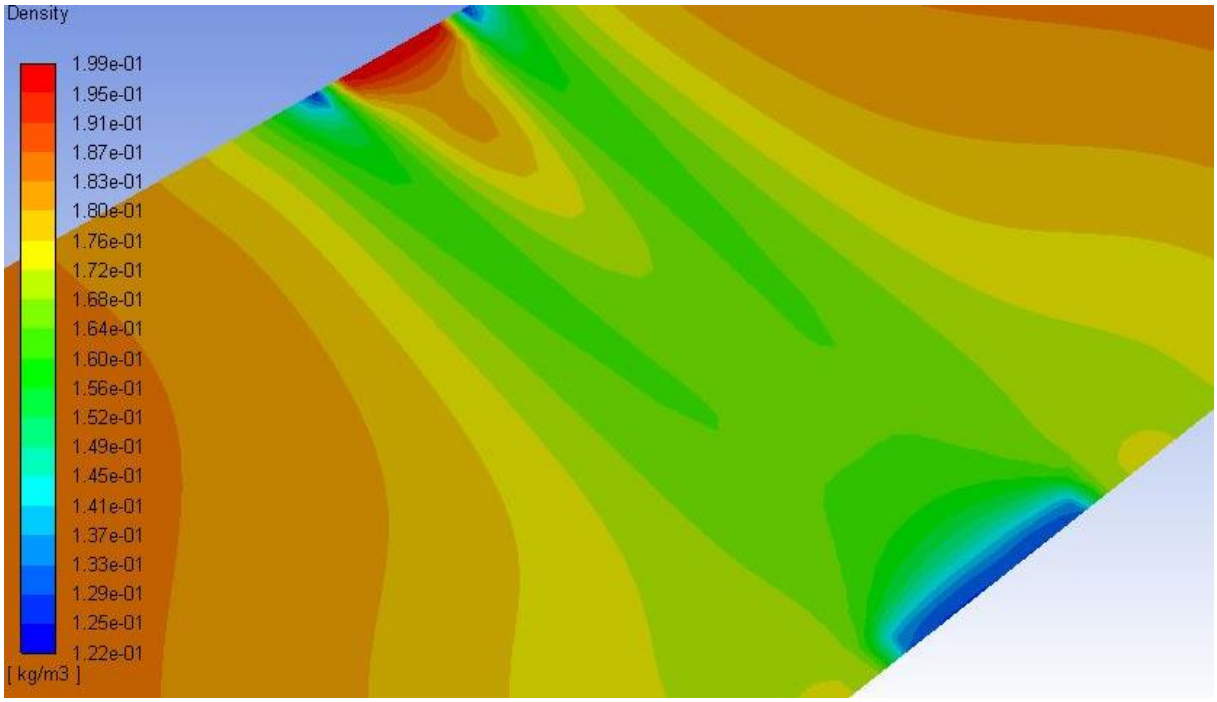

Figure 40: Density evolution along the horizontal plane in the centre of the domain.

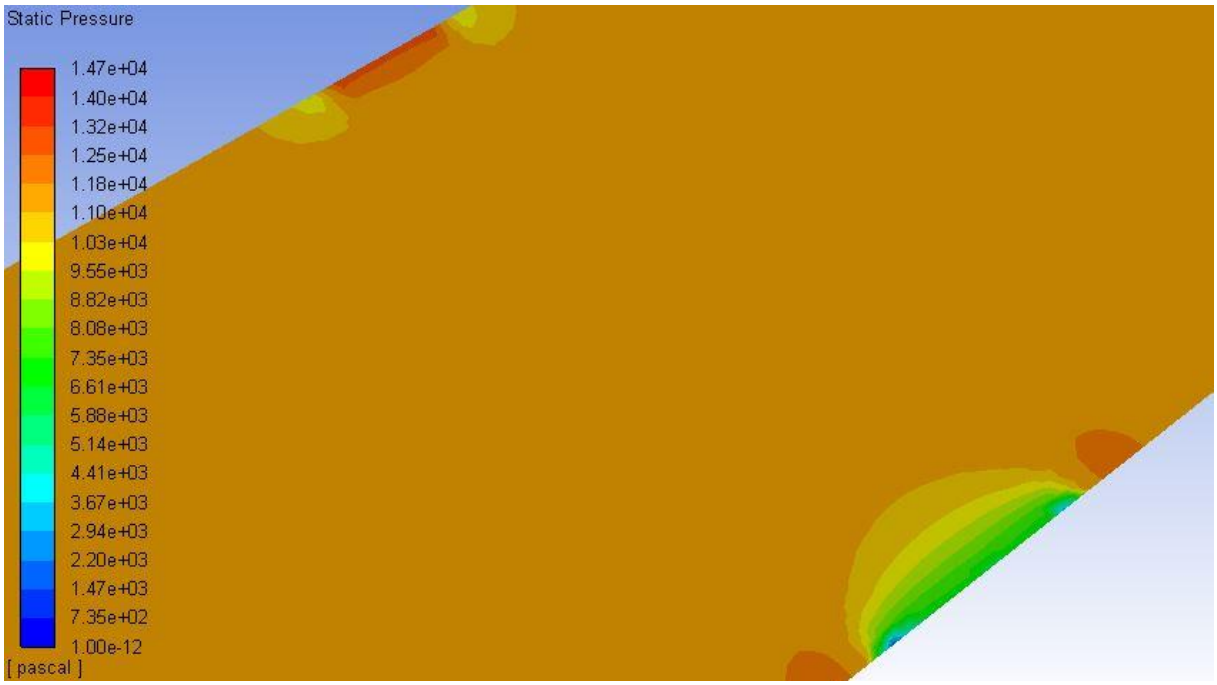

Figure 41: Static pressure evolution along the horizontal plane in the centre of the domain.

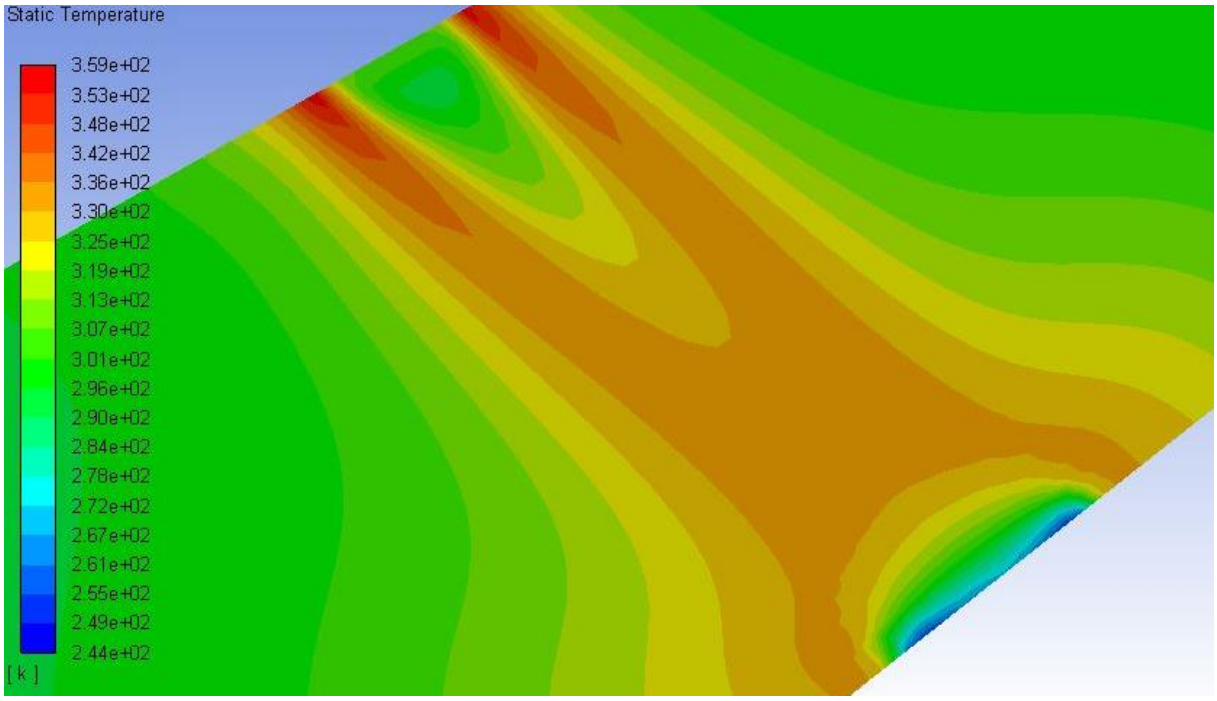

Figure 42: Static temperature evolution along the horizontal plane in the centre of the domain.

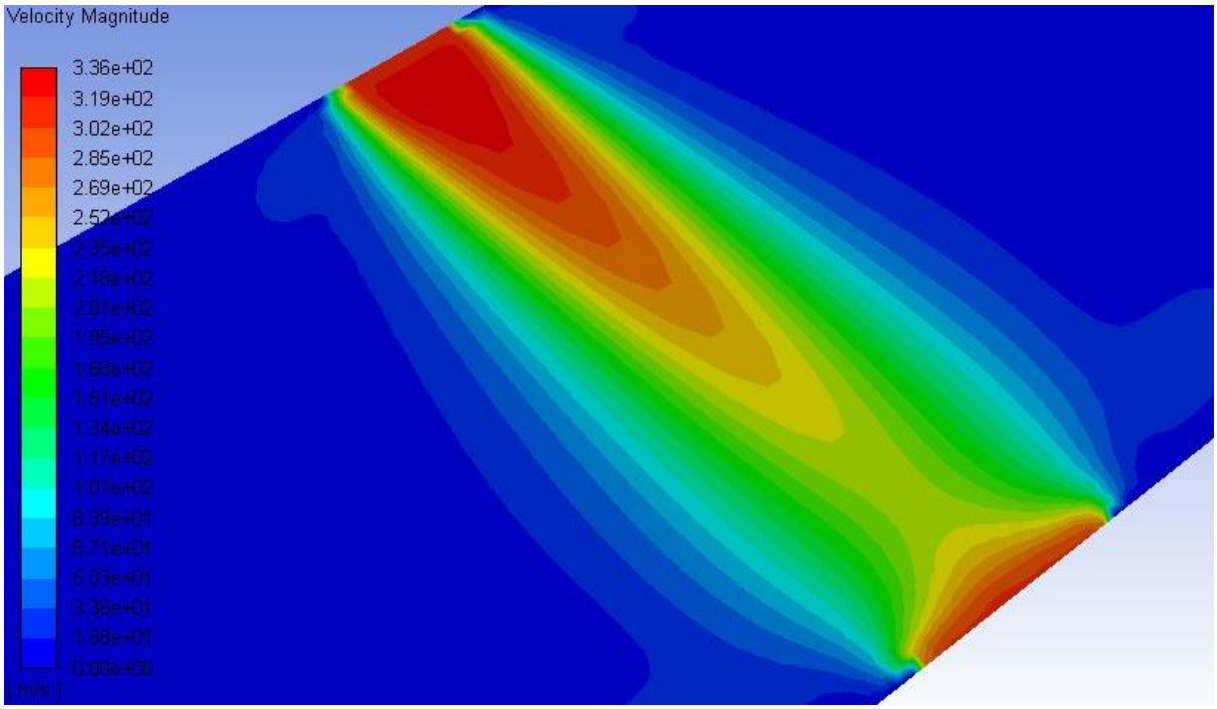

Figure 43: Velocity magnitude evolution along the horizontal plane in the centre of the domain.

The evolution of the parameters shown matches the one expected, since the results have been compared to a previous experiment in which the settings were implying a closed volume with an inlet and an outlet facing each other. Particularly for the velocity magnitude, the flow slowly decelerates as it is crossing the volume until it increases its speed again when approaching the outlet orifice, being this pattern the one already observed in the mentioned previous experience. Nevertheless, these results cannot be considered as correct in a quantitative way, since when they were extracted the mass flow rate convergence had not been achieved. This is due to the fact that a rough estimation on the flow behaviour was searched when performing this simulation in order to see if the flow evolution profile followed the expected pattern, and considering that this geometry is still far away from the final one, the quantitative results would not provide meaningful information. Therefore this simulation is not accounted for extracting further conclusions, but just for counting on a supporting point from which to continue building up the next cases.

4.5 Open channel with *30* inlet and *30* outlet orifices

4.5.1. Geometry definition

By means of this simulation the first realistic approach to the final model is performed. In this case, and bearing in mind the scheme depicted in the Figure 1, the geometry is composed by An opened *62 mm* length prism channel created from the *100* μm extrusion of the face that contains the inlets. This face has a height of *220* μm. The diameter of the inlets is *20* μm, and the one of the outlets is equal to *30* μm.

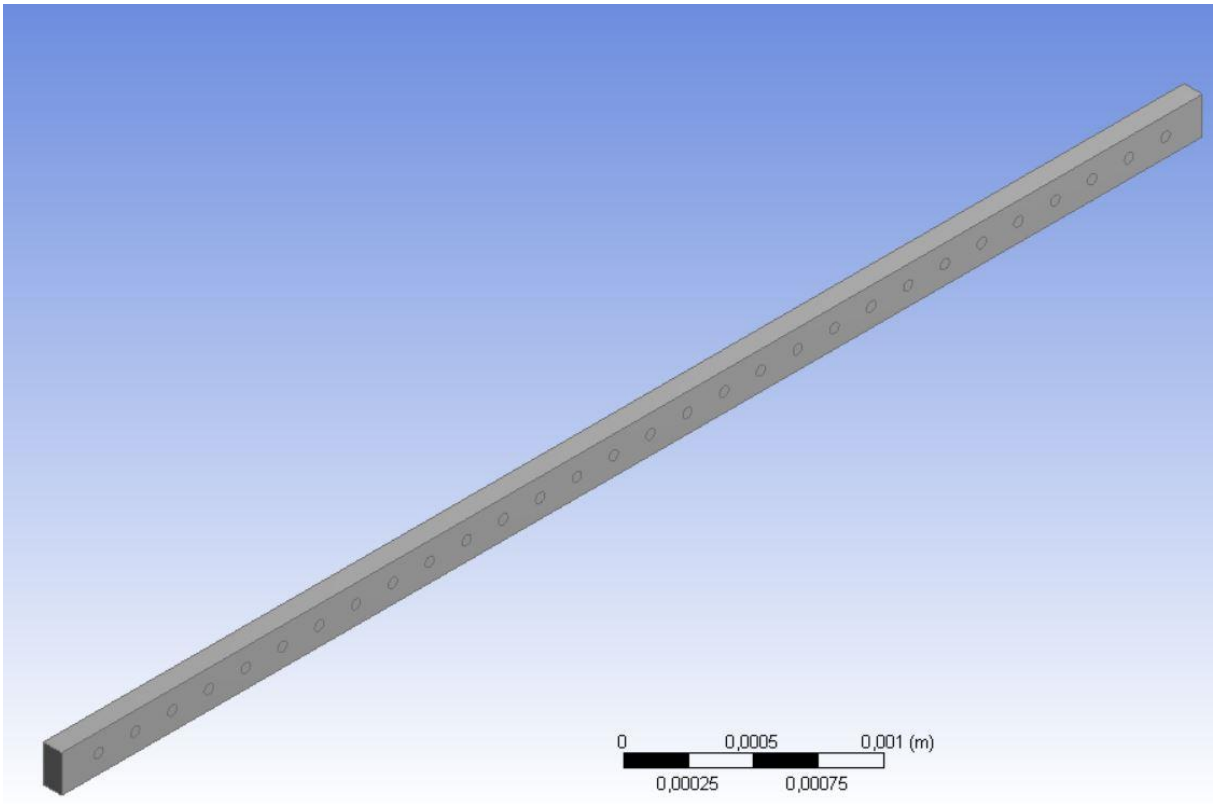

Figure 44: Geometry for the channel.

4.5.2. Meshing

As for the mesh settings:

Parameter	Value
Size Function	Proximity and curvature
Max Face Size *[m]*	$7.04 \cdot 10^{-6}$
Min Size *[m]*	$5.5 \cdot 10^{-8}$
Smoothing	High
Assembly Method	Cutcell

Table 10: Meshing settings.

4.5.3. Case setup

The case setup considered is the same one as the previous simulation.

4.5.4. Solution

Since the geometry is considerably more complex now the solution of the model is found by means of a transient solution. This is the only consideration that changes as for the solution settings in comparison with the previous case.

The aim of using a transient calculation method leans on the fact that it is necessary to verify if the flow behaviour, once it is developed, is constant with time and no interaction among the various inlets and outlets leads to a non-fixed result. In this case, and as it was stated previously, the transient option needs to be activated in the General panel of the Setup in the graphical interface of ANSYS Fluent. The rest of the settings remain constant, except for the Calculation section, in which additional parameters are now defined: the time step, the number of iterations per time step and the maximum number of time steps implemented. In order to roughly estimate the suitable time step the Courant number is used:

$$C = \frac{u_m \cdot \Delta t}{\Delta x} \tag{5}$$

Where u_m is the magnitude of the velocity, Δt the time step and Δx the length interval. The maximum value of this number that can be permitted depends on the type of solver used. For example, an explicit solver may require that the maximum C

is equal to *1*, while an implicit solver, as previously stated, is more stable and less sensitive to numerical instability, allowing a larger value of this constant.

Even though the solver used is the implicit one, since this setting is the one offered by default in Fluent and no change was made on it, in order to make an initial estimation the value of the time step used is calculated considering the minimum size defined for the meshing process, the velocity at the inlet and a Courant number equal to one. From this calculation the obtained time step is around $4 \cdot 10^{-7}$ seconds. Nevertheless, this value is not determinant since Fluent enables the option to define an adaptive time step that the program will update as the simulation develops, so this initial value will only be consider at the beginning of the simulation.

In an analogue way to the already covered steady simulations, the maximum number of time steps is set to *10000*. As for the number of iterations per time step, they will be initially set to *220*, lowering this value sequentially after observing that the residuals evolution is no longer decreasing as the iterations go by in a time step. In any case, the ideal procedure would be to set the number of iterations per time step in a way that the residuals evolution can drop three orders of magnitude for a given time step.

When observing the obtained results, it needs to be taken into account that not all the couples of faced inlet-outlet orifices will describe the same profile of parameters, since the ones that are located closer to the extremes of the main channel will feel more the "suction" effect of the open extremes of this. Therefore, in this case instead of visualizing one contour plot for each parameter, and since the ultimate parameter of interest is the density, a XY and a YZ plot of the evolution of density along the X axis between the central inlet and its corresponding outlet, and of the evolution of the density along the centre of the main channel in the Z axis, respectively, are considered. This is due to the fact that the evolution of the flow behaviour through a couple of an inlet and an outlet orifices at the centre of the main channel is practically the same to the one observed in the previous setup, where a closed volume with an inlet and an outlet was tested. Paying attention to the evolution of the density at this point by means of a *2D* plot, the obtained result is the following one:

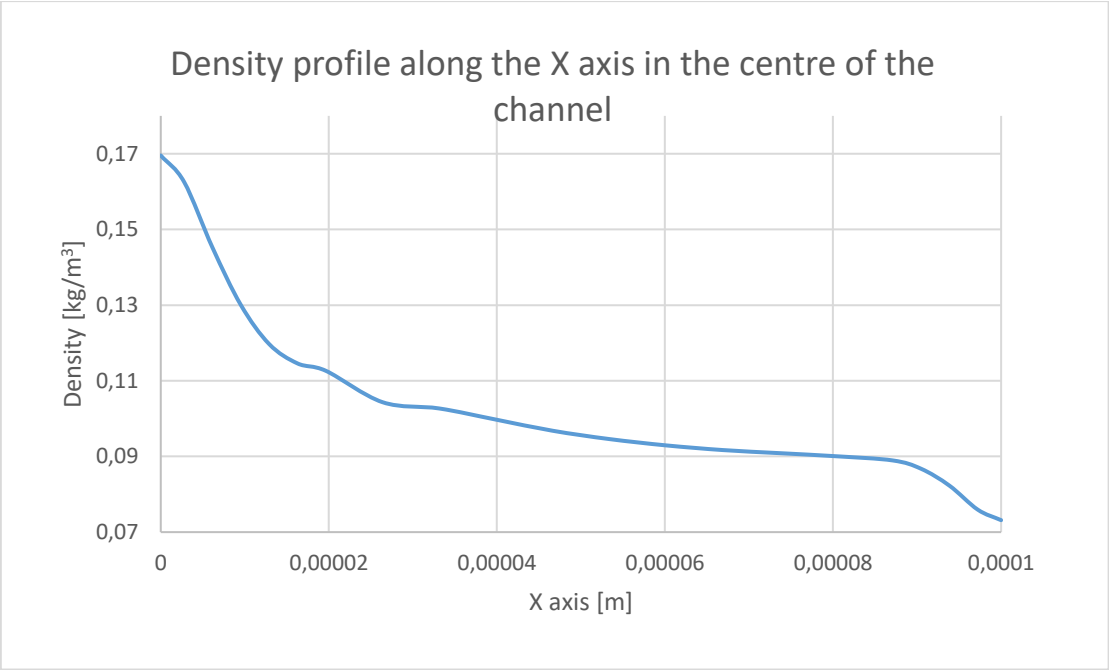

Figure 45: Density profile evolution along the X axis in the middle of the channel.

But when the attention is focused on the extremes of the channel, the distortion created on this pattern by the influence of the open ends is visible. In order to quantify such difference in a more intuitive way, the evolution of the density along the centre of the main channel is described:

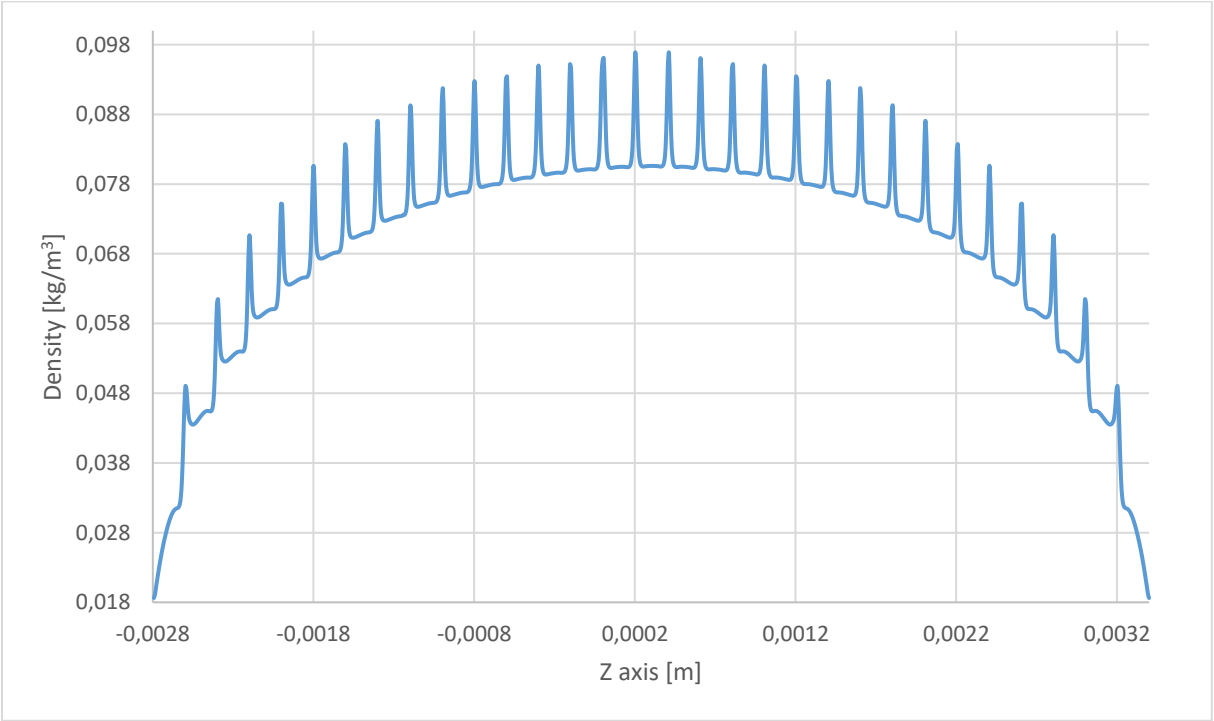

Figure 46: Density profile evolution along the Z axis in the middle of the channel.

The purpose of the target model is to create a pattern along the main channel through which the density follows a variable distribution, with the aim to create the desired XUV laser signal, as it has been commented at the beginning of the report. The obtained density profile along the Z axis fits, in a qualitative way, into the desired evolution. A comment to outline is that the previous plot is drawn with the values of density along the centre line, which would correspond, for the centre inlet, to the intersection of the line of the plot along the X axis with the value of $x = 50\ \mu m$. This assumption is stated since the laser is expected to travel along the channel through the middle part of it. But if the plot was obtained from a line closer to the inlets, a greater difference among the peaks and the back density would be obtained.

As for the convergence criteria:

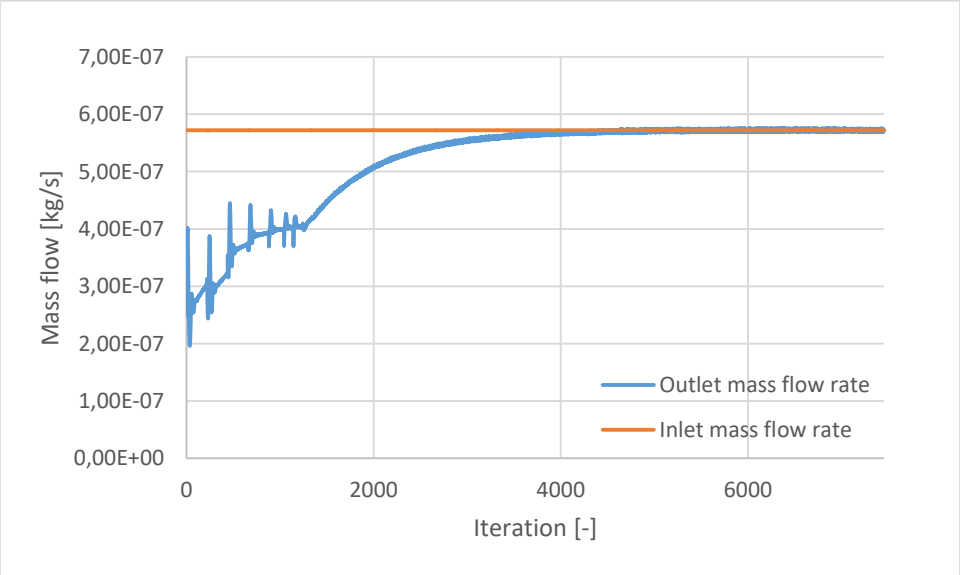

Figure 47: Mass flow rate convergence.

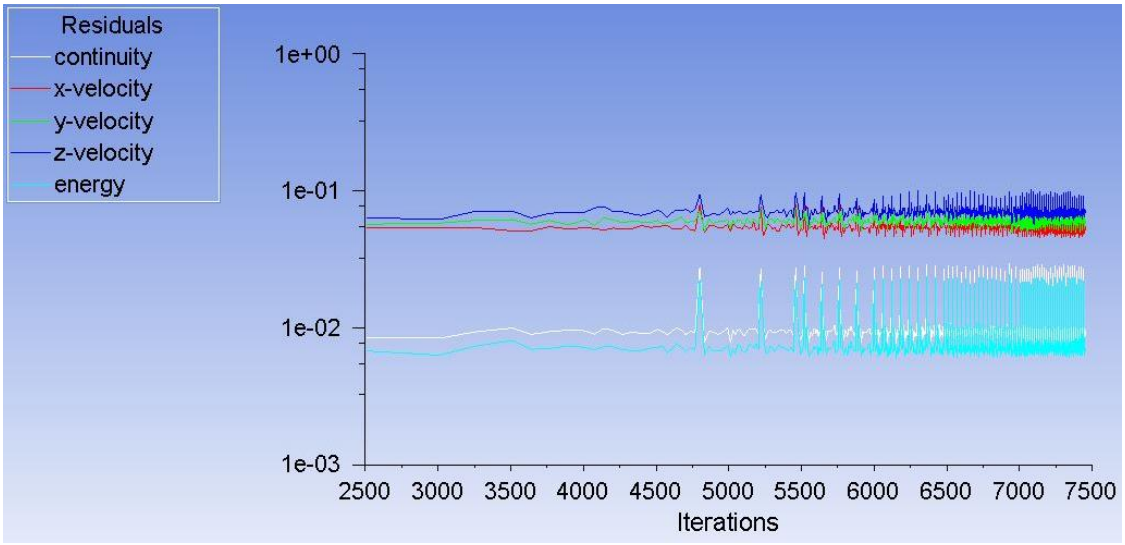

Figure 48: Evolution of the residuals.

In this case the evolution of the residuals is far away from the one obtained so far for the initial approximations, but since they stabilize around the same value and do not increase nor decrease, and considering that the mass flow rate is fully converged since the middle of the simulation, the solution can be considered as converged, even though the accuracy of the results given will have a worse quality that the one given by the initial approaches.

Regarding the final purpose of the model, the desired density profile has not been defined yet, so from the fluid dynamic point of view it is interesting to define how the variations of geometry will influence this density profile. The modifications to test will cover the size of the diameter of the outlets, as well as the amount of them.

4.6 Open channel with *30* inlet and *30* outlet orifices; outlet diameter *40 µm*

4.6.1. Geometry definition

The geometry considered is the exact same one of the previous case, but setting the value of the outlet diameter to *40 µm* instead of *30*.

4.6.2. Meshing

In an analogue way, no modifications have been implemented concerning the meshing settings.

4.6.3. Case setup

The case setup remains as the one of the previous simulation.

4.6.4. Solution

It is seen that, qualitatively, the evolution of the variables in this case follows the one defined by the previous simulation. For this model the density profiles are:

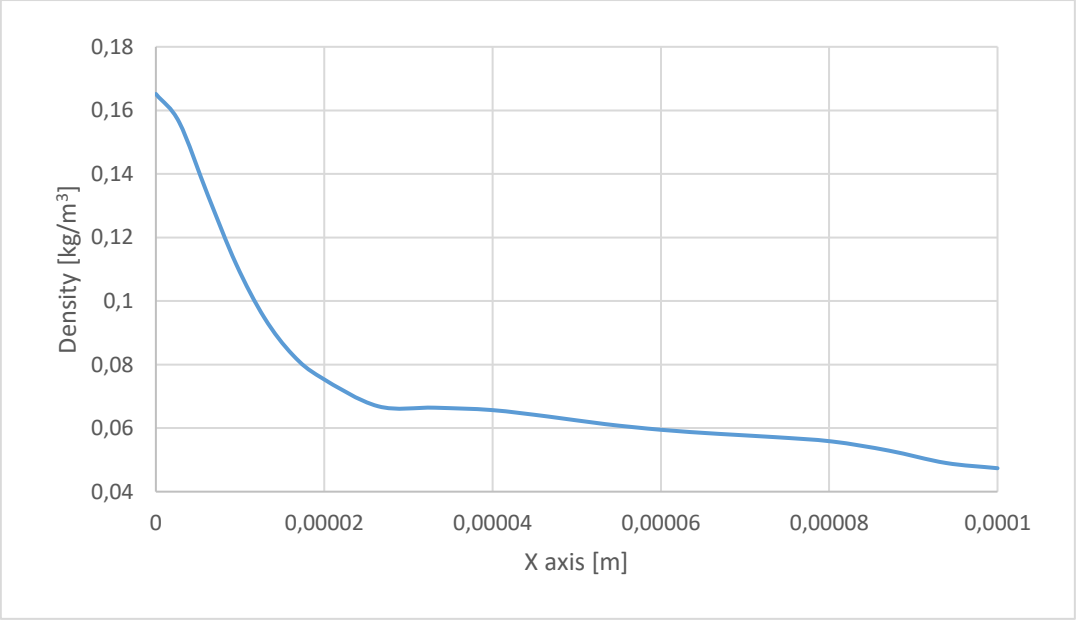

Figure 49: Density profile evolution along the X axis in the middle of the channel.

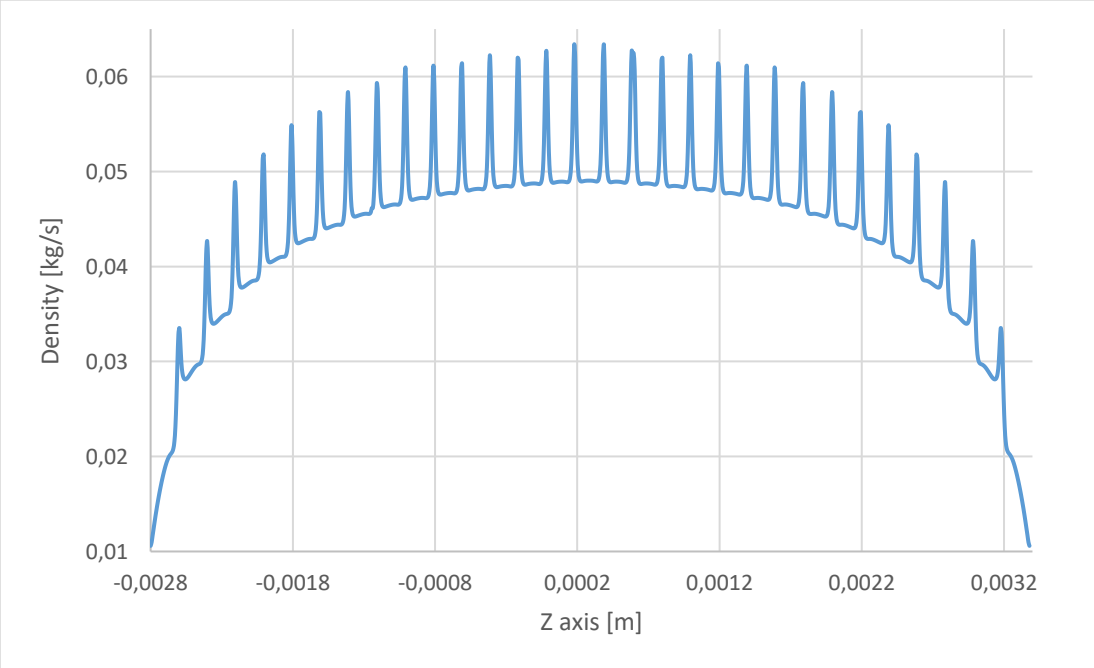

Figure 50: Density profile evolution along the Z axis in the middle of the channel.

In comparison with the original setup, in this case the density value drops faster in the X direction, phenomena that provides a profile evolution in the Z direction with smoother peaks.

Regarding the convergence of the solution, the residuals evolution remains close to the one of the original model. The mass flow rate convergence is verified.

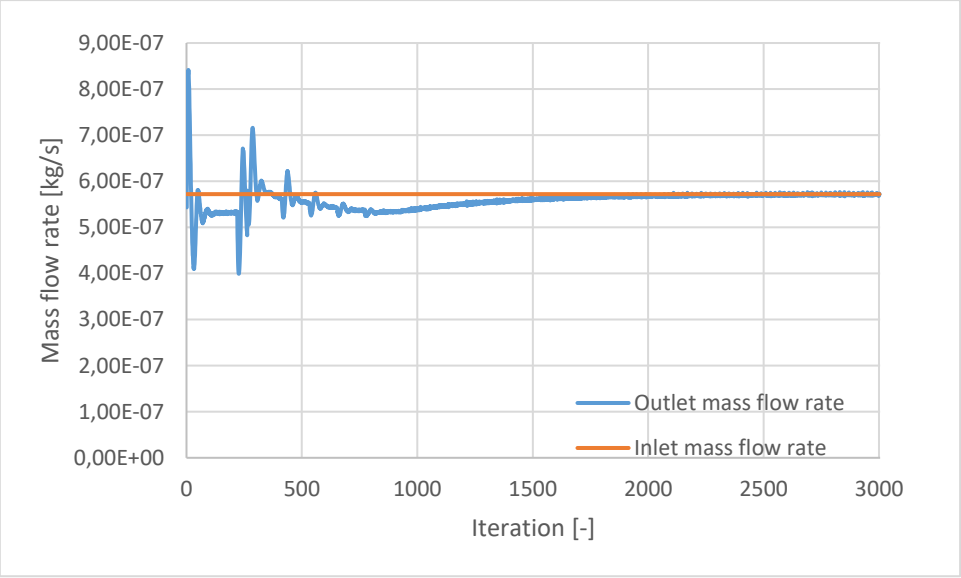

Figure 51: Mass flow rate convergence.

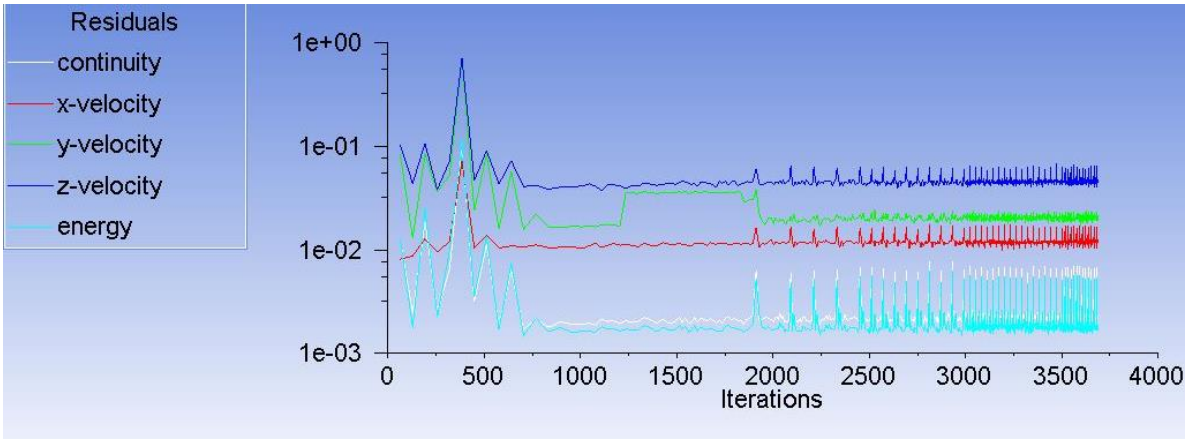

Figure 52: Evolution of the residuals.

4.7 Open channel with *30* inlet and *30* outlet orifices; outlet diameter *50 μm*

4.7.1. Geometry definition

The geometry is kept constant with the only difference of the outlet diameter that is updated to *50 μm* instead of *40*.

4.7.2. Meshing

The mesh settings are kept constant.

4.7.3. Case setup

In this case also the setup is conserved.

4.7.4. Solution

It is observed that the pattern provided by the solution is very similar to the previous settings, being possible to appreciate better the density evolution details through the already used plots:

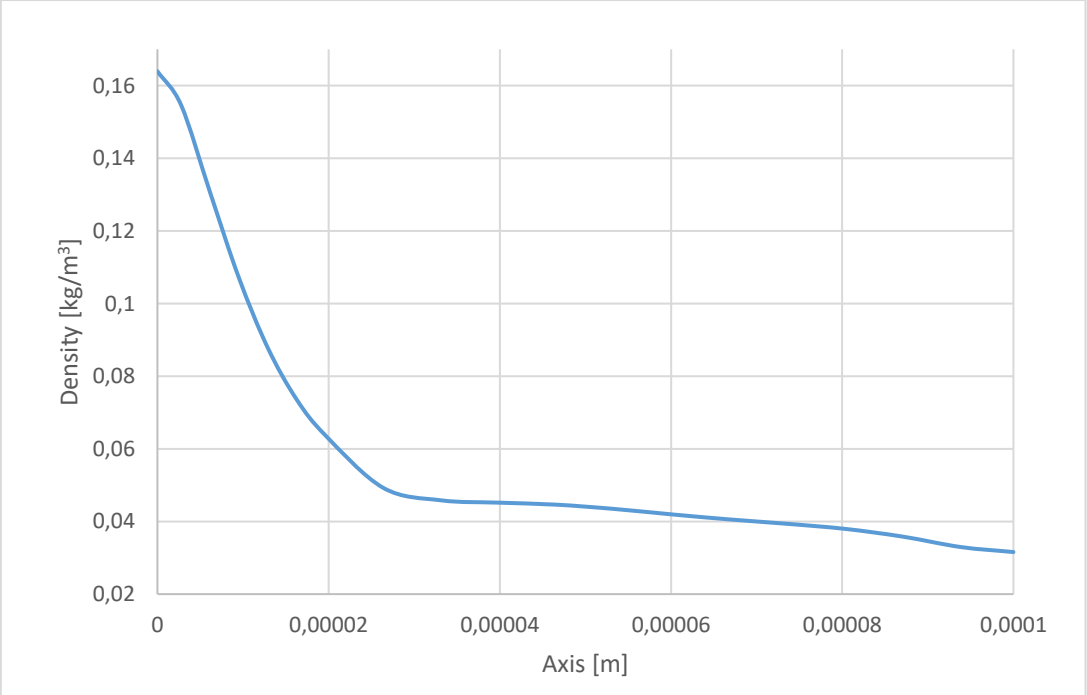

Figure 53: Density profile evolution along the X axis in the middle of the channel.

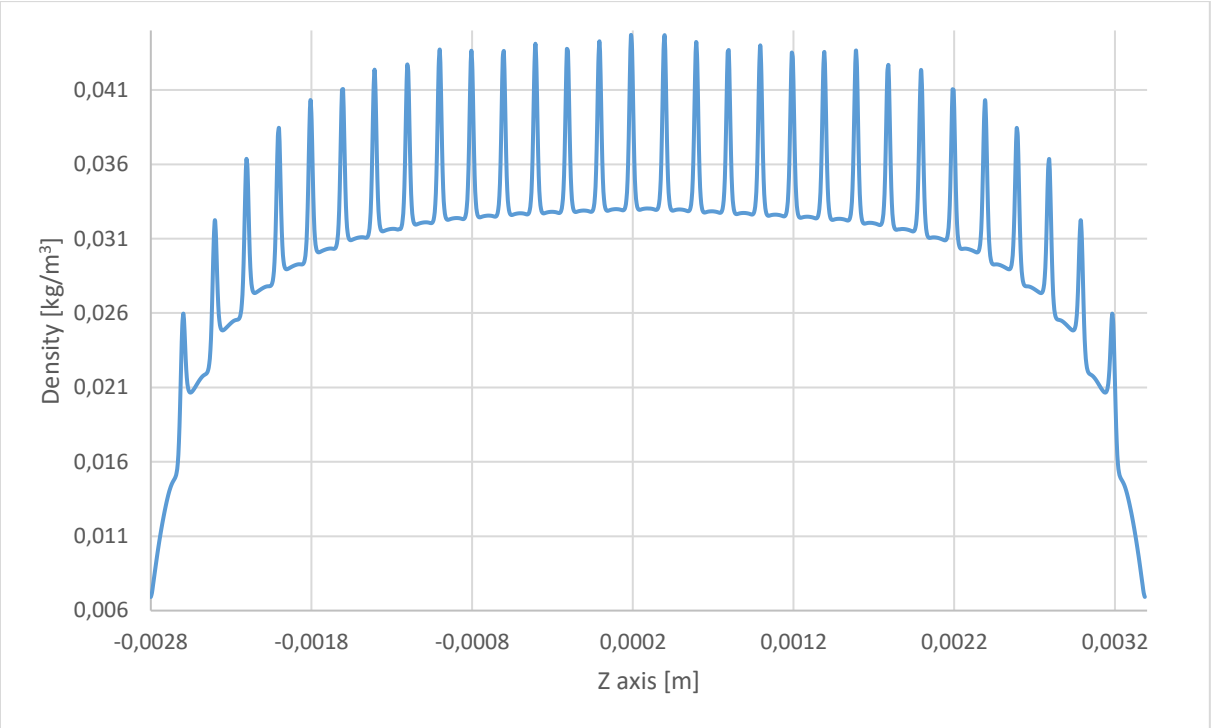

Figure 54: Density profile evolution along the Z axis in the middle of the channel.

The observations dropped from this result are analogous to the ones of the previous one when it was compared to the original setting: in this time the density peak is slightly lower and the decrease in density along the X axis takes place approximately at the same point as the setting with $40\ \mu m$ diameter for the outlet takes.

Regarding the convergence of the solution:

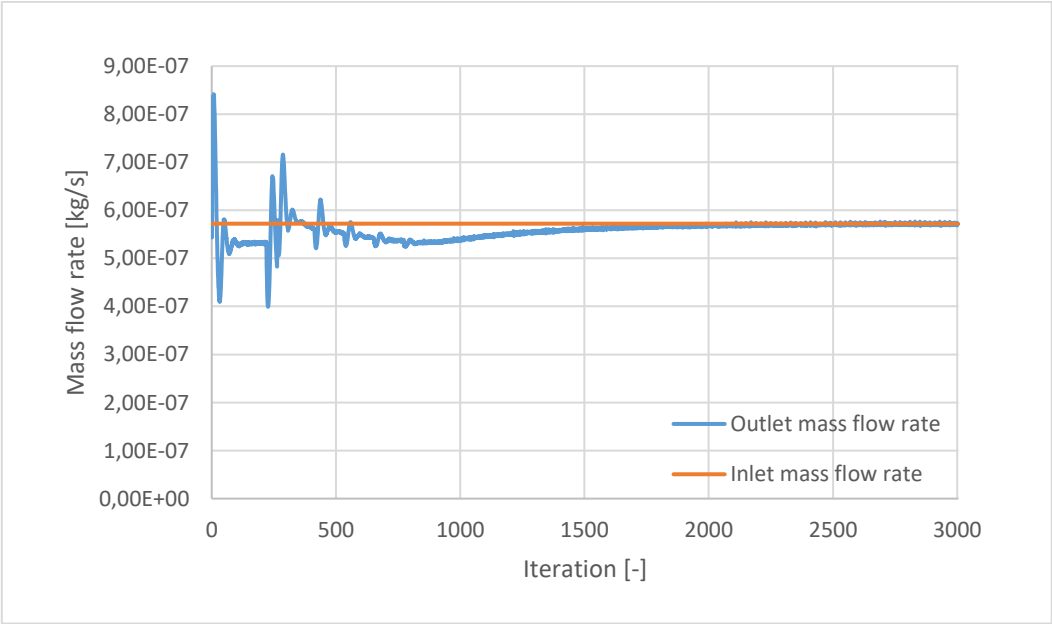

Figure 55: Mass flow rate convergence.

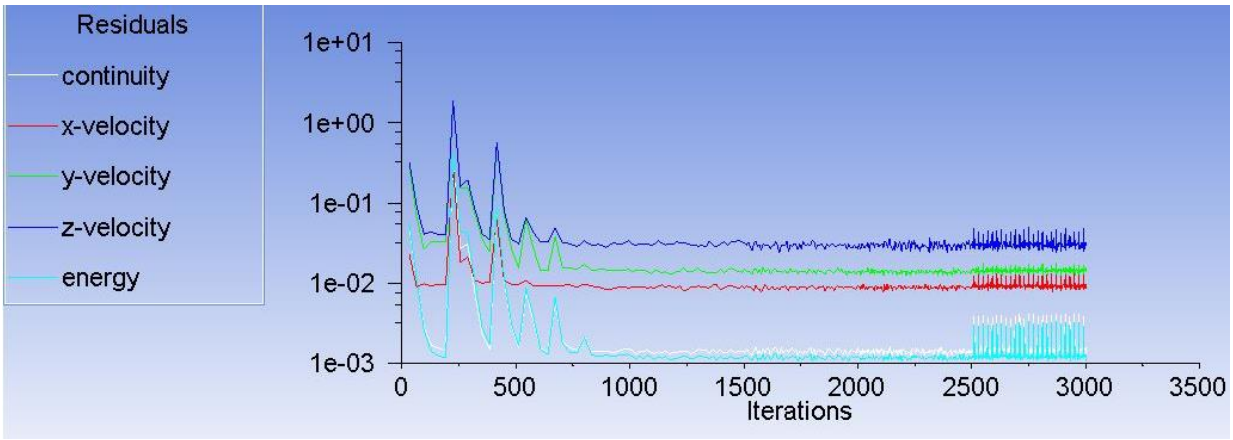

Figure 56: Evolution of the residuals.

4.8 Open channel with *30* inlet and *31* outlet orifices; outlet diameter *30 µm*

4.8.1. Geometry definition

The next suggested variation of the original geometry consists now on setting the outlet orifices not aligned to the inlet orifices along the X axis, but displaced in order to locate them in the middle of two inlets. Therefore the final number of outlets present in the geometry would be *31*.

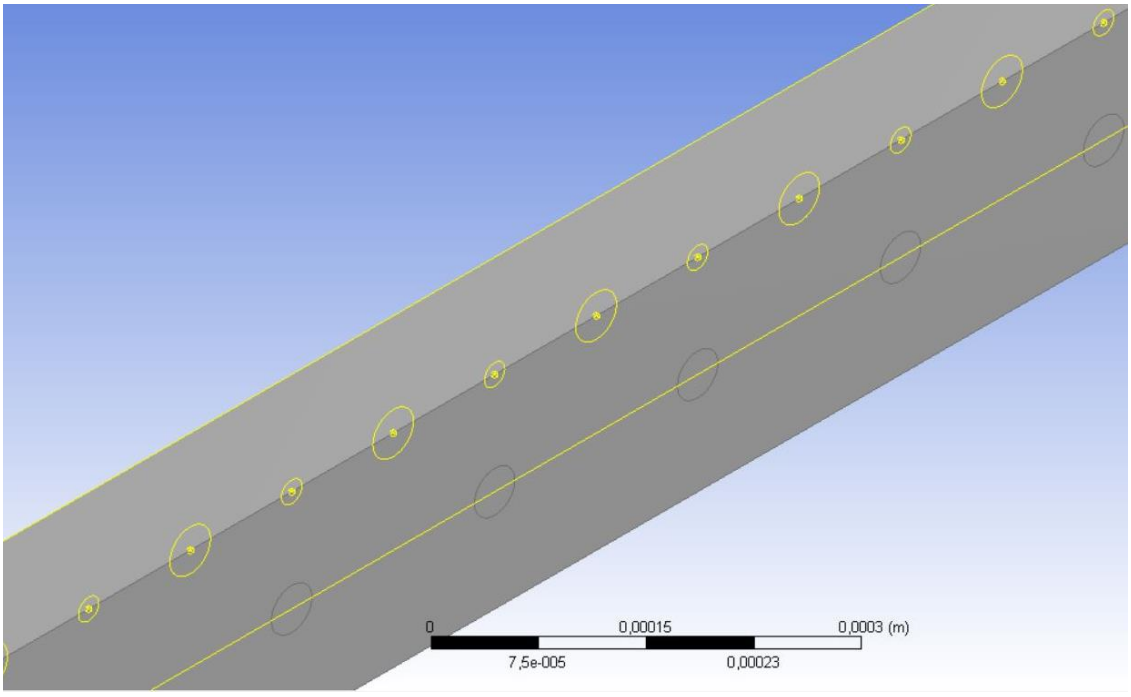

Figure 57: Geometry variation of the channel. The yellow lines represent the original sketch from which the volume has been extruded, the big circumferences represent the outlets, and the smaller ones are the inlets.

In the previous figure the geometry is shown by also marking out the sketch from which it was created in order to make visible the relative location of the inlets with respect to the outlets.

4.8.2. Meshing

The settings of the meshing procedure, though, remain the same.

4.8.3. Case setup

As for the case setup, no modifications have been implemented.

4.8.4. Solution

As it could be expected, in this occasion the evolution along the plane of the variables is not the same as the one seen so far. When the flow exits the inlet the profile is similar, but as it advances along the X direction the flow adapts in order to exit the volume through the outlets, that are no longer aligned with the inlet orifices.

As for the evolution of the density profile:

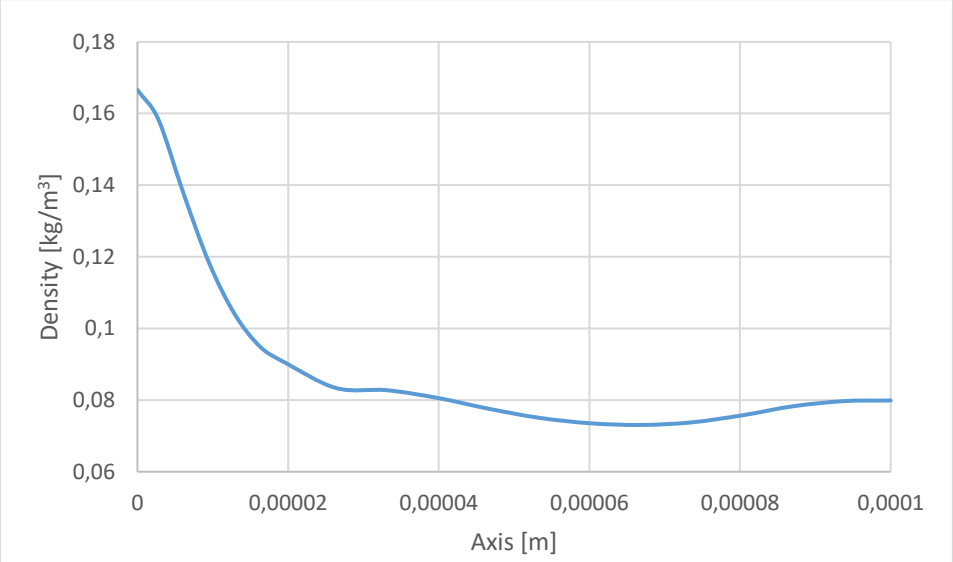

Figure 58: Density profile evolution along the X axis in the middle of the channel.

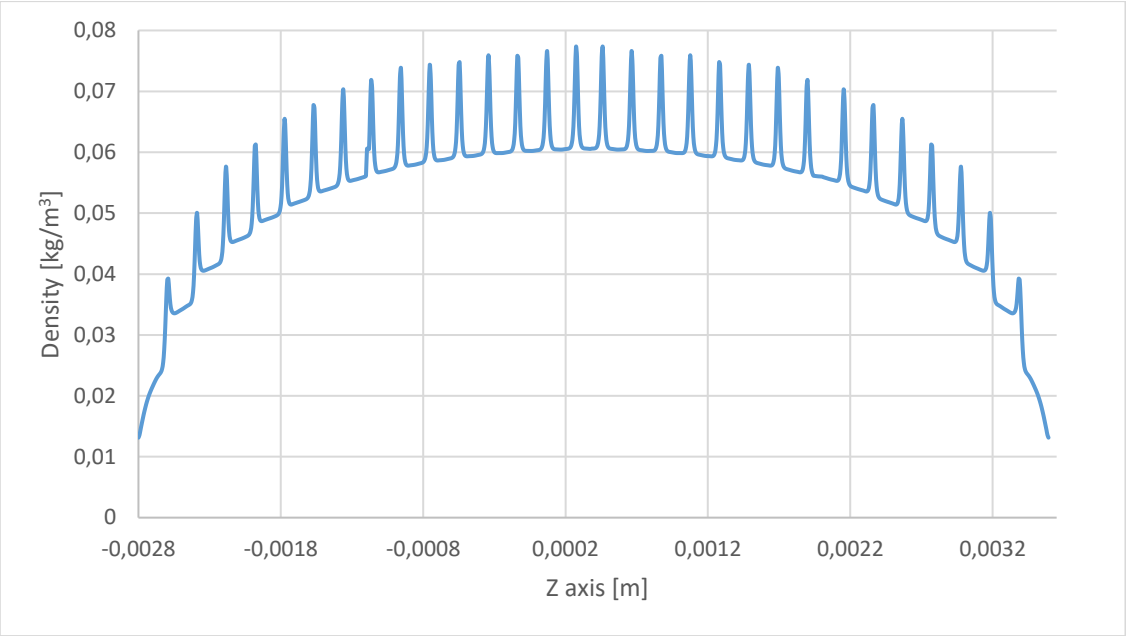

Figure 59: Density profile evolution along the Z axis in the middle of the channel.

A different behaviour is registered in the X direction point when the flow approaches the end of the volume. The profile obtained for the density along the main direction of the channel, though, remains the same as the already seen.

The convergence verification is stated through the following evolutions:

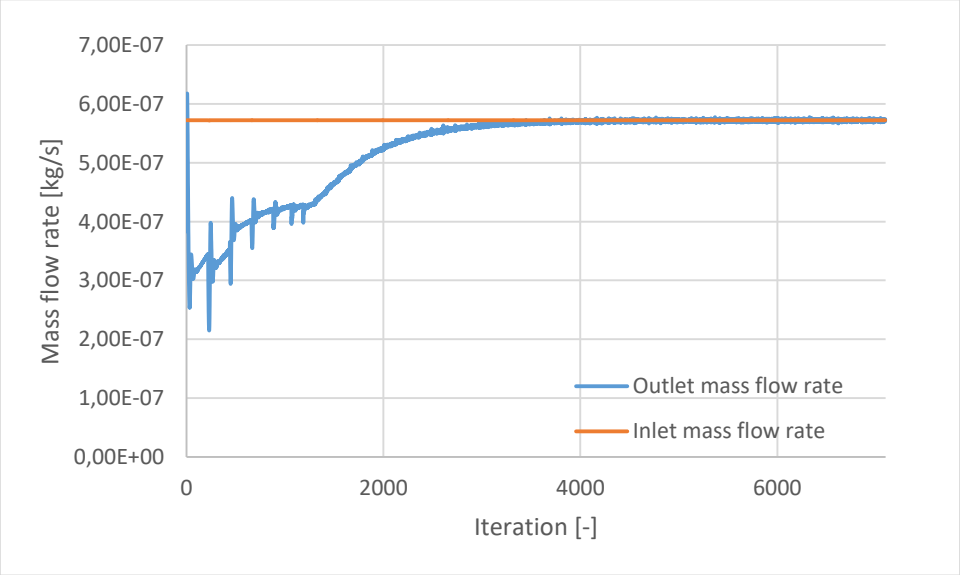

Figure 60: Mass flow rate convergence.

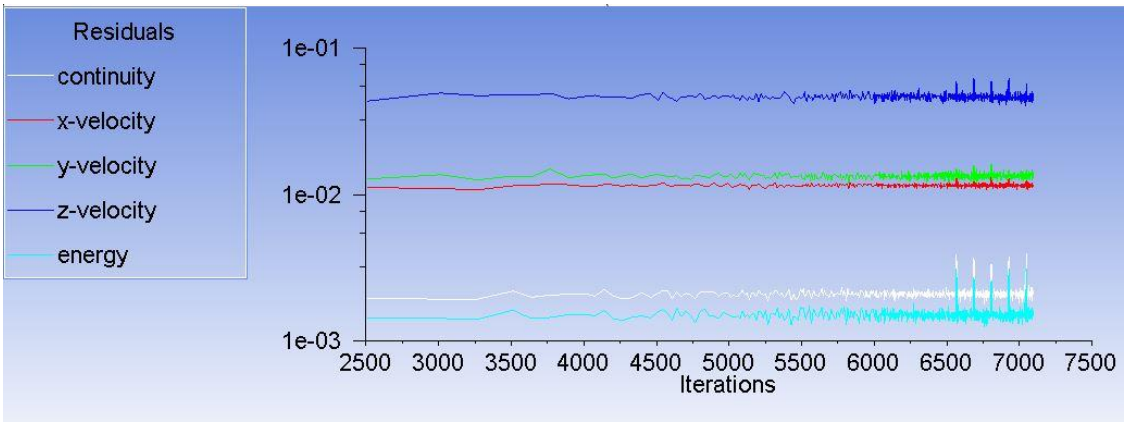

Figure 61: Evolution of the residuals.

4.9 Open channel with *30* inlet and *60* outlet orifices; outlet diameter *30 μm*

4.9.1. Geometry definition

This case results from the original model considered and the last one tested. In this setup every inlet along the channel will have its own inlet faced towards it at the end on the volume, but there will also be an additional outlet between of these original outlets.

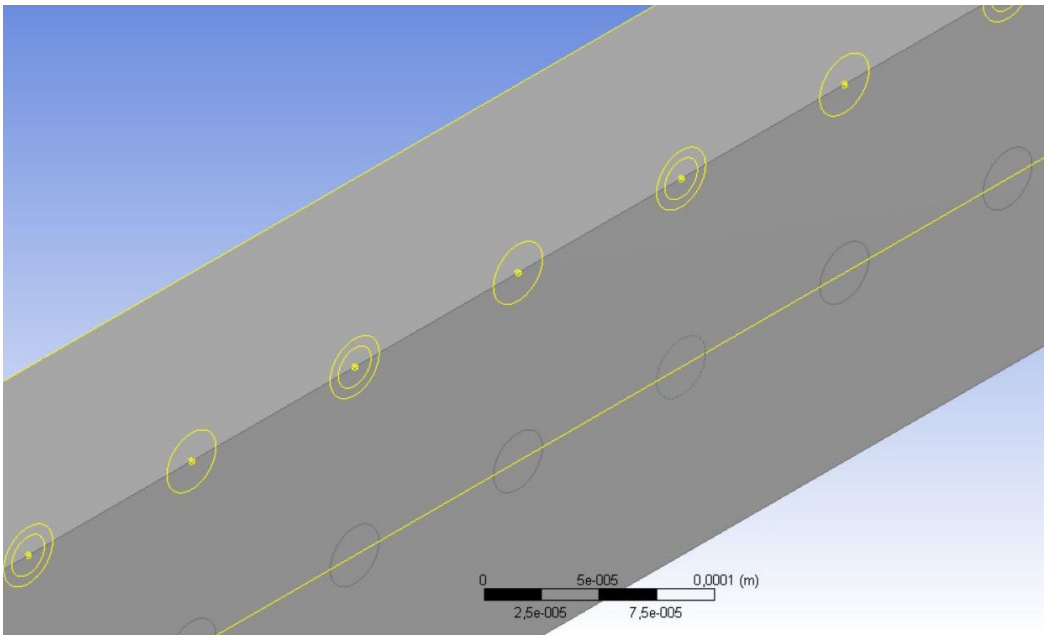

Figure 62: Geometry of the new setup. The yellow lines represent the original sketch from which the volume has been extruded, the big circumferences represent the outlets, and the smaller ones are the inlets.

4.9.2. Meshing

No modifications are implemented in this part.

4.9.3. Case setup

The case setup remains as it has been used so far.

4.9.4. Solution

The results obtained are a combination of the model with *30* outlets and the model with *31*, as it could be expected. As for the evolution of the density:

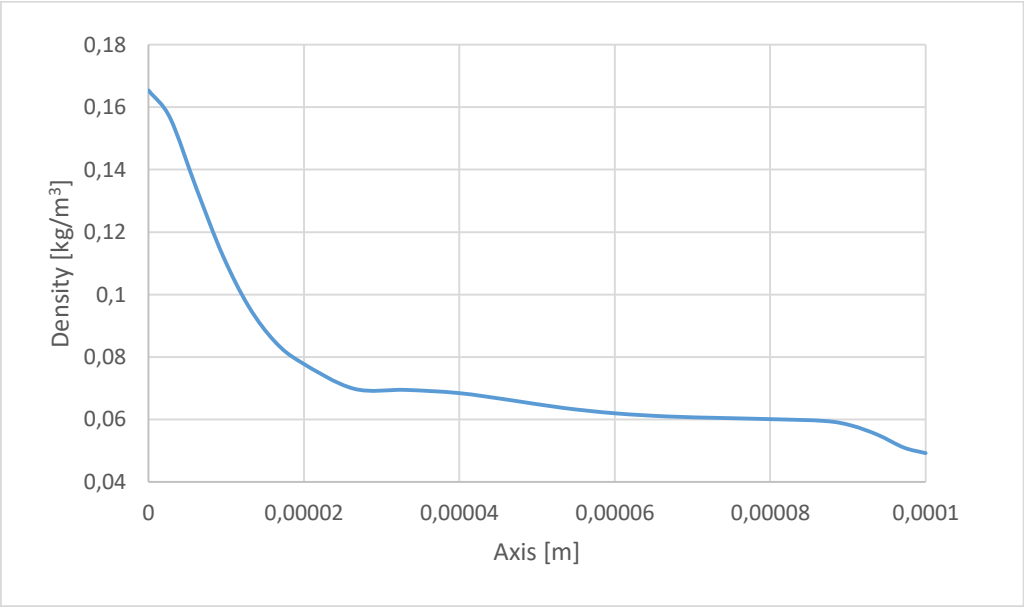

Figure 63: Density profile evolution along the X axis in the middle of the channel.

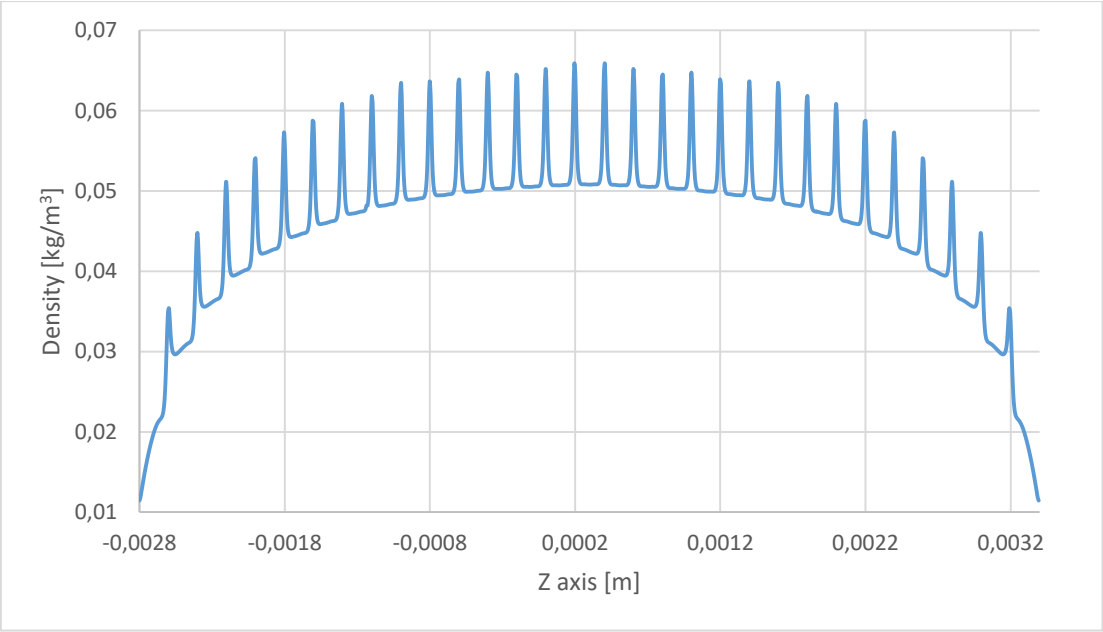

Figure 64: Density profile evolution along the Z axis in the middle of the channel.

In this case the density evolution along the X axis looks more similar than the one provided by the original case, but the parameter values in the middle of the channel is lower.

As for the convergence of the solution:

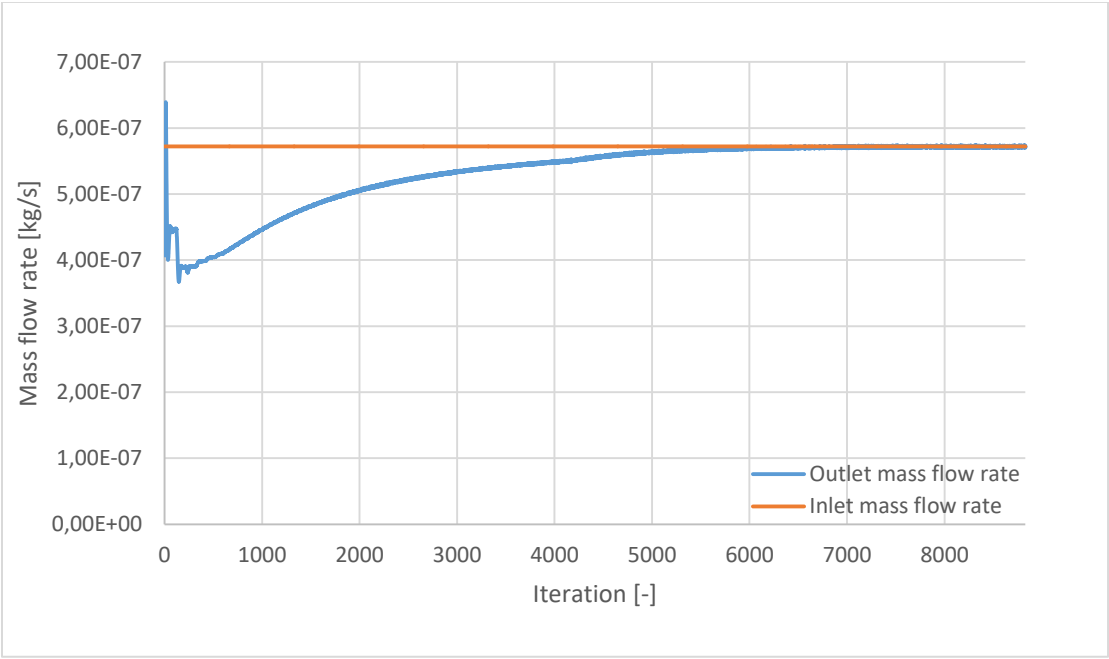

Figure 65: Mass flow rate convergence.

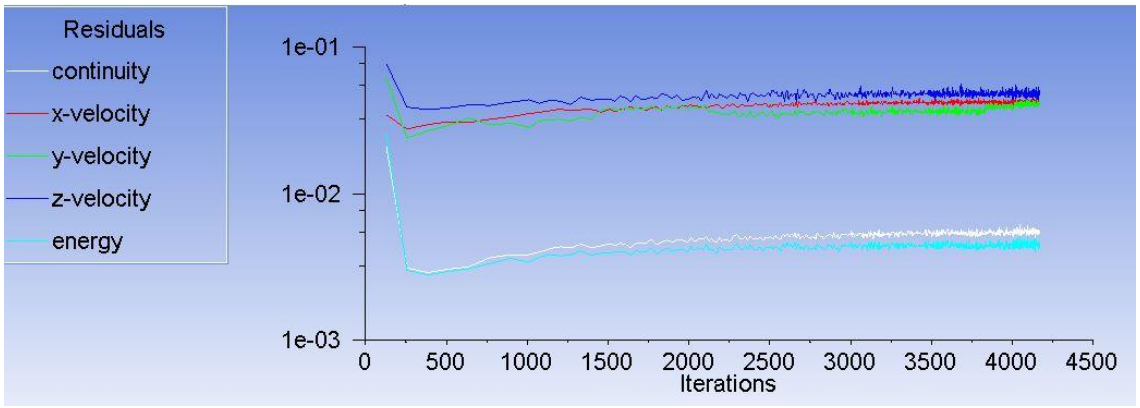

Figure 66: Evolution of the residuals.

4.10 Comparison of the density profiles provided by each of the geometries tested

It is interesting now to compare the results obtained for all the models in order to evaluate the differences of the density profiles produced by all of them. Therefore three plots are discussed: the evolution of the density along the X axis for the centred inlet in the middle of the channel, the evolution of the density along the Z axis in the middle of the channel and the increment of density that the first of the plots provides with respect to the background density. The results obtained are the following ones:

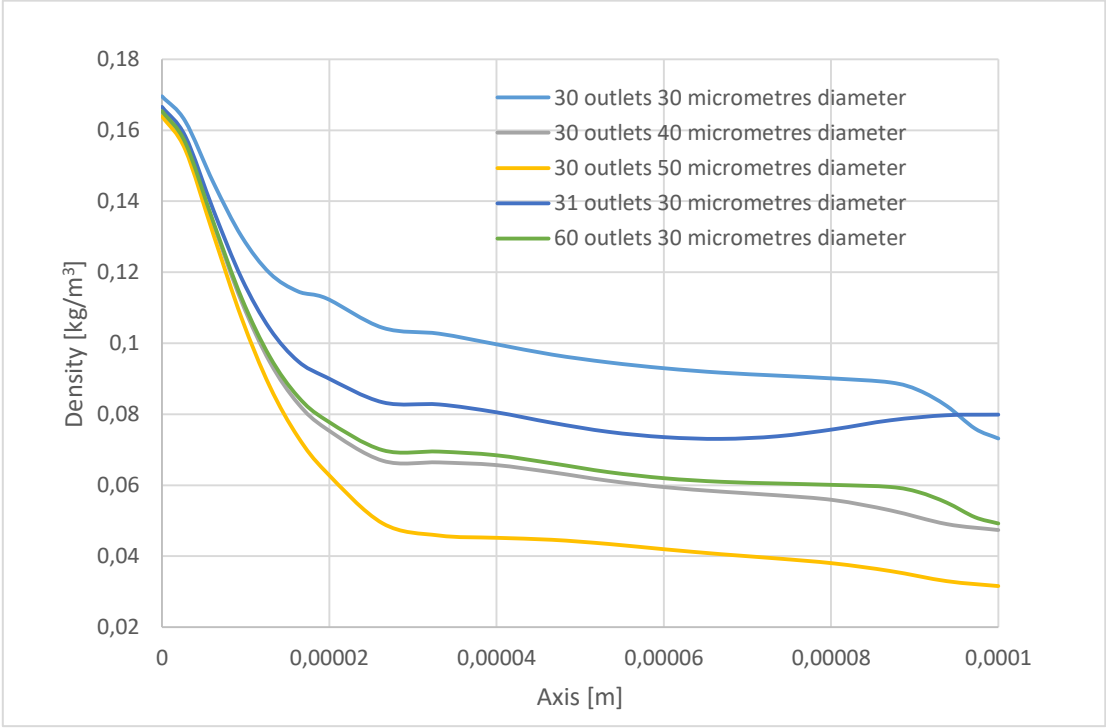

Figure 67: Comparison of the density profile along the X axis considering the different setups implemented.

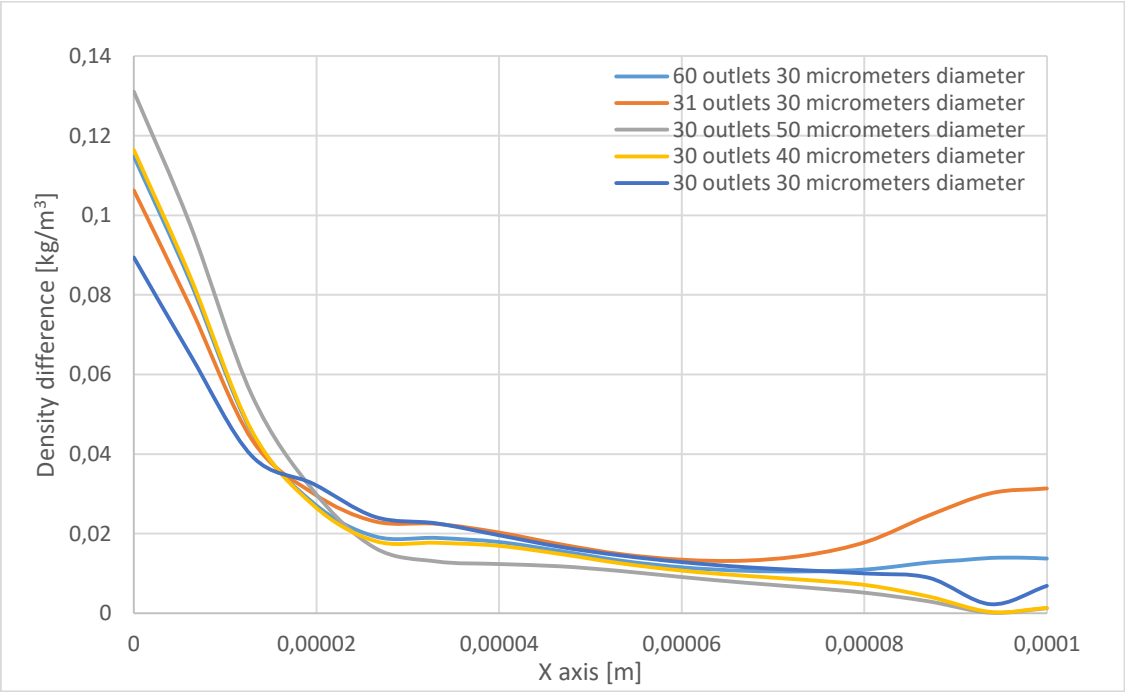

Figure 68: Comparison of the density profile difference along the X axis considering the different setups implemented.

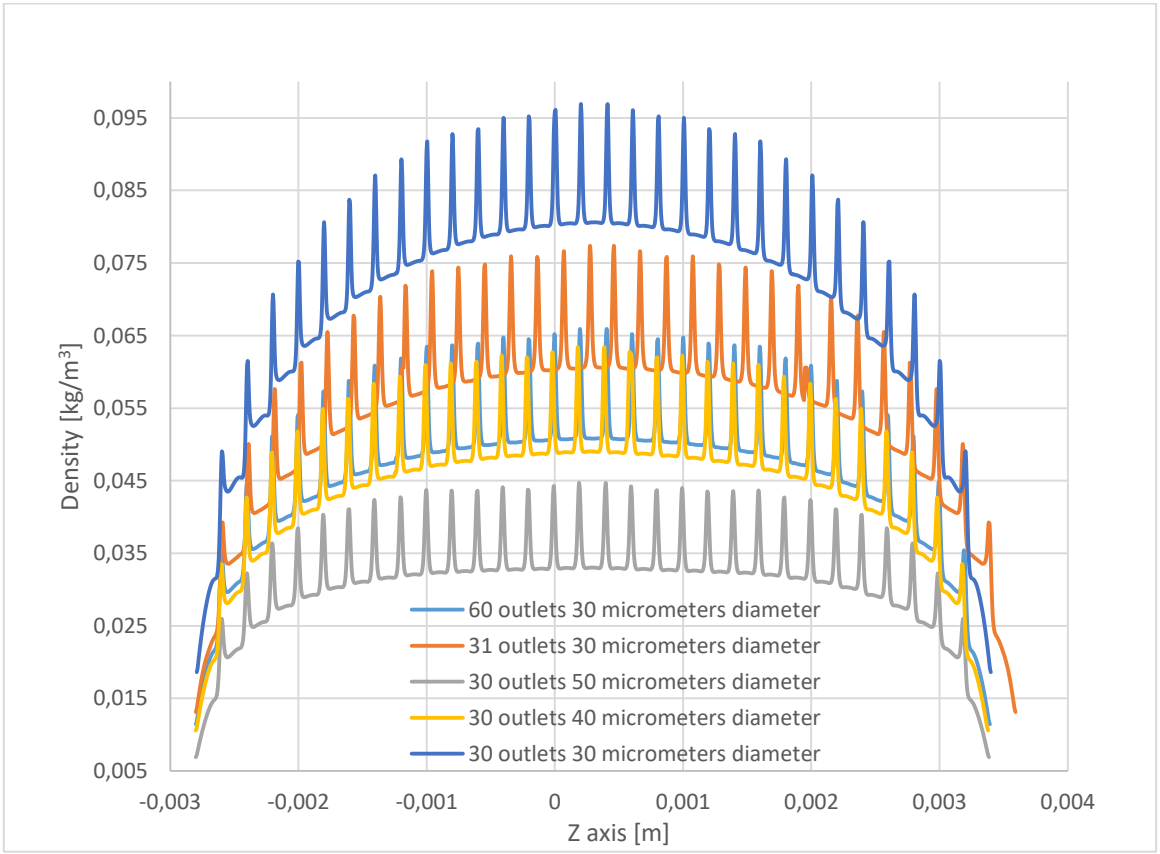

Figure 69: Comparison of the density profile along the Z axis considering the different setups implemented.

From the three graphs it is seen that the highest values of density are provided by the original model. But it is also necessary to point out that this configuration is the one that most feels the influence of the extremes of the main channel, that drain the flow deforming the profile along the Z axis in the shape of an arch. Tis effect is also noticeable in the other configurations, but in those cases the strength of it decreases as the maximum density reached by the peaks decreases. Therefore, from this point of view the channel that least would be affected by the extremes influence would be the one with *30* outlets of *50* μm of diameter, generating a more uniform profile.

Considering this observation, the conclusions obtained from the graph of the evolution of the density profiles along the X axis is analogous. Nevertheless, moving to the second one the consequences are not so evident. In this second graph the evolution represented is the difference in magnitude between the density profile along the X axis for the centre inlet of the channel, and the background density, which would be the lowest pressure that the laser would encounter when crossing the channel, also visible in the valleys between the peaks of the last graph (density evolution along the Z axis). It is observed that the hierarchy of the results initially deduced is conserved, but in this case little difference is shown in the interval provided by each of the configurations, especially in the centre part which is the one of interest. Therefore from this point of view the choice of the final model would not be considerably relevant.

4.11 Open channel with *30* inlet and *30* outlet orifices; outlet diameter *30* μm. Influence of the channels of the inlets

By checking out the original scheme of the model, it is seen that the inlets are composed by individual channels that conduct the flow from a reservoir that is at a pressure belonging to the range of *120-300 mbar*. As an approximation it has been assumed that at the exit of the inlets the flow would be sonic and at such pressure, but that assumption is not accurate. The effect of the inlets channels has not been taken into account. Along this channels the flow evolves and the profile described will not be the same one in all the channels, since they are all fed by the same reservoir and such profiles are influenced by the conditions at the exit, the most remarkable one being in this case how close to the extremes of the main channel the considered inlet is located.

By means of simplifying considerably the flow structure that is developed in the channel, it is possible to estimate the conditions at the outlet of the inlet channels through the Hagen-Poiseuille formula for a compressible fluid:

$$\dot{m} = \frac{\pi R^4}{8\mu R' T L} \cdot \frac{{P_{in}}^2 - {P_{out}}^2}{2} \tag{5}$$

$$V = \frac{R^2}{8\mu L} \cdot \frac{{P_{in}}^2 - {P_{out}}^2}{2P_{out}} \tag{6}$$

$$\dot{m}_{in} = \sum_{i=1}^{15} \frac{\pi {R_{ic}}^4}{8\mu R' T L_{ic}} \cdot \frac{{P_1}^2 - P(x_i)^2}{2} \tag{7}$$

$$P(x_i) = P_{int} - \frac{P_{int} - P_0}{L_{mc}} x_i \tag{8}$$

$$\dot{m}_{out} = \frac{\pi {R_{mc}}^4}{8\mu R' T L_{mc}} \cdot \frac{{P_{int}}^2 - {P_0}^2}{2} + \sum_{i=1}^{15} \frac{\pi {R_{oc}}^4}{8\mu R' T L_{oc}} \cdot \frac{P(x_i)^2 - {P_0}^2}{2} \tag{9}$$

$$\dot{m}_{in} = \dot{m}_{out} \tag{10}$$

By means of this simplification, the structure of the main channel has been represented by half of it assuming the symmetry of the flow behaviour. The inlet mass is the one delivered by the set of *30* channels (considering only *15* due to the symmetry assumption), and equalling this value to the one of the outlet mass it is possible to obtain the value of the pressure at the exit of the inlet channels.

4.11.1. Geometry definition

The new geometry is shown in the following image, where the inlet channels can be appreciated:

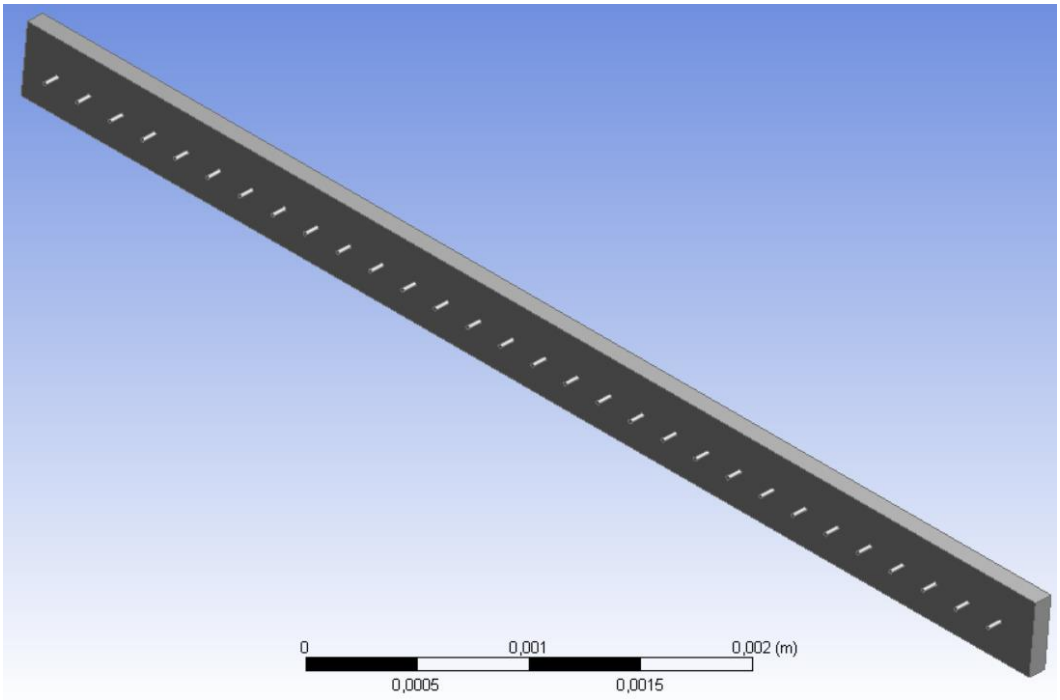

Figure 70: New geometry considering the inlet channels.

4.11.2. Meshing

No modifications are implemented in this part.

4.11.3. Case setup

The case setup remains as it has been used so far, testing the new geometry under two assumptions: considering the reservoir pressure is at *120* and *300 mbar*.

4.11.4. Solution

The results of the density profile for both cases is show in the following figure:

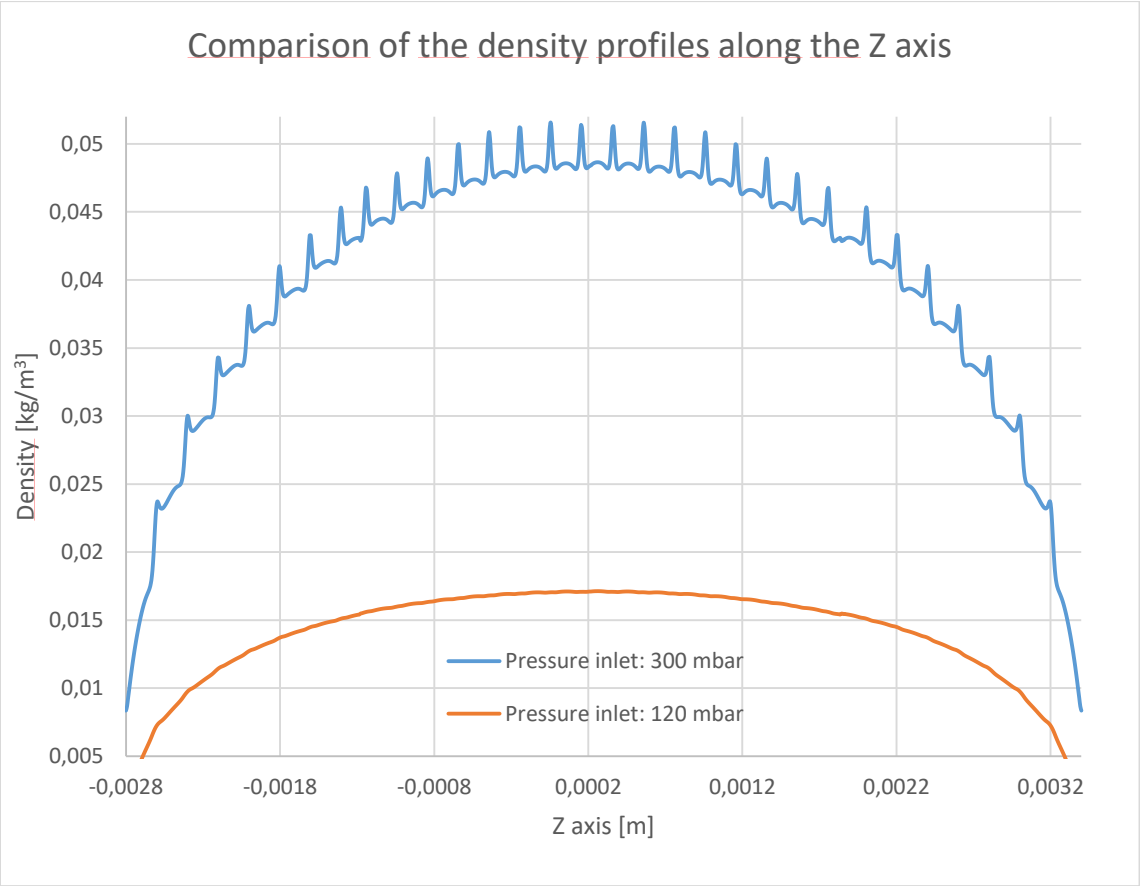

Figure 71: Comparison of the density profile along the Z axis considering the different setups implemented.

It is seen that, for the lowest reservoir pressure considered, the whole profile gives lower values of density in a flat shape. Besides in this case the density peaks are barely noticeable, and the consequence would be a poor modulation of the laser signal. In the case of the *300 mbar* of pressure for the reservoir, the density profile shows a parabolic shape similar to the one obtained in the original setup with no inlet channels. The peaks are noticeable in this case, but the magnitude of the whole density profile and the increase of it at the peaks are lower than the ones obtained for the original setup, meaning that it cannot be expected that the profile obtained is as sharp as the ones estimated initially.

If this analysis is considered, it is necessary to know if the gas behaves as a continuum fluid on the length scale, for which the gas obeys the Navier-Stokes equations of hydrodynamics. If this was not the case, rarefied gas dynamics would apply and the study implemented so far by means of ANSYS Fluent would not be valid. In order to define the nature of the gas, the Knudsen number is used. If the value of this parameter is lower than *0.001*, the gas behaviour will belong to the first situation mentioned: the continuum hypothesis is appropriate and the flow can be analysed using

the Navier-Stokes equations with conventional no-slip boundary conditions. For a range of Knudsen values between *0.001* and *0.1*, the gas is in the slip-flow regime: rarefaction effects start to influence the flow and the Navier-Stokes equations can only be employed provided tangential slip-velocity boundary conditions are implemented along the walls of the flow domain.

Considering the formula for the Knudsen number:

$$Kn = \frac{16\mu}{5L_{REF}\sqrt{2\pi R'T\rho}} \tag{11}$$

The results obtained for both configurations considered are the ones shown in the following table:

$\mathbf{P}_{\text{inlet}}$ $[mbar]$	$\mathbf{Kn}_{\text{MAX}}$ [-]
120	*0.0448*
300	*0.0192*

Table 11: Maximum values of the Knudsen number for the different settings.

It is seen that both Knudsen numbers are greater than *0.001*, which means that the slip-flow regime is the dominant condition on the inlets channels. Therefore, in order to obtain a more accurate approximation to the behaviour of the flow expansion, it would be necessary to redefine the boundary conditions on the walls of the inlets channels in order to account for this effect. This detail is important, since the convergence of the calculations has been ensured through the mass flow rate by comparing the inlet one to the outlet one, and the fact that the Knudsen number is greater than *0.001* implies that the mass flow rate calculated is not the one that is actually passing through the control volume.

Finally, as for the convergence criteria:

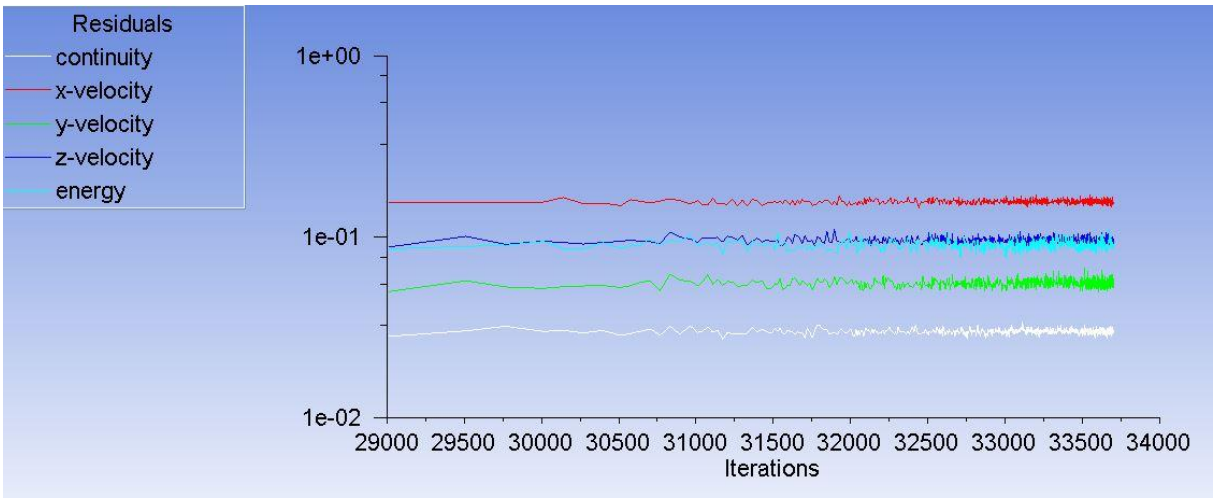

Figure 72: Evolution of the residuals for a reservoir pressure of *300 mbar*.

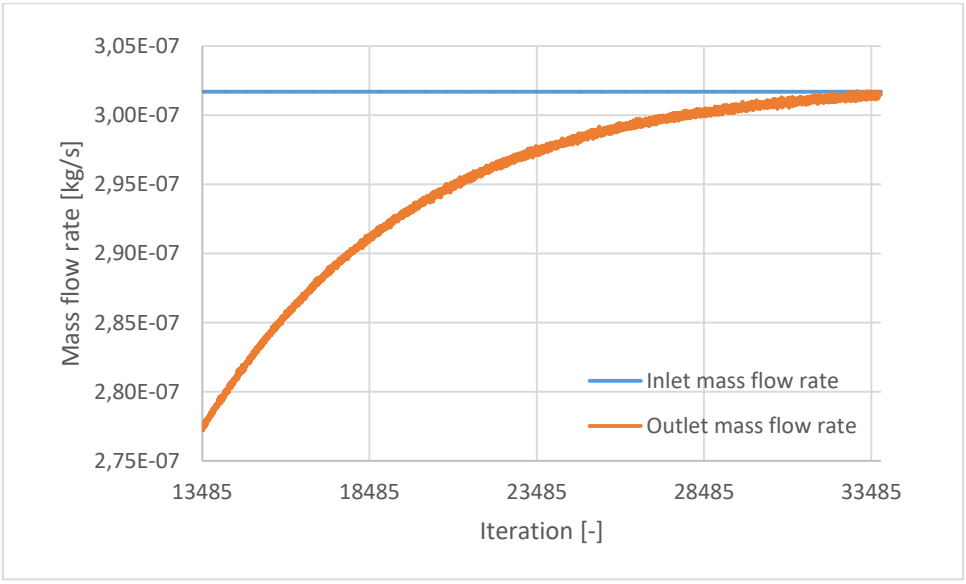

Figure 73: Mass flow rate convergence for a reservoir pressure of *300 mbar*. The plot is not showing all the convergence evolution since an error too place while storing the data.

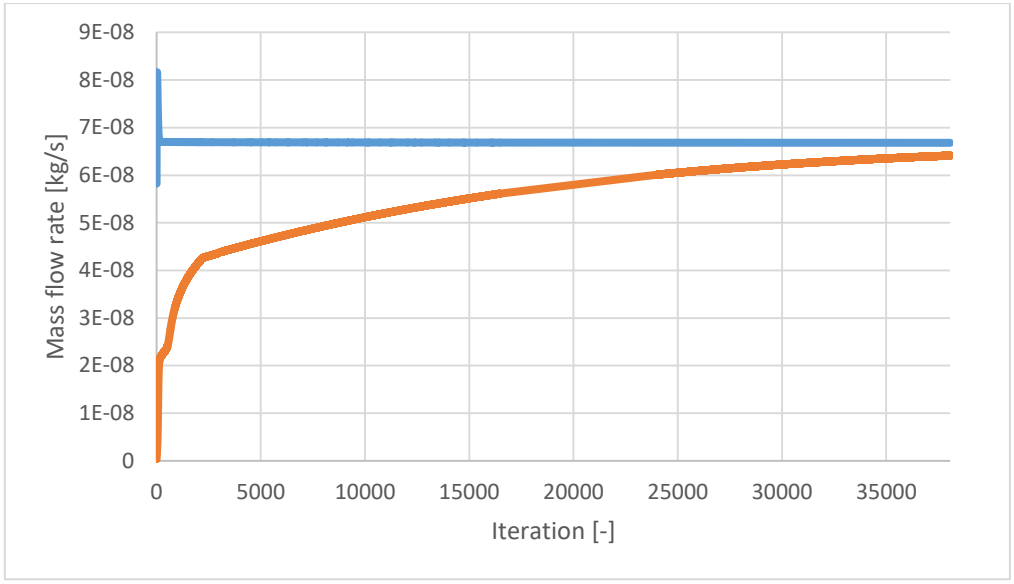

Figure 74: Mass flow rate convergence for a reservoir pressure of *120 mbar*. The blue line represents the inlet mass flow rate, and the orange line the outlet mass flow rate.

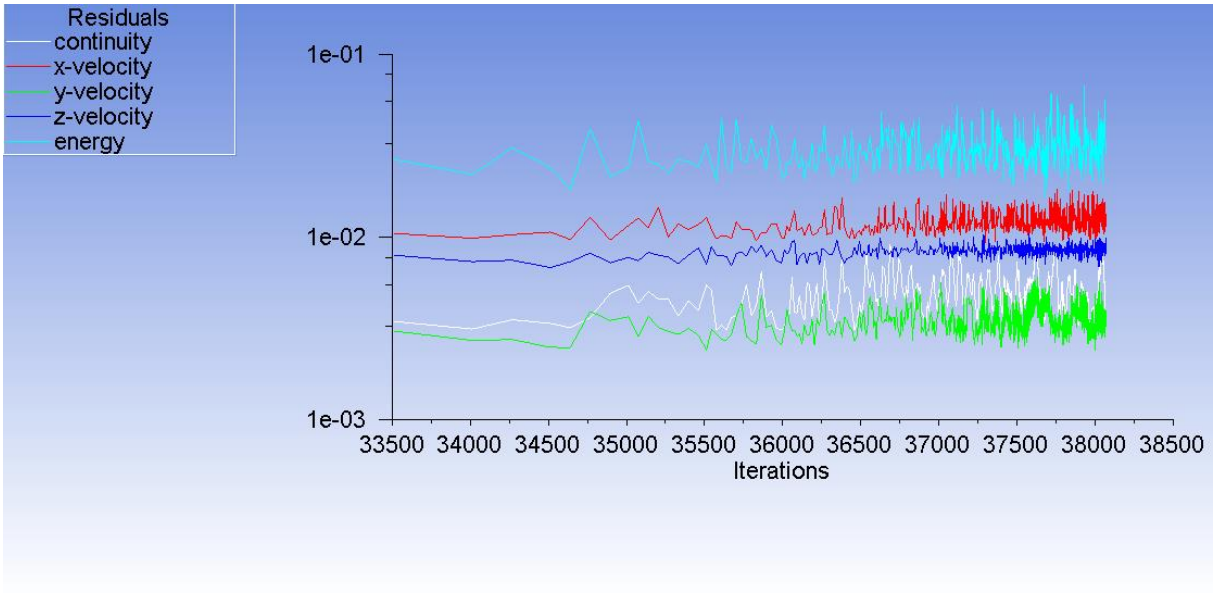

Figure 75: Evolution of the residuals for a reservoir pressure of *120 mbar*.

Chapter 5 Conclusions

Along this project, a study of the behaviour of the flow expansion taking place along a microchannel has been carried out. The results obtained by means of the different and progressive setups have been analysed and compared to the theory knowledge linked, and they all have been verified and assumed to be representative of the configuration considered.

Taking into account the final aim of the microchannel, in terms of modulating the laser signal through the creation of peaks in the density profile, the study has shown that, for these peaks to be as high as possible, it is necessary to increase the pressure of the reservoir from where the gas is injected in the main channel.

Besides, if the pattern of interest, regarding the density profile along the channel, follows a flat shape rather than a parabolic one, it is necessary to increase the diameter of the set of outlets in order to provide such tendency.

5.1 Further suggestions

Regarding the analysis performed by means of ANSYS Fluent, in order to make it more realistic and representative, a more accurate representation of the geometry would bring a more precise result: an example of it would be considering a circular cross section of the main channel instead of the rectangular one used so far. It would also be interesting to check whether symmetry simplifications could be applied to the original geometry in order to reduce the volume tested on the programme.

The boundary conditions on the walls of the inlets channels should also be redefined so that the slip-flow regime is accounted since, as it has been tested through the Knudsen number calculation, the no-slip condition on these walls is no longer valid and this affects the quality of the results obtained.

As for the mesh, the settings used along the project involve a structured mesh with a simple refinement near the inlet and outlet holes. Nevertheless, the mentioned configuration is not optimum and it could be improved with different methodologies: meshing the volume by parts with different levels of refinement would be the first option. In this case it should be necessary to analyse the zones of the volume in which the gradients of the variables are higher, or the zones where a development of the boundary layer is expected to happen, and provide a mesh with a smaller element size

and a greater refinement. In order to obtain the best element size for each of the zones, a mesh convergence study should be carried out in order to ensure the best relationship between the quality of the results obtained and the computational cost of the calculations. Regarding this issue it is necessary to bear in mind the fact that, depending on the ANSYS Fluent version that is used (the students one or the full version) the user may encounter a limit on the maximum number of elements to be defined in the volume.

Another option regarding the improvement of the mesh quality would be applying the dynamic mesh settings on Fluent: this way the program would evaluate itself the zones where more resolution would be needed in order to define the details of the flow behaviour. The drawback of this option is the increase of the computational cost.

Finally, the last suggestion to point out regarding the computational process and the calculations carried out involves the machine used. In order to perform the studies mentioned, having a powerful computer would save up computational cost considerably: the results would be obtained faster if the performance is compared to a more basic tool.

References

1. Extreme ultraviolet. (n.d.). Retrieved from
https://en.wikipedia.org/wiki/Extreme_ultraviolet
2. Extreme ultraviolet lithography. (n.d.). Retrieved from
https://en.wikipedia.org/wiki/Extreme_ultraviolet_lithography
3. OSA Publishing. (n.d.). Retrieved from
https://www.osapublishing.org/view_article.cfm?gotourl=https%3A%2F%2Fwww%2Eosapublishing%2Eorg%2FDirectPDFAccess%2F1AF3AFA0-977B-2491-7F227EB8348DE8F4_35581%2Fjosab-15-10-2620%2Epdf%3Fda%3D1%26id%3D35581%26seq%3D0%26mobile%3Dno&org=Consiglio%20Nazionale%20delle%20Richerche%2F%20Istituto%20Nazionale%20per%20la%20Fisica%20della%20Materia%20Politecnico%20di%20Milano%20%28INFM%29
4. What is CFD | Computational Fluid Dynamics? — SimScale Documentation. (n.d.). Retrieved from
https://www.simscale.com/docs/content/simwiki/cfd/whatiscfd.html
5. Meshing -- CFD-Wiki, the free CFD reference. (n.d.). Retrieved from
https://www.cfd-online.com/Wiki/Meshing
6. Notes of the subject "Computational and experimental fluid dynamics" ("Mecánica de fluidos computacional y experimental" in the original title) from Universitat Politècnica de València.
7. FLUENT 6.3 User's Guide - Contents. (n.d.). Retrieved from https://www.sharcnet.ca/Software/Fluent6/html/ug/node1.htm
8. Notes of the subjet "Heat transfer and termal analysis" from Politecnico di Milano.
9. Knudsen number - Wikipedia. (n.d.). Retrieved from https://en.wikipedia.org/wiki/Knudsen_number
10. KNUDSEN NUMBER. (n.d.). Retrieved from http://www.thermopedia.com/content/908/
11. Barber, R. W., & Emerson, D. R. (n.d.). The influence of Knudsen number on the hydrodynamic development length within parallel plate micro-channels. Retrieved from https://www.witpress.com/Secure/elibrary/papers/AFM02/AFM02019FU.pdf